Ref. Ares(2019)5612848 - 06/09/2019

GIS-Based Infrastructure Management System for Optimized Response to Extreme Events of Terrestrial Transport Networks

European critical hazards (natural) D2.1

GIS Map and identification of hot spots of sudden extreme natural hazard events, including database with impact and return periods

September 2019 (V1.0)

PUBLIC

This project has received funding from the European Union's Horizon 2020 research and innovation programme under grant agreement No. 769255.

SAFEWAY

GIS-BASED INFRASTRUCTURE MANAGEMENT SYSTEM FOR OPTIMIZED RESPONSE TO EXTREME EVENTS OF TERRESTRIAL TRANSPORT NETWORKS

Grant Agreement No. 769255

European Critical Hazards (natural) Deliverable D2.1

WP 2 Risk Factors and Risk Analysis

Deliverable ID	**D2.1**
Deliverable name	**GIS Map and identification of hot spots of sudden extreme natural hazard events, including database with impact and return periods**
Lead partner	**NGI**
Contributors	UMINHO, Ferrovial, Budimex, TØI, IMC, IP, NR

PUBLIC

SAFEWAY Project Synopsis

According to European TEN-T guidelines, due consideration must be given to the risk assessments and adaptation measures during infrastructure planning, in order to improve resilience to disasters. SAFEWAY's aim is to design, validate and implement holistic methods, strategies, tools and technical interventions to significantly increase the resilience of inland transport infrastructure. SAFEWAY leads to significantly improved resilience of transport infrastructures, developing a holistic toolset with transversal application to anticipate and mitigate the effects extreme events at all modes of disaster cycle:

1. **"Preparation":** substantial improvement of risk prediction, monitoring and decision tools contributing to anticipate, prevent and prepare critical assets for the damage impacts;
2. **"Response and Recovery":** the incorporation of SAFEWAY IT solutions into emergency plans, and real-time optimal communication with operators and end users (via crowdsourcing and social media);
3. **"Mitigation":** improving precision in the adoption of mitigation actions (by impact analysis of different scenarios) together with new construction systems and materials, contributing to the resistance & absorption of the damage impact.

SAFEWAY consortium has 15 partners that cover multidisciplinary and multi-sectorial business fields associated with resilience of transport infrastructure in Europe: national transport infrastructure managers & operators, a main global infrastructure operator, partners able to provide various data sources with large coverage in real time, comprehensive ITC solutions, and leading experts in resilience, risk databases, remote sensing-based inspection, and decision systems based on predictive modelling.

SAFEWAY will carry-out 4 real case studies distributed through 4 countries, linked to 5 corridors of the TEN-T Core Network. SAFEWAY has as main expected impacts:

1. at least 20% improvement in mobility; and
2. at least 20% lower cost of infrastructure maintenance.

Document Information

Document Name	European critical hazards (natural)
Version No.	V1.0
Due date Annex I	31/08/2019
Report date	02/09/2019
Number of pages	146
Lead Author	Unni Eidsvig (NGI), Luca Piciullo (NGI), Kristine Ekseth (NGI), Christina Ekeheien(NGI)
Other Authors	Sara Cuerva Navas (Ferrovial) Nataliya Aleksieva (NR) Julia Ratajczak (Budimex) Johanna Ludvigsen (TØI) Francisco Ganhão (IP)
Dissemination level	Public

Document History

Ver.	Date	Description	Authors	Checked by
0.1	24/06/2019	Version ready for review. Updated from Internal deliverable InD2.1	U. Eidsvig, L. Piciullo, K. Ekseth, C. Ekeheien	B. Riveiro E. Nabais
0.2	22/08/2019	Updated version, including review comments from UVIGO and INSITU.	U. Eidsvig, L. Piciullo, K. Ekseth, C. Ekeheien	C. Perez-Collazo
1.0	30/08/2019	Quality Check	C. Perez-Collazo	U. Eidsvig

Document Approval

Ver.	Name	Position in project	Beneficiary	Date	Visa
1.0	Dr. Belén Riveiro	Project Coordinator	UVIGO	02/09/2019	BR

Executive Summary

The main Objective of this deliverable is to identify risk factors, mainly with regard to natural hazards. This encompasses identification of critical natural hazards and their impact on the infrastructure (Section 2), review of natural hazard maps and data bases at European level (Section 3) and review of natural hazard maps at National or regional level for the Pilot areas (Section 4). The gathered information is used to describe the effect of climate change for the Pilot areas (Section 5) and to produce hot-spot maps for the Pilot areas (Section 6).

The first step was to identify the critical natural hazards, i.e. sudden natural extreme events leading to malfunctioning of terrestrial transport networks in Europe. Further, the impact or modes of malfunctioning of the infrastructure caused by each one of these events were described. The identification of critical hazards and failure modes was performed from a generic point of view, as well as specific for the Pilot areas. The generic approach considered all plausible failure modes with a natural extreme event trigger for roads and railways, is based on a literature review and a review of results from previous EU projects, and considers the vulnerability and resilience of terrestrial transport systems. The specific approach for Pilot areas considers the most important triggers and failure modes for Pilot areas. This assessment was performed by the infrastructure owners (*Infraestruturas de Portugal* and Network Rail) and railway infrastructure maintainer(Ferrovial):

- **Portugal:** Natural weather-related events with the greatest impact on road and rail transportation in the Portuguese Pilot are forest fires and floods.
- **Spain:** Natural hazards that have had the greatest impacts in the Spanish Pilot of the Mediterranean corridor (Demonstration site 2.A, in Málaga and Demonstration Site 2.B in Murcia) are flooding, landslides, earthquakes, heavy rain and hot/cold waves.
- **UK:** At asset level; the most critical natural hazards encompass, flooding, subsidence and landslides. Compensation payments for the London North-West (LNW) Route indicates that wind, flooding and snow-related events have had the most significant impact on interruption on the infrastructure service (network level).

The next step was to assess the likelihood of natural events. This is done by providing an overview of available inventories, databases and GIS maps of natural hazards at European level and at National level for the Pilot areas. Downloadable data at European level include:

- Flood hazard maps and catalogues
- Wild fire catalogues
- Hazard maps related to wind and temperature (heat)
- Landslide hazard maps
- Earthquake hazard maps and catalogues
- Rainfall catalogue and forecast analyses

In addition, other available information on European maps of weather-related hazards for current and future climate has been reviewed and summarised. Further, a brief overview of European dynamic hazard maps used for monitoring and forecasting has been provided.

For the Pilot countries, information about the following hazard types has been reviewed and described:

- **Portugal:** Wild fires and flood
- **Spain:** Flood, landslide, heatwaves (and wild fires), earthquakes, rainfall
- **UK:** Flood and wind

Section 6 provides hot-spot maps for the demonstration sites to better identify the most exposed parts of the infrastructure. The maps are obtained by overlapping different natural hazard maps with the road and railway tracks of the pilot areas. The aim is to highlight critical areas which need further investigations to mitigate dangerous situations.

Table of Contents

Glossary of Terms

Hazard	Probability that a particular danger (threat) occurs within a given period of time.
Impact	(Undesirable) effects on human and natural systems including direct and indirect effects. Direct effects related to the failure of critical infrastructures commonly trigger cascading effects.
Threshold	The level of magnitude of a system process at which sudden or rapid change occurs. It is a point or level at which one relatively stable state or regime gives way to another.
Failure mode	A way that failure can occur, described by the means by which element or component failures must occur to cause loss of the sub-system or system function.
Pilot	A near-real life operational environment designed to test and validate the effectiveness and transferability of technologies and methodologies defined in the framework of the SAFEWAY project.
Demonstration Site	A particular geographical location or transport network infrastructure section, within a project pilot, where one or more project technologies or methodologies will be tested and validate its effectiveness and transferability in relation to one or more adverse events (Natural or human-made)
Scenario	An outline of a possible future event that assess the outcomes that an extreme event may have on a transport infrastructure – i.e., affecting one or more critical assets and/or disrupting users. Scenarios are defined within the so called "scenario-based risk analysis", which is the process of analysing a set of multiple scenarios or "alternative words" with the aim of identifying potential risk and their linked hazards, to increase preparedness to handle them and minimize their impact.

1. Introduction

Transportation is an important component of a society to maintain its functions and its economic and social development. Many different types of adverse weather conditions challenge transportation networks, such as storms, intense precipitation, extreme temperatures, as well as weather-related hazards like floods, erosion, landslides, and forest fires. Negative impacts include accidents, damage to infrastructure or to components of the infrastructure, delays and malfunctioning of the transportation network, resulting in economic consequences. Climate change is anticipated to lead to an escalation of such negative impacts if no counter-measures are taken.

1.1 Framework for risk assessment

The IS0 31000:2009 represent a globally accepted standard for risk management. The principles of effective risk management in ISO 31000 are that it should (Purdy; 2010):

1. Create and protect value;
2. Be an integral part of all organizational processes;
3. Be part of decision making;
4. Explicitly address uncertainty;
5. Be systematic, structured, and timely;
6. Be based on the best available information;
7. Be tailored;
8. Take into account human and cultural factors;
9. Be transparent and inclusive;
10. Be dynamic, iterative, and responsive to change;
11. Facilitate continual improvement of the organization.

In the risk management framework established by ISO 31000, risk assessment includes risk identification, risk analysis and risk evaluation, and is followed by risk treatment (decision making and execution of regarding risk reduction). In the following, each element in the risk management process is presented in more detail.

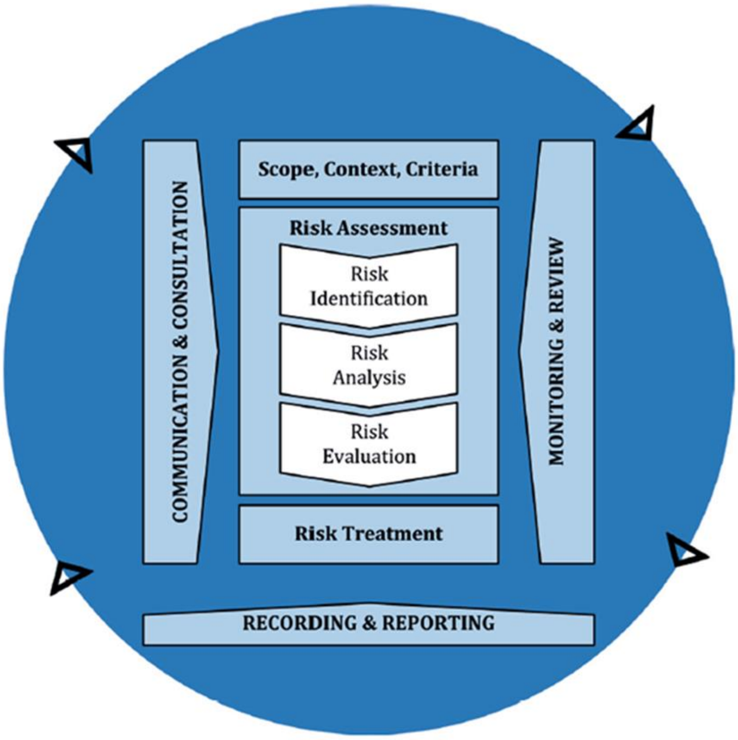

Figure 1: Risk management process. (Source: ISO-31000: 2018)

1.1.1 Establishing the context

According to ISO 31010, establishing the context defines the basic parameters for managing risk and sets the scope and criteria for the rest of the process. It considers background studies to the particular risks being assessed. In this phase, the risk assessment objectives, risk criteria, and risk assessment programme should be determined and agreed. For a specific risk assessment, establishing the context should include:

a) Establishing the external context (e.g. cultural, political or financial factors, perceptions and values of external stakeholders).
b) Establishing the internal context (e.g. internal information flow, decision process, internal stakeholders, standards and internal processes).
c) Establishing the context of the risk management process (e.g. responsibilities, extent of project, defining risk assessment methodologies, risk criteria, identification of decision and action processes, identifying required resources, evaluation of risk assessment and management process).
d) Defining risk criteria (e.g. use and character of probabilities, type of consequences, risk treatment decision process)

1.1.2 Risk assessment

Risk assessment includes risk identification, risk analysis and risk evaluation. Risk assessment provides an understanding of risks, their causes, consequences and their probabilities, which provides an input to decisions about:

- whether an activity should be undertaken;
- how to maximize opportunities;
- whether risks need to be treated;
- choosing between options with different risks;
- prioritizing risk treatment options;
- the most appropriate selection of risk treatment strategies that will bring adverse risks to a tolerable level.

1.1.3 Risk treatment

Risk treatment is a part of risk management performed in parallel with or after the risk assessment study. It involves the decision making process of how to mitigate the risk (if needed) and the actual execution of mitigation work, which can be physical means and/or non-physical means for example of an organisational character. It involves selecting and agreeing on one or more relevant options for either (a) reduce the probability of occurrence of the hazard phenomena or (b) reduce the consequence once the hazard phenomena occurs, or both. Once the mitigation program is decided, it should be implemented. This is part of a cyclical process of assessing and reassessing the level of risk, with a view to determining its tolerability against the criteria previously set, in order to decide whether further treatment is required.

1.1.4 Risk communication and consultation

Risk communication is an essential part of risk management, both internally in the risk management project group itself, and with various types of external stakeholders. Establishing a communication plan, and involving external stakeholders early in the project phase is a key success factor for the project, and can contribute to:

- defining the context appropriately;
- ensuring that the interests of stakeholders are understood and considered;
- bringing together different areas of expertise for identifying and analysing risk;
- ensuring that different views are appropriately considered in evaluating risks;
- ensuring that risks are adequately identified;
- securing endorsement and support for a treatment plan.

1.1.5 Monitoring and review

Risk management is a continuous process. All risk projects at some point needs verification of the correctness of the premises for, and findings from, the project. It is therefore recommended to carry out monitoring and review actions on a regular basis in order to verify that:

- assumptions about risks remain valid;
- assumptions on which the risk assessment is based, including the external and internal context, remain valid;
- expected results are being achieved;
- results of risk assessment are in line with actual experience;
- risk assessment techniques are being properly applied;
- risk treatments are effective.

1.2 Scope of report

This report encompasses collection of data on natural events, relevant for hazard and impact assessment. In the hazard assessment, likelihood could be described using various parameters, derivable from each other: return period, frequency or probability[1].For impact assessment, also the magnitude or intensity is an important property of the natural event. The data on return period/frequency/probability and on magnitude/intensity of the natural events are contained within different data bases. The most relevant data (e.g. for the pilot area countries) will be integrated into the SAFEWAY Infrastructure Management System (WP7). In this report the impacts of the different events are described verbally in terms of failure modes (Table 1 and Table 2). To each failure mode, the impact is classified as either reduction of mobility in the network or damage to infrastructure assets – or both. Strategies, tools and data for quantification of the impacts will be established in D2.2, D2.3 and applied within WP5.

The work to be accomplished in WP 2 (and the application of the results) are related to different steps of the risk management process in Figure 1:

- **Establishing context:** The type of impact to be assessed was established in cooperation with WP 5 and 6 and include: Reduction of mobility (reduction of capacity/loss of service for the transportation line or speed reductions due to difficult driving conditions) and deterioration of infrastructure assets.
- **Risk identification:** Section 2 of this deliverable identifies failure modes and impact types, including identification of trigger.
- **Risk assessment:**
    - Hazard assessment: This deliverable identifies and collects hazard data for the most critical natural events through review and collection of European hazard maps and data bases. The hazard data encompass static hazard maps/data bases and maps considering long term and short-term changes (long-term: climate change; short term: dependent on current weather conditions and meteorological parameters).
    - Impact assessment: This deliverable assesses the impacts qualitatively, by linking natural event triggers to impacts and failure modes of the infrastructure. Methodology for quantitative assessment of direct material impact as well as impacts on mobility will be outlined in D2.2 (for man-made hazards) and D2.3 (for natural

[1] For example, the return period of a flood might be 100 years; otherwise expressed as its probability of occurrence being 1/100, or 1% in any one year. This does not mean that if a flood with such a return period occurs, then the next will occur in about one hundred years' time - instead, it means that, in any given year, there is a 1% chance that it will happen, regardless of when the last similar event was.

hazards). WP 5 will work further with application of quantitative impact assessment.

- **Risk treatment:**
    - Help decisions regarding maintenance and operation: Input to models for optimisation of maintenance and resilience. Input to decision support systems. (Input to WP 5 and further to WP 6)
    - Input to action plan for long-term resilience (WP8)

2. Risk identification

2.1 Identification of plausible weather-triggered failure modes for terrestrial transportation lines

The risk identification comprises a review of all plausible failure modes with extreme weather event trigger for road and rail. The review has considered papers and projects considering vulnerability and resilience of terrestrial transport systems towards natural events. The failure modes are summarised in Table 1. The table is based on summaries from EEA(2017), VTT(2011) and Snelder and Calvert(2016).

Table 1: Description of failure modes for transportation lines triggered by extreme weather events or related hazards

Extreme weather event or related hazard	**Impacts on transport with classification:** **S: Relevance for the infrastructure service, i.e. affecting mobility** **M: Material impacts on assets, affecting transportation line health and maintenance needs**			
	Road		**Rail**	
Heat waves	Damage to pavements	M, S	Rail buckling	M, S
	Vehicle failure (tyres)	S	Material fatigue	M, S
	Fatigue of drivers	S	Increased instability of embankments	M
			Overheating of equipment	M
			Thermal expansion on bridge expansion joints and paved surfaces	M
Forest fires	Reduced visibility	S	Dangerous conditions	M, S
	Dangerous driving conditions	S	Damage and deformation of railway assets	M, S
	Structural damage of infrastructure, especially pavements	M, S	Loss of stability and capacity	M, S

Extreme weather event or related hazard	Impacts on transport with classification: S: Relevance for the infrastructure service, i.e. affecting mobility M: Material impacts on assets, affecting transportation line health and maintenance needs			
	Road		**Rail**	
	Damage of barriers, panels	M	Damage of barriers, panels	M
Forest fires (cont.)	Growing vegetation on slopes is destroyed. It can lead to soil degradation and slope slide	M	Growing vegetation on slopes is destroyed. It can lead to soil degradation and slope slide	M
Heavy precipitation	Reduced visibility and surface friction	S	Change of the ballast position	M
	Mass transport by surface water in or along the embankment	M	Mass transport by surface water in or along the embankment	M
	Embankment and slope damage	S	Embankment and slope damage	S
	Material and terrain washed away under the foundation of the viaduct	M	Material and terrain washed away under the foundation of the viaduct	M
Flooding (urban, river, flash floods, storm surge)	Water on road and in underground transport system	S	Water on line and in underground transport system	S
	Erosion and destruction of embankment	S, M	Erosion and destruction of embankment	S, M
	Erosion (scouring) and damage to bridge supports	S, M	Erosion (scouring) and damage to bridge supports	S, M
	Subsidence of element	S, M	Subsidence of element	S, M
	Structural collapse of construction elements	S, M	Structural collapse of construction elements	S, M
	Damage or deformation of protection barriers	M	Deficiencies in the railway track bed	M
	Damage of pavement due to destruction and instability of vegetation along the path	S, M	Damage or deformation of protection barriers	S, M

Extreme weather event or related hazard	Impacts on transport with classification: S: Relevance for the infrastructure service, i.e. affecting mobility M: Material impacts on assets, affecting transportation line health and maintenance needs			
	Road		Rail	
	Damage of lightening system	S	Damage due to destruction and instability of vegetation along the path	S, M
Landslides	Blocking of transportation line	S	Blocking of transportation line	S
	Destruction of transportation line	S, M	Destruction of transportation line	S, M
Wind	Difficult driving conditions; exposed parts of roads (e.g. bridges) closed due to strong wind gusts	S	Exposed parts of line (e.g. bridges) closed due to strong wind gusts	S
	Obstacles on the road owing to fallen trees and other objects	S	Obstacles on the road owing to fallen trees and other objects	S
	Reduction of drainage capacity	M	Damage to infrastructure such as signals, catenary, etc. (e.g. owing to falling trees)	S, M
	Deformation of lightning system	S	Change of the ballast position	S, M
	Damage/movement of fencing, acoustic panels	M	Stripping of gravel	M
			Reduction of drainage capacity	M
			Damage/movement of fencing, acoustic panels	M
Fog	Reduced visibility	S	Reduced visibility	S
Storms (thunderstorms, hail, blizzards, i.e. strong wind	Reduced visibility and surface friction	S	Reduced visibility and surface friction	S
	Obstacles on road	S	Obstacles on rail line	S

Extreme weather event or related hazard	Impacts on transport with classification: S: Relevance for the infrastructure service, i.e. affecting mobility M: Material impacts on assets, affecting transportation line health and maintenance needs			
	Road		Rail	
gusts, intense snowfall)	Failures in transport control system	S,M	Failures in transport control system	S,M
Cold spells	Reduced surface friction	S	Reduced surface friction	S
	Technical failure of vehicles	S	Deterioration of infrastructure	
	Deterioration of infrastructure	M	Change of temperatures in the rails, which leads to deformation without proper dilatation	
	Material damage of infrastructure	M	Material damage of rails	M
Cold Spells (cont.)	Structural damage of the concrete structure degradation in extremely low temperatures	S, M	Structural damage of the concrete structure degradation in extremely low temperatures	S, M
	Frozen culverts may be blocked and cause structural damage	S, M	Frozen culverts may be blocked and cause structural damage	S, M
	Cracks close to contraction joints in the cement concrete pavement.	S, M		
Snowfall	Reduced visibility and surface friction	S	Obstacles on rail line owing to snowdrift, broken branches etc.	S, M
	Obstacles on roads owing to snowdrift and broken branches	S, M	Increasing slope erosion which may cause local slope damage	M
	Increasing slope erosion which may cause local slope damage	M	Ice and snow in culverts leading to reduced drainage capacity and water on the rail structure or flooding	S, M

Extreme weather event or related hazard	Impacts on transport with classification: S: Relevance for the infrastructure service, i.e. affecting mobility M: Material impacts on assets, affecting transportation line health and maintenance needs			
	Road		Rail	
	Ice and snow in culverts leading to reduced drainage capacity and water on the road structure or flooding	S, M		

2.2 Risk identification for the Pilots

The pilot and demonstration activities are small-scale, short-term projects that test and validate the innovative methodologies and technologies which were being developed in WPs 2-4 for future replication or scaling up.

For the weather-related events, the focus is on:

- Pilot 1: Portugal, region of Santarém/Leiría.
- Pilot 2: Spain, Murcia and Malaga regions.
- Pilot 3: United Kingdom, rail infrastructure between Manchester and London

The first Pilot will take place in Portugal in two demonstration sites: one in the region of Santarém (Demonstration Site 1.A) and another in Leiría (Demonstration Site 1B). They include both railway and road sections of the Atlantic corridor.

This second Pilot will take place in Spain, along the Mediterranean Corridor, and considers two demonstration sites: Demonstration site 2.A, in Málaga, includes a section of high-speed railway (154km of length) including four stations. The Demonstration Site 2.B in Murcia includes conventional railway, comprising older infrastructure whose conservation may be worse than the high-speed infrastructure of Demonstration Site 2.A.

The third Pilot will take place in UK. The only demonstration site for this Pilot (Demonstration Site 3.A) is placed in Stoke-On-Trent, covering a 10-mile section of the London-Manchester railway line, which is the most frequented train line in the United Kingdom. This line is part of the London North Western route, the biggest in the country, running the railways in the North West and West Midlands and, thus, a critical component of the North Sea-Mediterranean corridor of the TEN-T network.

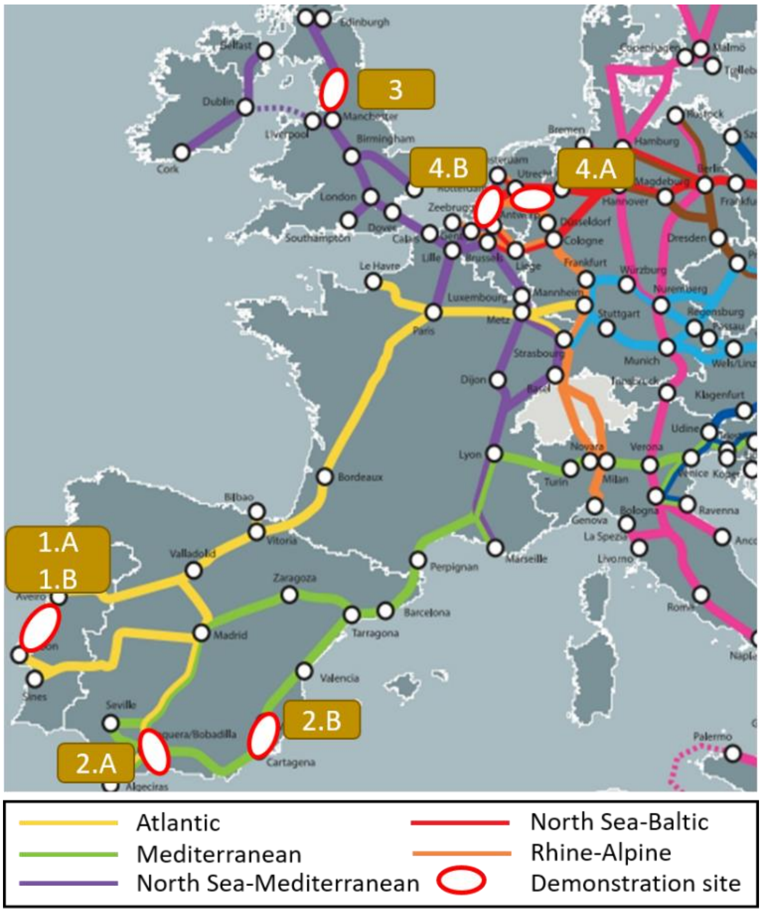

Figure 2: Map of Pilots and demonstration sites

2.2.1 Risk identification/failure modes Portugal, natural events

Various types of adverse events will be considered for the definition of scenarios in the Portuguese pilot. The natural hazards taken into account depend on the selected demonstration site; floods in the case of Santarém and both floods and wildfires in Leiría (UVIGO, 2019).

The most critical natural hazard events in the Santarém demonstration site are considered to be related to floods, because roads and railway included in this site are placed along the basin of the Tagus River.

In the Leiría demonstration site, the most critical natural hazard events encompass wildfires, events that are closely related with heatwaves occurrence. The number, duration and amplitude of heatwaves is expected to increase in the future according to climate change projections. Flooding is also an event to be considered in this demonstration site.

The Demonstration Site 1.A (Santarém) includes both road and railway transportation modes, so it can be validated in a multimodal context. Regarding the road section, the available information includes 49 pavement sections that cover a total of 311 km (both directions considered separately in highway sections). Similarly, the railway area is subdivided in 31 sections from four different railway lines, covering a total of approximately 92 Km.

Apart from the pavement and rail sections, there is information available regarding bridges and viaducts. There are data from more than 150 assets in road sections, and a similar number for the rail sections

For the Demonstration Site 1.B (Leiría), the available information is divided in road and railway assets (similarly than for Demonstration Site 1.A, bridges and viaducts), with approximately 40 assets for each transportation mode.

Failure mode at asset level is presented in Table 2, based on information from the descriptions of the scenarios (UVIGO, 2019). Further information on critical assets can be found in Planetek (2019).

Table 2: Failure modes at asset level; weather related natural hazards, in the Portuguese Pilots

Meteorological trigger or related hazard	**Assets**	**Impacts on transport with classification:** **S: Relevance for the infrastructure service, i.e. affecting mobility** **M: Material impacts on assets, affecting transportation line health and maintenance needs**	
Flood	Pavement and Tracks	Material damage (washing away), water overtopping.	S,M
	Retaining wall	Water leak, settlement, sliding rotation	S, M
	Embankments	Settlement, lateral spreading, slope stability failure	S, M
	Bridges	Washing away of access tracks, water overtopping, pier/abutment sinking and rotation (local scour)	S, M
Forest fire	Pavement and tracks	Burning/burnt obstacles, structural damage	S, M
	Retaining walls	Rotation, settlement, burning, sliding	S, M
	Embankment	Settlement, burning, lateral spreading, slope stability failure	S, M

Meteorological trigger or related hazard	Assets	Impacts on transport with classification: S: Relevance for the infrastructure service, i.e. affecting mobility M: Material impacts on assets, affecting transportation line health and maintenance needs	
	Bridges	Structural damage, partial/total collapse	S, M
	Vegetation	Vegetation damaged or completely burnt by flames, which could worsen the slope stability and eventually lead to landslides	M

2.2.2 Risk identification/failure modes Spain, natural events

For this pilot, the identified natural hazards encompass earthquakes, flooding, storms / heavy Rain, hot / cold waves and landslides (UVIGO; 2019).

Further failure modes were identified at asset level. Ferrovial (2018) link each critical asset belonging to the case studies in the Mediterranean corridor with the possible events, natural or man-made, that lead the asset to malfunctioning. Table 2 summarise the failure modes triggered by natural, weather-related events in the Spanish case study.

Table 3: Failure modes at asset level; weather related natural hazards, in the Spanish Pilots

Meteorological trigger or related hazard	Assets	Impacts on transport with classification: S: Relevance for the infrastructure service, i.e. affecting mobility M: Material impacts on assets, affecting transportation line health and maintenance needs	
Flood	Viaduct	The terrain under the footing of the viaducts washed away	S,M
Flood	Cut slope and embankment	Increased slope erosion affecting service life and potentially causing landslides or embankment failure	S, M

Meteorological trigger or related hazard	Assets	Impacts on transport with classification: S: Relevance for the infrastructure service, i.e. affecting mobility M: Material impacts on assets, affecting transportation line health and maintenance needs	
Flood	Drains, culverts	Blocking of culverts by debris (branches, leaves etc.), preventing drainage. Water accumulate in the upslope ditch, potentially causing landslide or embankment failure.	S, M
Flood	Fencing and protection elements	Damage, movement or removal of protection elements by flood	M
Flood	Vegetation	Damage, movement or removal of vegetation, worsening slope stability	M
Flood	Rail track	Mechanical failure of tracks, ultimately leading to derailment	M, S
Flood	Ballast	Destabilization of the ballast bed, modifying track stability	M, S
Heavy rain	Ballast	Saturation of surrounding areas of the track to full capacity Water reaching the ballast level, leading to materials drag, modifying the safety of the track.	M, S
Heavy rain leading to flood	Same as for floods, except failure of viaduct and rail track.		
Landslide	Overpass and underpass	Differential strains in underpasses and overpasses in the transition to the cut slope	M
Landslide	Viaduct	Differential strains in viaducts in the transition to the cut slope	S,M
Landslide	Cut slope and embankment Tunnel entrance, cut and cover	Failure of cut slope or embankment	S, M
Landslide	Drains, culverts	Blocking of culverts preventing drainage. Water accumulate in the	

Meteorological trigger or related hazard	Assets	Impacts on transport with classification: S: Relevance for the infrastructure service, i.e. affecting mobility M: Material impacts on assets, affecting transportation line health and maintenance needs	
		upslope ditch, potentially causing landslide and destruction of track.	
Landslide	Fencing and protection elements	Damage, movement or removal of protection elements by landslide	M
Landslide	Vegetation	Damage, movement or removal of vegetation, worsening slope stability	M
Landslide	Rail track	Mechanical failure of tracks, ultimately leading to derailment	M, S
Landslide	Ballast	Destabilization of the ballast bed, modifying track stability	M, S
Hot/cold waves	Cut slope and embankment	Change of the terrain properties, potentially causing **landslides**	M, S
Hot/cold waves	Drains, culverts	Pipe outlet blocked with ice, preventing drainage. Water accumulate in the upslope ditch, potentially causing landslide or embankment failure.	M,S
Hot/cold waves	Vegetation	Vegetation surrounding the track killed during heatwave, worsening slope stability.	M
Hot/cold waves	Rail track	Ambient **temperature gradient** increase might cause unexpected rail fatigue. Railway steel contracts at low temperatures and expands at high temperatures. An increase of the temperature gradient might cause a premature rail wear. No information available yet about how the temperature gradient might reduce the rail life cycle.	M
Hot/cold waves	Fish plate joint	Hot/cold waves might lead to mechanical failure of fish plate joints. If several contiguous fish plate joints are for example	M,S

Meteorological trigger or related hazard	Assets	Impacts on transport with classification: S: Relevance for the infrastructure service, i.e. affecting mobility M: Material impacts on assets, affecting transportation line health and maintenance needs	
		fractured, the rail could overlap and consequently provoking derailment of trains	
Hot/cold waves	Expansion joint	If the expansion joint expands too much because of the temperature, the tracks might overlap, potentially derailing trains.	M,S

In addition to the weather-related failure modes in Table 3, earthquakes also pose a threat to the transportation lines. Earthquakes, depending on the time, its location and magnitude might affect underpasses and overpasses, tunnels, viaducts, slope of embankments and culverts. Earthquakes can damage, move or remove handrails and anti-climb fencing, fencing elements and vegetation (and further worsening slope stability).

2.2.3 Risk identification/failure modes UK, natural events

For the UK Pilot sudden weather events are frequent, especially heavy rain causing floods. For Stoke-on-Trent demonstration site, the critical natural hazards encompass subsidence, flooding and landslide (UVIGO, 2019).

NetworkRail (2019) presents the failure mode at asset level. which is completed with information from the descriptions of the scenarios (UVIGO, 2019) in Table 4.

Table 4: Failure modes at asset level for weather related natural hazards in the UK Pilot

Meteorological trigger or related hazard	Assets	Failure mode description Relevance for loss of service (S), affecting transportation line health and need for long-term maintenance (M).	
Flooding	Under bridges	Scour of bridge foundations. Three assets are over canal	S, M
Flooding	Culvert	Culvert capacity exceeded during flood or reduced after flood due to mass transport	S,M
Heavy rainfall/ landslide	Retaining wall	Landslides/geotechnical movement	S,M
Subsidence	Bridges	Cracking, pier/abutment, settlement, total or partial collapse	S, M
	Retaining walls	Cracking, partial or total collapse	S, M
	Culverts	Blockage, water accumulation leading to landslides and/or collapse	S, M
	Tunnels	Settlement, cracking, partial or total collapse	S, M

Further information on critical assets can be found in Planetek (2019).

Additionally, an assessment of the most critical natural hazards at network level is performed, based on costs for disruption (compensation payment). NetworkRail (2014) present analysis of the compensation payments to train and freight operators for network disruption (Schedule 8 performance costs) during the period 2006/07 to 2013/14. The analysis clearly shows that wind, flooding and snow-related events have had the most significant impact on the Route. Vegetation incursion on the overhead line equipment and track as a result of high wind speeds has been the most significant factor on the London North West (LNW) Route.

Table 5: Most severe weather-related impact based on compensation payment for network disruption (Schedule 8 costs) (Source: NetworkRail; 2014)

Weather-related impact	Schedule 8 costs[1]	Projected future impacts	Prioritisation
Wind	£2.2m	Wind changes difficult to project, however, generally projected to increase	High
Flooding	£1.2m	Up to17% increase in February mean daily precipitation[2]	High
Snow	£1.75m	Up to 2.6°C increase in January mean daily minimum temperature[2]	Medium
Adhesion	£0.8m	Complex relationship between adhesion issues and future climate change.	Medium
Heat	£0.5m	Up to 3°C increase in July mean daily maximum temperature[2]	Medium
Earthslips	£0.4m	Up to17% increase in February mean daily precipitation[2]	Medium
Cold	£0.4m	Up to 2.6°C increase in January mean daily minimum temperature[2]	Low
Sea level rise	Not recorded	0.2m increase in sea level rise[3]	Low
Lightning	£0.3m	Storm changes difficult to project, however, generally projected to increase	Low
Fog	£3k	Complex relationship, however, research suggests fog events may decrease	Low

1 Annual average 2006/07 to 2013/14
2 UKCP09 projection, 2050s High emissions scenario, 50th percentile, against 1970s baseline
3 UKCP09 projection, 2050s High emissions scenario, 50th percentile, against 1990 baseline.

3. Hazard maps and data bases at European level

3.1 Overview

Data from EMDAT (Figure 3 a, b; EMDAT, 2017) clearly shows that the number of natural disasters and the economic damage have dramatically increased in the last three decades. This is mainly due to the increase in number and intensity of events due to climate change and continuous urbanization in areas often exposed to natural hazards.

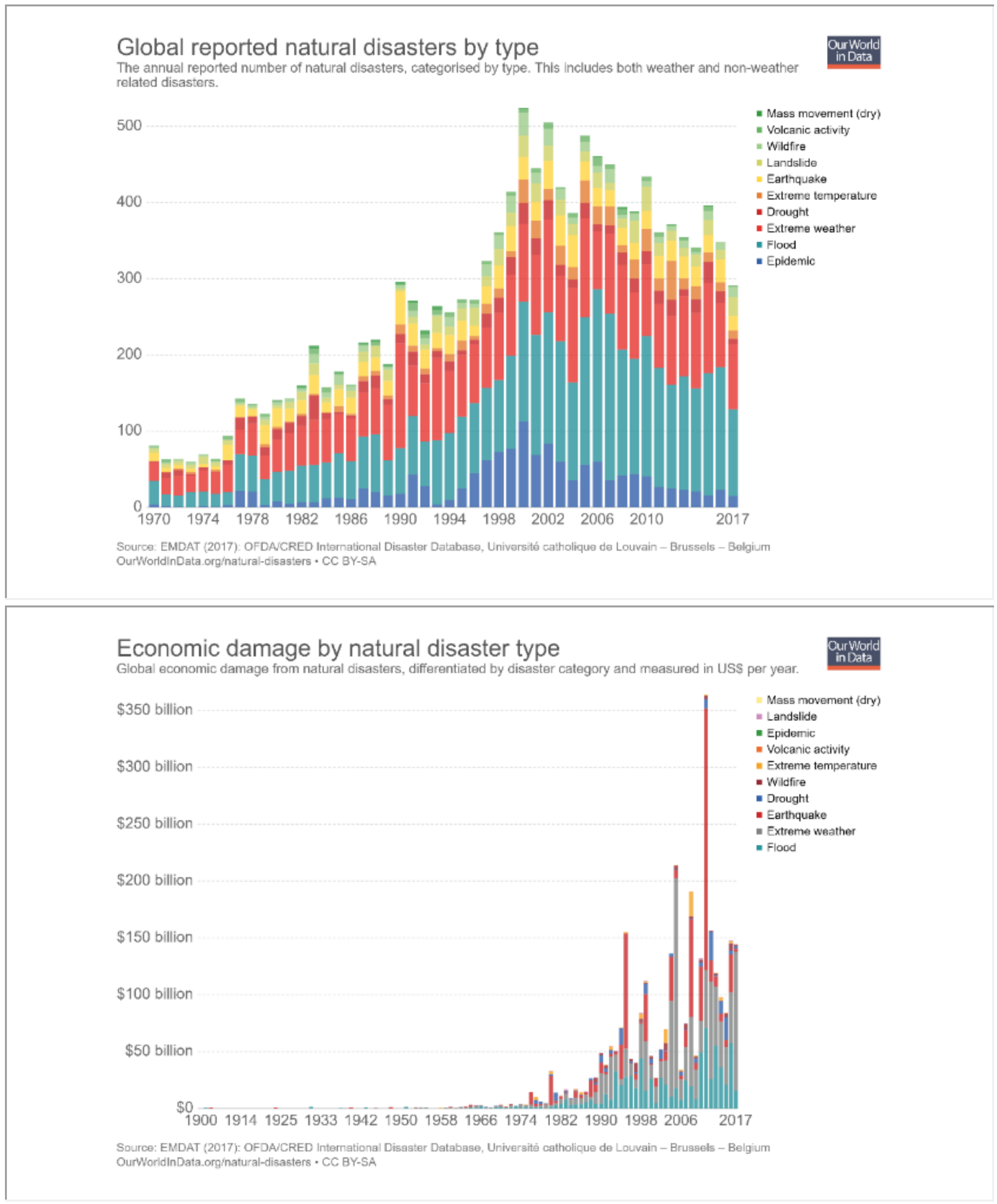

(a)

(b)

Figure 3: (a) global reported natural disasters by type for the period 1970-2017; (b) economic damage by natural disaster type for the period 1900-2017. (Source: EMDAT;2017)

An increased number of governmental and research institutions are involved, or have been involved in the last decade, with natural hazards analysis and mapping. The aim often focused on the definition of hazard maps and/or on the monitoring and forecasting of extreme natural events. Detailed hazard maps, as well as reliable forecasts of such events, are important parts of risk management of natural hazards, with the ultimate goal to reduce fatalities and economic damages to buildings and infrastructures caused by natural hazards. The aim of this section is to provide maps that allows the visualization of extreme weather conditions and natural hazard risk 'hot spots'. The most relevant data will be integrated into the SAFEWAY IMS. The identification is conducted by review and evaluation of existing Global and European databases on weather and natural hazards. A list of databases produced for mapping of natural hazards is reported in the tables A1-A8. The name of the database, the detail on the type of data available and the link for downloading the dataset are some of the information gathered. Furthermore, the tables are organised by the type of natural hazards: flood, wildfire, wind, heat, landslide, earthquake. There are some databases gathering datasets for different natural hazards, such as the Global Risk Data Platform (GRDP), the Global Risk Data Platform and the Socioeconomic Data and Applications Centre (SEDAC). Overview of data sources are given in Table 6.

Table 6: List of available data sets from various EU projects and official data sources in Europe

Name/project	Map theme	Description
LAMPRE	Landslides	Hazard maps
ANYWHERE	Meteorological data, floods, flash floods, debris flow, landslides, storm surges, heatwaves, forest fire, drought, storm, severe winds, snowfall	Dynamic data
INTACT	Extreme weather events	Predictions of future hazard situation.
Improver	Natural hazards: floods, earthquakes, landslides, forest fires, meteorological extreme events due to climate change	Hazard maps and climate change
SafeLand	Landslides	Hazard/hotspots maps
EWENT	Extreme weather events	
RAIN	Extreme weather event probability	
Infrarisk	Landslides	
Matrix	Natural hazards	
Floodsite	Flood	Hazard maps

Name/project	Map theme	Description
European Environment Agency, EEA	Extreme weather events, floods, forest fires	Effects of climate change on frequency of EWE and related hazards
EU Joint Research Centre (JRC)	Flood, Landslides	Hazard maps
Global Risk Data Platform	Flood,	Exposure and risk index.
Global Risk Data Platform	Landslides	Hazard maps
Global Risk Data Platform	Flood, forest fires	Events catalogue
Global Assessment Report on Disaster Risk Reduction(GAR) 2017	Flood, earthquakes	Hazard maps
Socioeconomic Data and Applications Center (SEDAC)	Flood, wildfires, earthquakes	Hazard maps
NASA earth observations	Wildfires, temperatures	Events catalogue
The Global Wind Atlas	Wind speed	Observations
European Monthly wind speed (MAPPE model)	Wind speed	Observations
European Climate Assessment (ECAD)	Wind parameters, temperature parameters	Hazard maps
E-OBS data access	Temperature	Observations
SHARE	Earthquakes	Events catalogue
International seismological centre	Earthquakes	

Name/project	Map theme	Description
I-REACT	Flood	Forecast/early warning
Copernicus EFAS	Flood	Monitoring and forecast
EFFIS	Forest fire	Monitoring and forecast

The main databases and their origins have been described in detail in the next section. The most relevant data will be integrated into SAFEWAY IMS (WP7).

3.2 Description of downloadable European hazard maps/data bases

3.2.1 Joint Research Centre Data Catalogue

The Joint Research Centre (JRC) is the European Commission's science and knowledge service. The headquarters are in Brussels but there are research sites in five Member States: Geel (Belgium), Ispra (Italy), Karlsruhe (Germany), Petten (the Netherlands) and Seville (Spain). The work is largely funded by the EU's budget for Research and Innovation. The JRC provides scientific and technical support to the European Commission Services for the implementation of the EU Thematic Strategy for Soil Protection, both through its own work activities and in collaboration with national research organizations, mapping agencies and academia.

The JRC data catalogue contains 94 collections about several topics: environment, energy supplies, sustainable mobility and consumer health and safety. The Floods collection consists in 13 datasets about flood hazard maps at European (6) and global scale (7).

Flood Hazard Maps at European and Global Scale

This collection contains pan-European flood hazard maps at 100-meter resolution for several return periods, from 10 to 500 years. A combination of distributed hydrological and hydraulic models was set up for the European domain (Alfieri et al., 2014) to realize the maps. Then, an observed meteorological data set is used to derive a long-term streamflow simulation and subsequently coherent design flood hydrographs for different return periods along the pan-European river network.

The maps are provided in GeoTIFF file and can be opened with a GIS software. They depict flood-prone areas in Europe for flood events with different return periods. The cell values indicate water depth in meter (Figure 4).

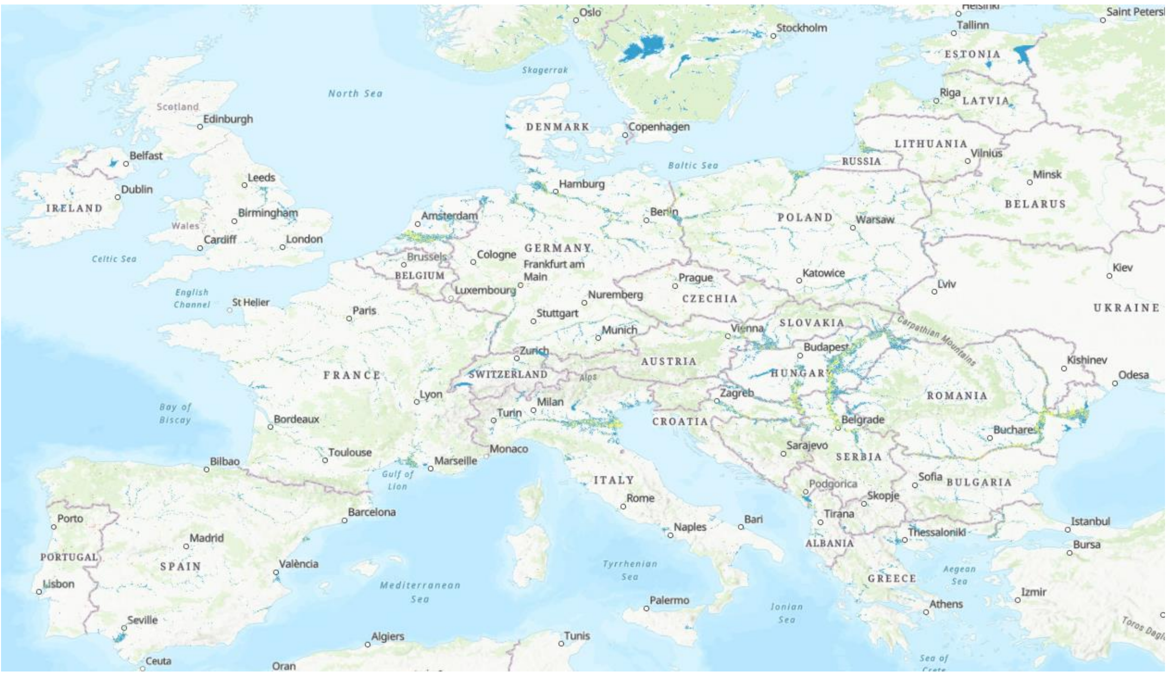

Figure 4: Map of the flood prone areas in Europe for flood events with 10-year return period. Cell values indicate water depth (in m). (Source: JRC data catalogue on Floods)

European Landslide Susceptibility Map (ELSUS v2)

ELSUS v2 shows levels of spatial probability of landslide occurrence (landslide susceptibility) at European scale. It covers all European Union member states except Malta, and several neighbouring countries. The map has been produced by regionalizing the study area based on elevation and climatic conditions, followed by spatial multi-criteria evaluation modelling using pan-European slope angle, shallow sub-surface lithology, and land cover spatial datasets as the main landslide conditioning factors. In addition, the location of over 149,000 landslides across Europe, provided by various national organizations, has been used for model calibration and map validation (Wilde et al., 2018).

3.2.2 Global risk data platform

The Global Risk Data Platform replaces the previous PREVIEW initiative launched in 1999 by UNEP/GRID-Geneva to share spatial data information on global risk from natural hazards. Currently, the collection of data is made via a wide range of partners. The Global Risk Data Platform has been developed as a support to the Global Assessment Report on Disaster Risk Reduction (GAR). Many improvements were made on the data and on the application. At present the Global Risk Data Platform allows to visualise, download or extract data on past hazardous events, human & economical hazard exposure and risk from natural hazards. It covers tropical cyclones and related storm surges, drought, earthquakes, biomass fires, floods, landslides, tsunamis and volcanic eruptions. In the following the indicators important for SAFEWAY project are briefly described.

Flooding

The Global risk data platform provides different maps and datasets regarding floods: events; physical exposure; economical exposure; risk. A catalogue of the past flood events in the period 1999-2007 is available in a shape file format. The observed floods are obtained from the Dartmouth Flood Observatory (DFO). The physical exposition dataset is provided in a GeoTIFF format and it estimates the expected average annual population (2007 as the year of reference) exposed (inhabitants) to flood. The economical exposition dataset provides an estimate of the annual economical exposition to flood in a GeoTIFF format. A Global Domestic Product grid for the year 2010, provided by the World Bank, has been used to realize this dataset. It describes the expected average annual GDP (2010 as the year of reference) exposed in US $. Finally, a global estimated risk index for flood hazard has been defined combining together the information of the other maps. The dataset is provided through a GeoTIFF format and it represents the risk index in 5 classes (from low, 1, to extreme, 5; Figure 5).

Fire events

The Global risk data platform provides two maps regarding fire events: events; density. The fire events dataset is a catalogue over the period November 1995 - March 2011. The data is presented in monthly global fire maps, in GeoTIFF, obtained by satellite images (Gregoire et al., 2001) from the European Space Agency (ESA-ESRIN) World Fires Atlas Program (ATSR). The fire density map includes an average of fires density over the period 1997-2010 (Figure 6). The variable described is the expected average number of event per 0.1 decimal degree pixel per year multiplied by 100 (e.g. 64 value means 0.64 events per year). The dataset is provided in a GeoTIFF format.

Figure 5: Estimated risk index induced by flood hazard. Unit is estimated risk index from 1 (low) to 4 (extreme). (Source: Global risk data platform)

Figure 6: An average of fires density over the period 1997-2010. (Source: Global risk data platform)

Earthquakes

The database on earthquakes includes several maps: catalogue of events; earthquakes modified Mercalli intensity; physical exposure; economical exposure. The earthquakes catalogue gathers events with magnitude higher than 5.0 as reported by the Advanced National Seismic System (ANSS) Catalogue over the period January 1970 - June 2015. The ANSS Composite Catalogue is a world-wide earthquake catalogue created by merging the master earthquake catalogues from contributing ANSS institutions and then removing duplicate solutions for the same event. The global estimate of the Modified Mercalli Intensity dataset is based on Global Seismic Hazard Assessment Program (GSHAP) dataset, converted to Modified Mercalli Intensity (MMI) using the methodology developed by Wald et al. (1999). The dataset on the annual physical exposition to earthquakes includes MMI categories higher than a given value (5,7,8,9) over the period 1973-2007. It is based on two data sources: 1) Modified Mercalli Intensity map available in the Shakemap Atlas from USGS (Figure 7); 2) A population grid for the year 2010, provided by LandScanTM Global Population Database. The map shows the average annual population (2010 as the year of reference) exposed (inhabitants). The economical exposure to earthquakes is like the previous one. The difference is that a Global Domestic Product grid for the year 2010, provided by the World Bank, has been used to carry-out the analysis. The variable described is the expected average annual GDP (2010 as the year of reference) exposed in US $ (year 2000 equivalent).

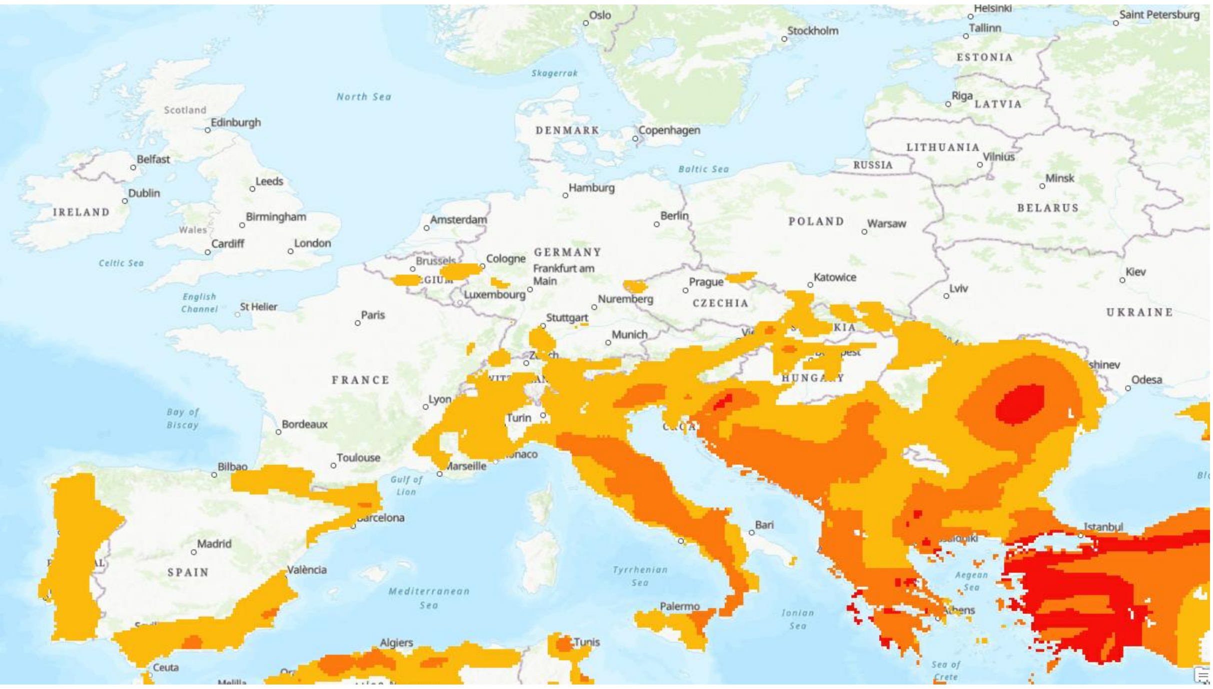

Figure 7: Global estimate of the Modified Mercalli Intensity. (Source: Global risk data platform)

3.2.3 Socioeconomic Data and Applications Center (SEDAC)

SEDAC is one of the Distributed Active Archive Centers (DAACs) in the Earth Observing System Data and Information System (EOSDIS) of NASA. SEDAC focuses on human interactions in the environment. Its mission is to develop and operate applications that support the integration of socioeconomic and earth science data and to serve as an "Information Gateway" between earth sciences and social sciences (http://sedac.ciesin.columbia.edu/about). The SEDAC provides maps and information on different natural hazards: floods, droughts, wildfires, landslides, earthquakes and multi-hazards.

Flooding

The SEDAC provides two maps concerning floods: the Global Flood Hazard Frequency and Distribution; and the Global Flood Proportional Economic Loss Risk. The maps are both structured as a 2.5-minute grid. The first represents the relative frequency of flood occurrence (Dilley et al., 2005). The greater the grid cell value in the final data set, the higher the frequency (figure 8). The map has been derived from a global catalogue of extreme flood events between 1985 and 2003 compiled by Dartmouth Flood Observatory. The second map (figure 9) depicts the flood proportional economic loss by weighting the value of the Gross Domestic Product (GDP) exposure to flood for each grid cell by a vulnerability coefficient (Sachs et al., 2001; Dilley et al., 2005).

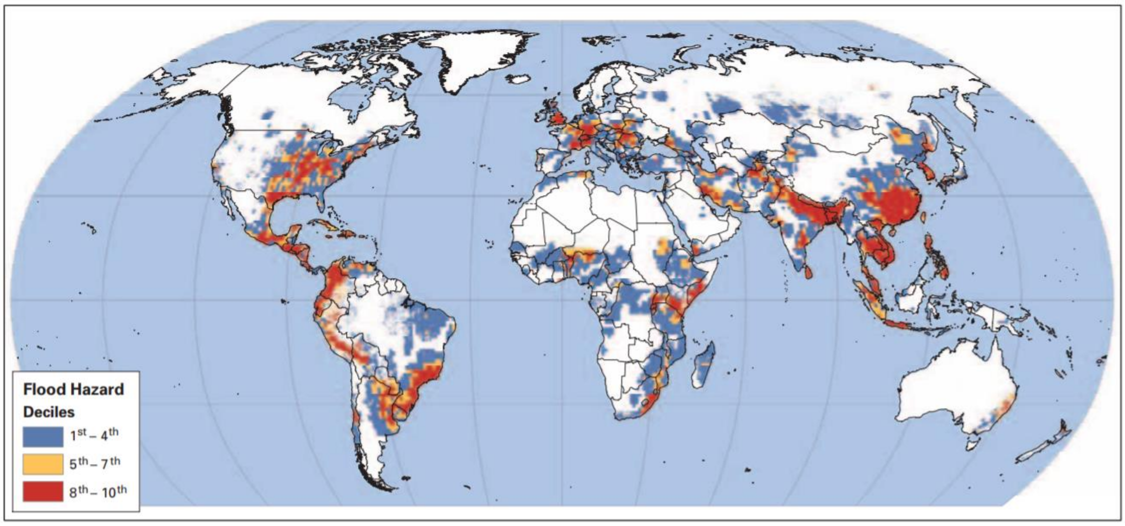

Figure 8: Distribution of flood hazard. (Source: Dilley et al., 2005)

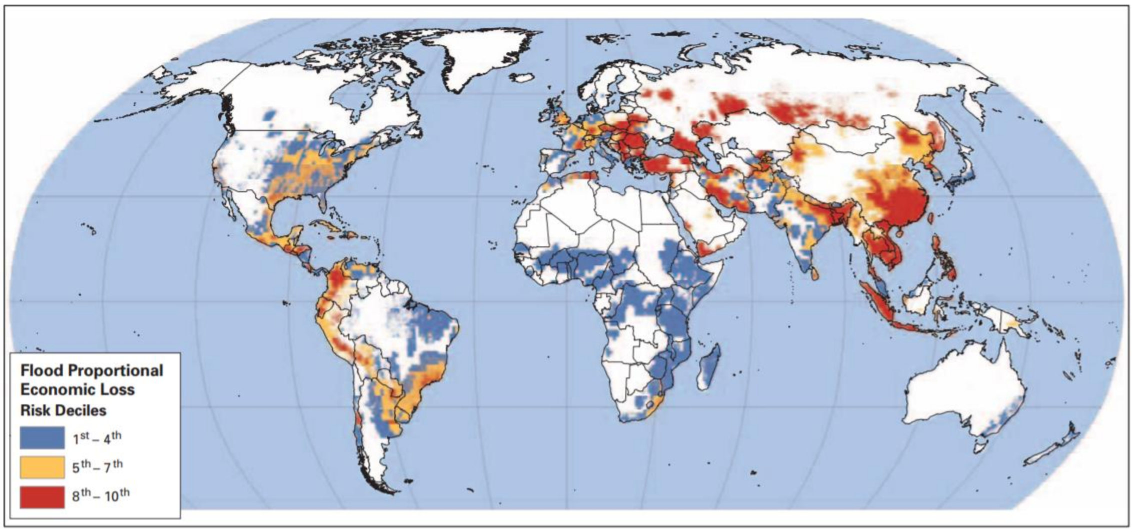

Figure 9: Economic loss due to flood as a function of the GDP density (Source: Dilley et al., 2005)

Earthquakes

The two maps available for assessing earthquake hazards have been generated considering two different data sets. The first based on the Global Seismic Hazard Program (GSHAP) data that incorporate expert opinion in predicting localities where there exists a 10 percent chance of exceeding a peak ground acceleration (pga) of 2 meters per second in a 50-year time span (Dilley et al., 2005). The latter dataset uses the Advanced National Seismic System (ANSS) Earthquake Catalogue data of actual earthquake events exceeding 4.5 on the Richter scale during the period 1976-2002.

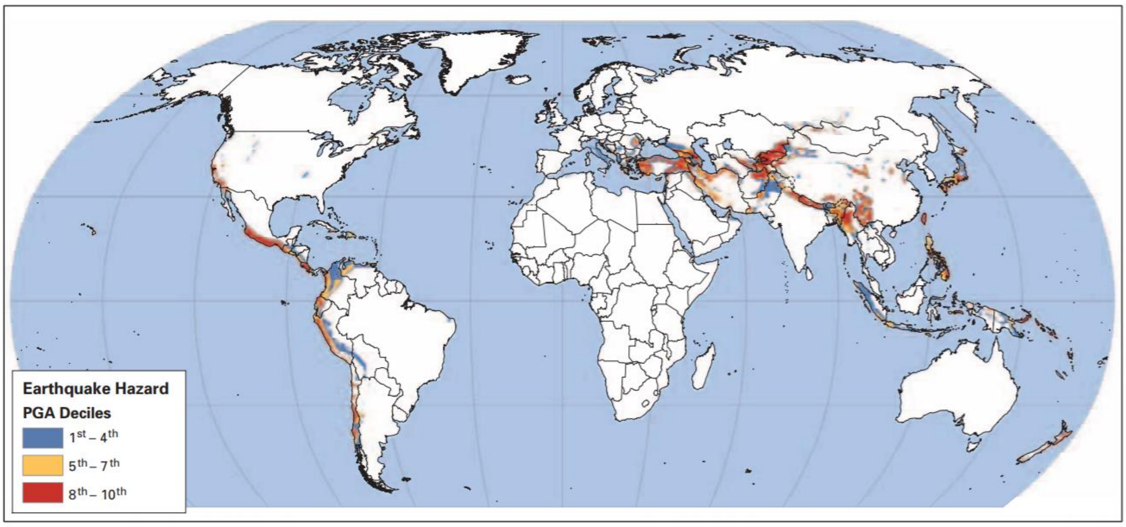

Figure 10: Global Earthquake Hazard Distribution - Peak Ground Acceleration (Source: Dilley et al., 2005)

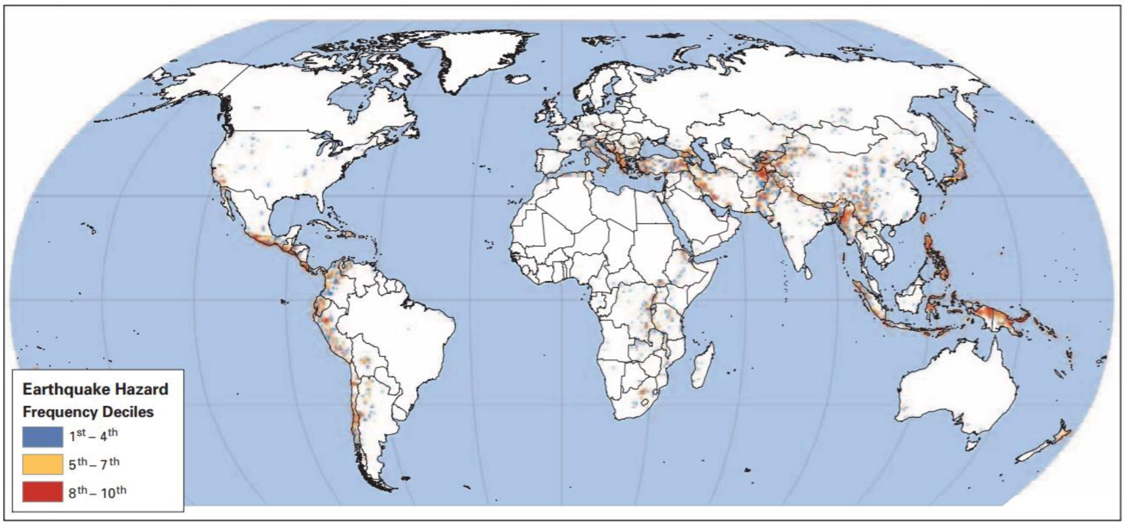

Figure 11: Global Earthquake Hazard Frequency and Distribution (Source: Dilley et al., 2005)

3.2.4 NASA Earth Observations (NEO)

NEO is part of the EOS Project Science Office located at NASA Goddard Space Flight Center. The mission is to collect information about Earth's ocean, atmosphere, and land surfaces through satellite images, in order to depict climate and environmental changes as they occur on the planet. The images in NEO are freely available for public use without further permission in both CSV (comma separated values) and floating point GEOTiff files. The database gathers information on different branches: atmosphere, energy, land, life, ocean; and are continuously updated.

Fire events

The Moderate Resolution Imaging Spectroradiometer (MODIS) Fire Product provides information on the location of a fire, its emitted energy, the flaming and smoldering ratio, and an estimate of area burned. The red, orange, and yellow pixels on these maps show the locations where the MODIS instrument detects actively burning fires (figure 12).

Indicators for extreme weather conditions

The NEO database provides several interesting indicators for describing the climate change. The global temperature anomaly, the land surface temperature anomaly and the land surface temperature, seem to be the most useful database for the purposes of SAFEWAY project. The global temperature anomaly analysis specifies the temperature anomaly at a given location as the weighted average of the anomalies for all stations located within 1,200 kilometres of that point, with the weight decreasing linearly with distance (figure 13). Shades of red and orange indicate areas where the average annual temperatures are warmer than they were in that area during the base period from 1951-1980. The dataset contains information for the period 01/1880-04/2019.

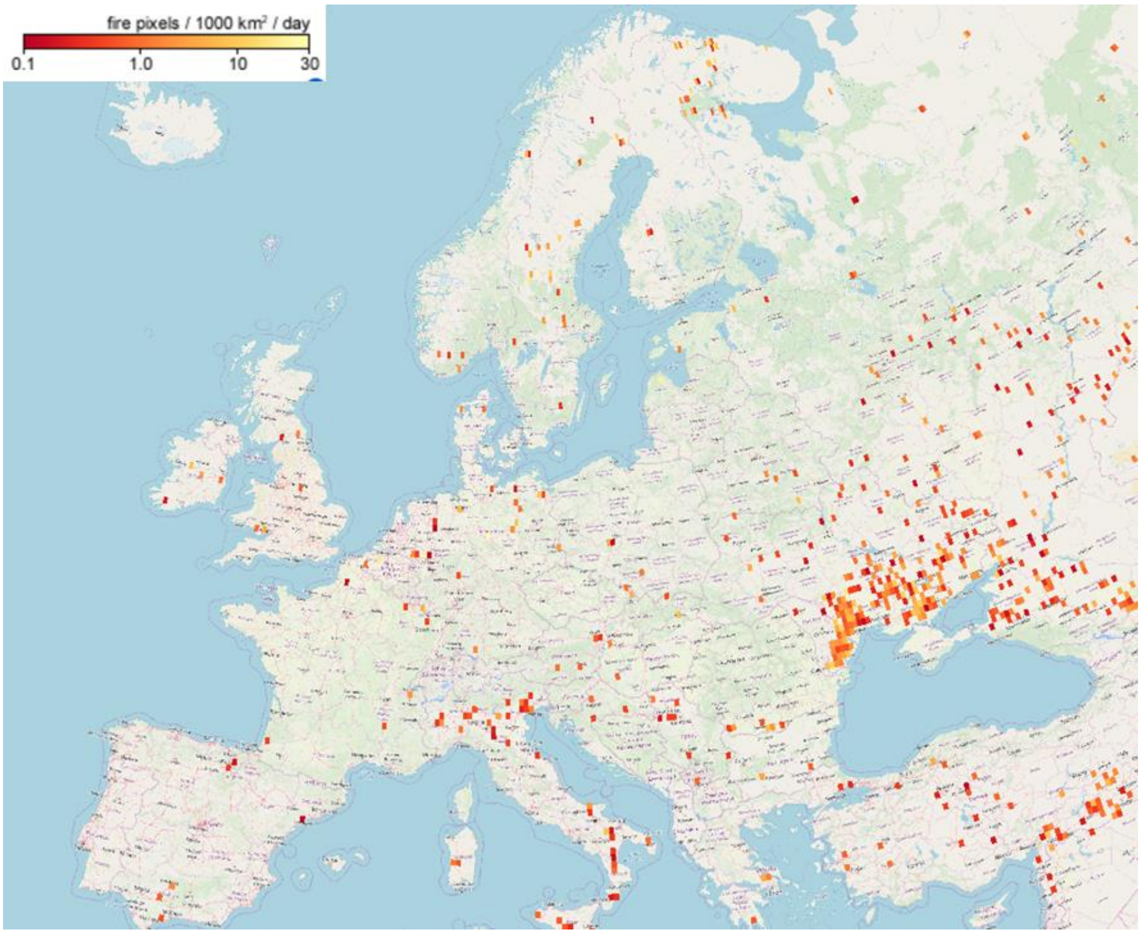

Figure 12: Locations where the MODIS instrument detects actively burning fires. The colours represent a count of the number of fires observed within a 1,000-square-kilometer area for July 2018. (Source: MODIS; https://modis.gsfc.nasa.gov/data/)

The land surface temperature anomaly and the land surface temperature are datasets representing temperature patterns of the top millimetre (or "skin"), for both day-and night-time, of the land surface — including bare land, snow or ice cover, urban areas, and cropland or forest canopy — as observed by MODIS in clear-sky conditions for the period 2000-2019. The land surface temperature anomaly dataset shows land surface temperature anomalies for a given day, week, or month compared to the average conditions during the period 24/02/2000-25/06/2019. Figure 14 compares the temperature patterns of the top millimetre (or "skin") of the land surface in Celsius degrees and the land surface temperature anomalies for July 2018.

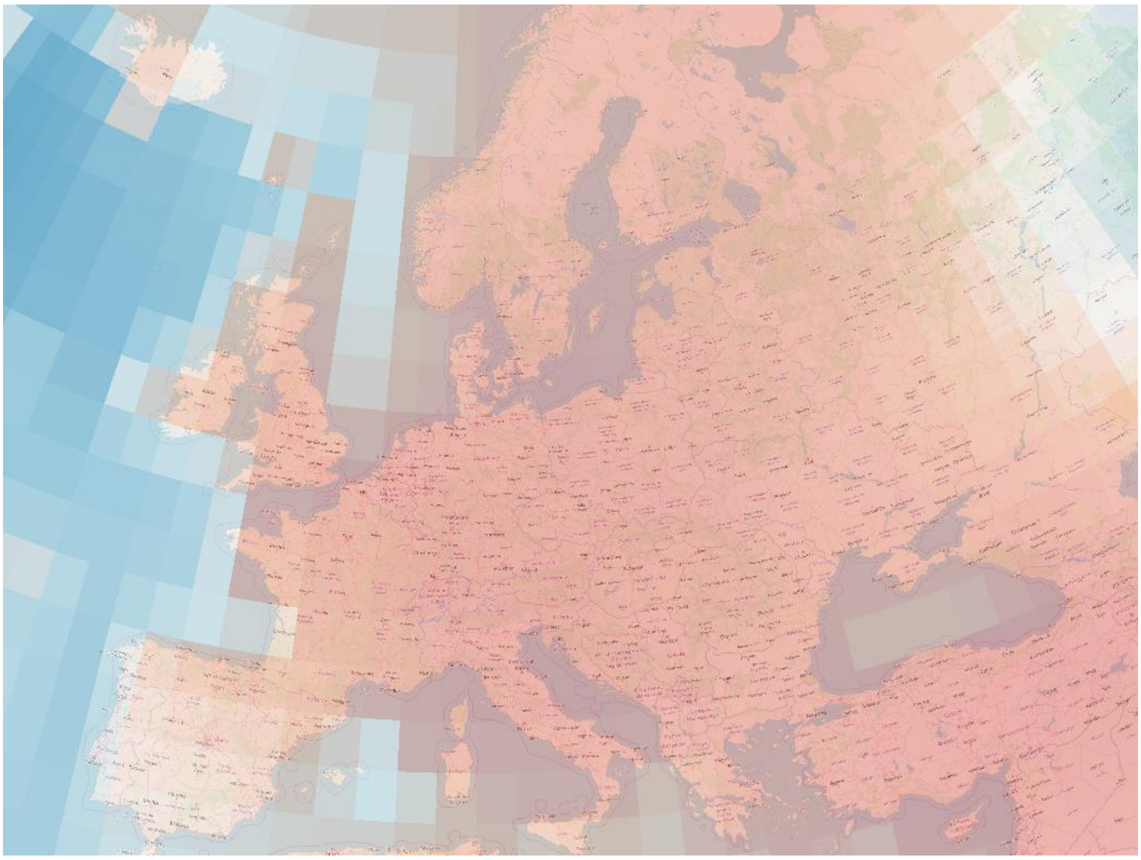

Figure 13: Global temperature anomaly in Europe for the year 2017. Shades of red and orange indicate areas where the average annual temperatures (in Celsius degree) are warmer than they were in that area during the base period from 1951-1980. (Source: NASA earth observations(NEO))

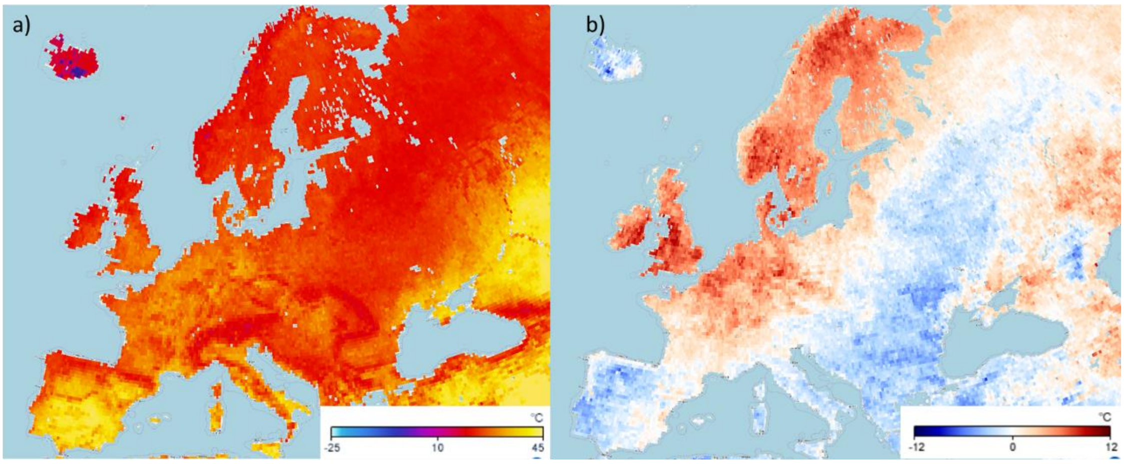

Figure 14: a) The temperature patterns of the top millimetre (or "skin") of the land surface in Celsius degrees for July 2018; b) Land surface temperature anomalies for July 2018 compared to the average conditions during that period between 2001-2010. (Source: NASA earth observations(NEO))

3.2.5 Global Assessment Report on disaster risk reduction (GAR)

The Global Assessment Report on Disaster Risk Reduction (GAR) is a biennial global assessment of disaster risk reduction and comprehensive review and analysis of the natural hazards that are affecting humanity. The GAR contributed to achieving the aims of the Hyogo Framework for Action through monitoring risk patterns and trends and progress in disaster risk reduction while providing strategic policy guidance to countries and the international community. The GAR is produced in collaboration and consultation with a wide range of stakeholders, including various UN agencies, governments, academic and research institutions, donors and technical organizations and specialists.

The GAR Atlas presents the output of a Global Risk Model (GRM) that can estimate the disaster risk associated with different kinds of hazard (earthquakes, tsunamis, flooding, cyclonic winds and storm surge) faced by national economies throughout the world. This model has been developed by a consortium of leading scientific and technical organisations, under the coordination of UNISDR. The main purpose of the GAR Atlas is to broadly identify high risk areas at global level and identifying areas where more detailed data should be collected and where detailed risk assessments are to be performed.

Flood hazard

The GAR Atlas global flood hazard assessment uses a probabilistic approach for modelling riverine flood major river basins around the globe. This has been possible after compiling a global database of stream-flow data, merging different sources and gathering more than 8000 stations over the globe in order to calculate the range of possible discharges from very low to the maximum possible scales at different locations along the rivers. The calculated discharges were introduced in the river sections to model water levels downstream. This procedure allowed for the determination of stochastic event-sets of riverine floods from which hazard maps for several return periods (25, 50, 100, 200, 500, 1000 years) were obtained. The hazard maps are developed at 1kmx1km resolution and have been validated against satellite flood footprints from different sources (DFO archive, UNOSAT flood portal) performing well especially for big events. For smaller events (lower return periods), the GAR Atlas flood hazard maps tend to overestimate with respect to similar maps produced locally (hazard maps where available for some countries and were used as benchmark). The main issue being that, due to the resolution, the GAR Atlas flood hazard maps do not take into account flood defenses that are normally present to preserve the value exposed to floods. More information about the flood hazard assessment can be found in the background paper (Rudari et al., 2015).

Earthquakes and seismic hazard

For the GAR Atlas, a fully probabilistic seismic hazard analysis at global level was developed by CIMNE and INGENIAR Ltda. This hazard model is a continuation and improvement of the one developed in the framework of GAR13 where a set of tectonic provinces were identified and characterized by means of a set of parameters that describe the future seismic activity on each of them based on historical records together with relationships to obtain hazard intensities as a function of magnitude and distance. The hazard analysis was performed using the program CRISIS2014, a state-of-the-art tool for these kinds of tasks and widely known and acknowledged by experts in the field across the world. More details about the probabilistic seismic hazard analysis can be found in Cardona et al. (2015). The chosen variables for hazard intensity measure were the spectral acceleration (respectively of 0,2; 0,5; 1 seconds) and the peak ground acceleration. Hazard maps considering different return periods for both variables have been considered (see figure 15).

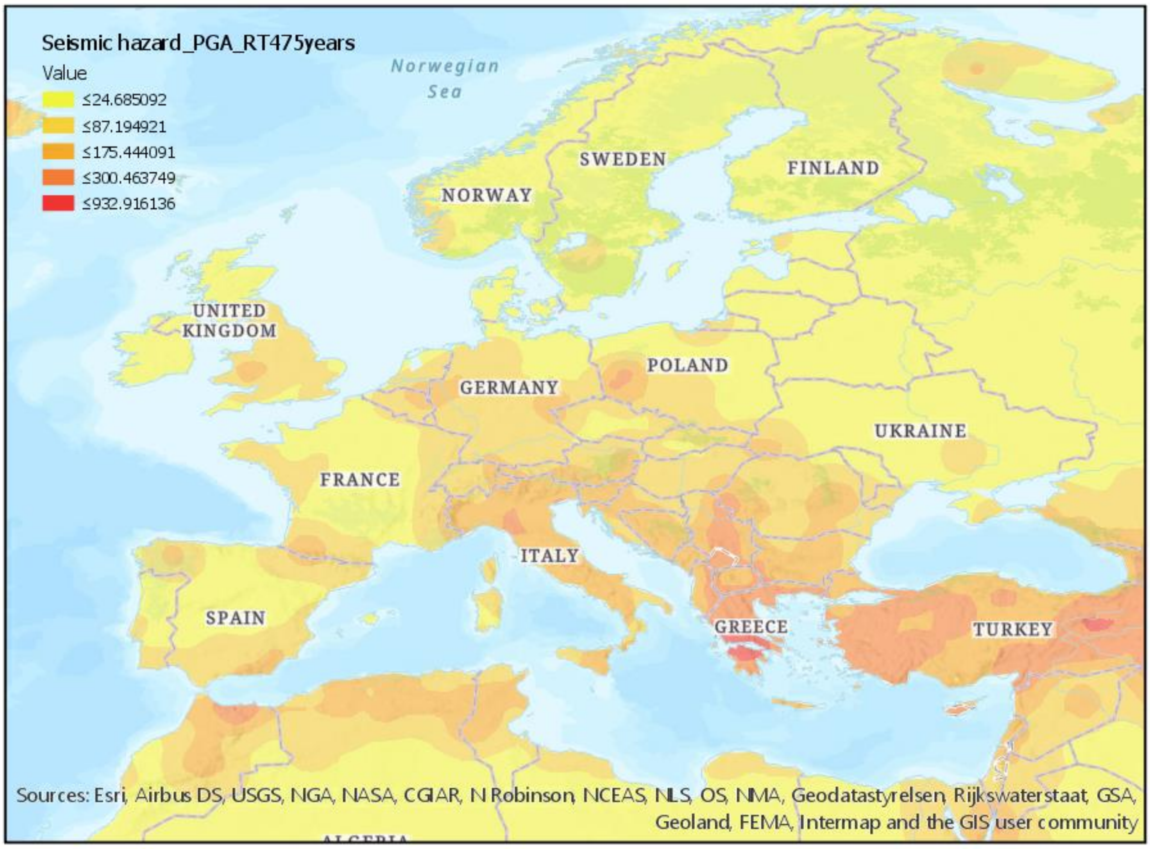

Figure 15: Seismic hazard considering the peak ground acceleration for 475 years return period. (Source: GAR Atlas database)

3.2.6 European Climate Assessment & Dataset project (ECA&D)

The European Climate Assessment & Dataset project (ECA&D) was initiated in 1998 and has received financial support from EUMETNET and the European commission. Between 2003 and 2008 the project has been partially funded by European Meteorological Network (EUMETNET). From 2009 onwards, the Royal Netherlands Meteorological Institute (KNMI) has committed itself to fund ECA&D. ECA&D has now obtained the status of Regional Climate Centre (RCC) for high resolution observation data in WMO Region VI (Europe and the Middle East). Currently, there are 69 National Meteorological and Hydrological Services, observatories and universities from Europe and the Mediterranean sharing long-term daily resolution climatic time series from meteorological stations. The objective of ECA&D is to analyse, aggregate and validate the meteorological data collected by the stations in the WMO region VI. For each station 72 indices are calculated monthly, describing changes in the mean or extremes of climate. The indices are grouped in different categories describing weather characteristics: cloudiness, cold, compound, drought, heat, humidity, pressure, rain, snow, sunshine, temperature. The full dataset covers the period 1950-2018. It has originally been developed and updated as parts of the ENSEMBLES (EU-FP6) and EURO4M (EU-FP7) projects. Currently it is maintained and elaborated as part of the UERRA project (EU-FP7).

3.2.7 *Extreme weather event hazard maps from the INTACT project*

Simple extremes are characterized by the occurrence of an extreme value for a single variable (such as temperature), whereas complex extremes involve a critical combination of variables associated with a weather or climate phenomenon, such as a cyclone (rainfall and wind) or drought and many others. The INTACT project was focusing specifically on four types of extreme weather:

- Temperature extreme
- Precipitation extreme (also including snowfall)
- Wind extreme
- Complex extreme (including 2 different parameters among temperature, precipitation and wind)
  - Combined temperature and precipitation extreme
  - Combined temperature and humidity extreme

Most of the indices considered in INTACT have been defined following the recommendations of the CCl/CLIVAR/JCOMM Expert Team on Climate Change Detection and Indices (ETCCDI)

Extreme indicators based on temperature

Different climate indices are available to address the different aspects (frequency, amplitude and persistence) of the extreme temperature events. The INTACT project considers only some of them. In particular, there are indices calculating the number of days exceeding a specific threshold, which can be a fixed value or based on the percentile of the different (minimum, maximum or mean) temperature distribution (percentile-based indices could be more useful to express anomalies relative to local climate). Other indices evaluate the number of consecutive days in which a specific threshold is exceeded (or not), while others evaluate the absolute extreme value reached. Usually, temperature indices include indices to classify both high and low temperature extreme events. At the same time, depending on the features of the extreme event to be classified, the distribution of the mean, maximum or minimum daily temperature is considered.

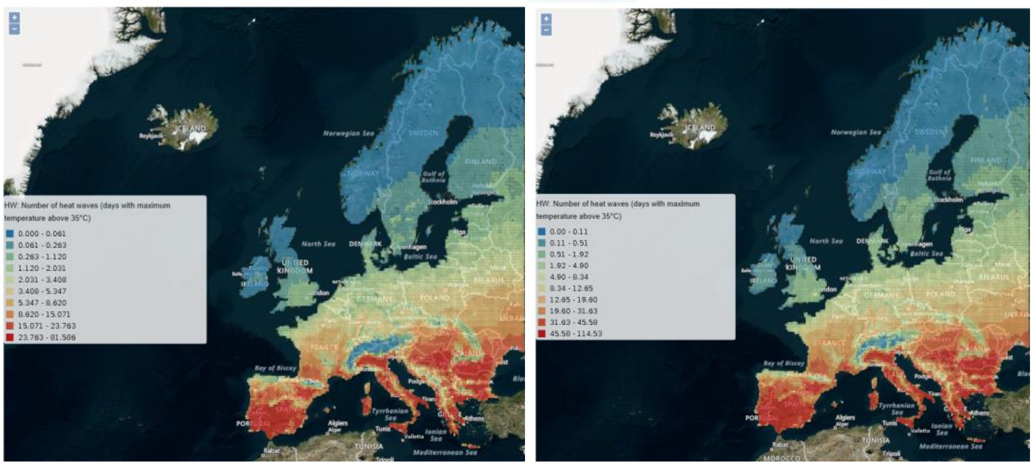

Figure 16: Predictions of number of heatwaves(days with a maximum temperature above 35°C) per year for time periods 2011 - 2041 (left) and 2071-2100(right). (Source: INTACT-Wiki; http://scm.ulster.ac.uk/~scmresearch/intactnew/index.php/Extreme_weather_maps)

Extreme indicators based on precipitation

Concerning precipitation EWI, they are quite similar to the temperature ones, including frequency, amplitude and persistence of extreme precipitation events. Precipitation extreme indicators can characterize events with high precipitation, but also extremely dry conditions. Most indicators are based on the number of days or consecutive days overcoming a fixed daily precipitation threshold, while others are derived from the number of days exceeding (high precipitation events) or not (low precipitation events) a specific percentile of daily precipitation distribution. There are also others concerning the absolute extreme value of cumulated precipitation on a selected time span (1 day, 2 days or 5 days, typically).

Extreme indicators based on snow

Regarding snow, five different indices have been selected: the first based on the frequency of the snow days (snow precipitation higher than 1 mm); the second and the third are related to the frequency of days exceeding an assigned threshold for the snowfall. The fourth is related to the amount of maximum yearly snowfall. The last index provides information about the contribution of the four seasons to the yearly snowfall.

Extreme indicators based on wind

Two basic typologies of indicators have been selected to characterize extreme wind events: indices based on the frequency of daily wind intensity (considering different threshold values); indices based on the maximum daily value reached by the mean wind intensity and by gusts. Gusts are sudden, rapid and brief changes in the wind speed. Wind extreme values have a significant importance for engineering application. Unfortunately, due to the difficulty to obtain homogeneous high-frequency wind data, these indices have been barely considered in literature.

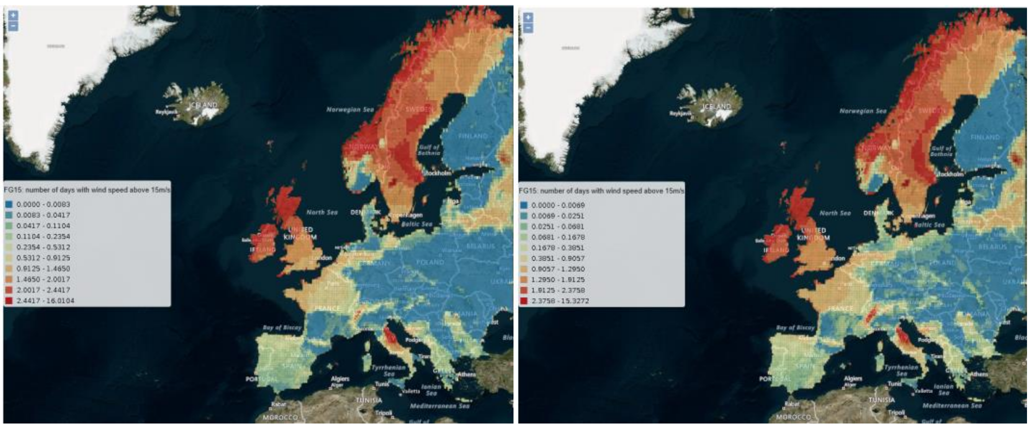

Figure 17: Number of days with wind speed above 15m/s per year for time periods 2011 - 2041 (left) and 2071-2100(right). (Source: INTACT-Wiki; http://scm.ulster.ac.uk/~scmresearch/intactnew/index.php/Extreme_weather_maps)

3.2.8 Other datasets

For the Multimedia Assessment of Pollutant Pathways in the Environment (MAPPE) project several datasets were developed. A set of 12 maps of monthly mean wind speed is available. The maps describe the average wind per month for the period 01/01/2002-31/12/2006.

The SAFELAND project ("Living with landslide risk in Europe: Assessment, effects of global change, and risk management strategies") proposes hotspots of landslide, hazard and risk maps identified by three GIS based analysis that cover all of Europe with the same approach and locally validated with available landslide inventories.

The SHARE European Earthquake Catalogue, compiled in the frame of the SHARE project 2006 by GFZ Potsdam, is an earthquake catalogue for the period 1900-2016.

Another earthquake catalogue is compiled by the International Seismological Centre for the period 1904-2018.

The Global Wind Atlas is a web-based application developed to facilitate online queries and provide freely downloadable datasets. Users can download, in a .pdf file, high-resolution maps showing global, regional, and country wind resource potential. Information on the datasets and methodology used to create the Global Wind Atlas can be found in the Methodology (https://globalwindatlas.info/about/method) and Datasets (https://globalwindatlas.info/about/dataset) sections.

E-OBS is a database on daily gridded observational dataset for precipitation, temperature and sea level pressure in Europe. ECA&D staff maintains and updates the E-OBS gridded dataset (http://c3surf.knmi.nl/dataaccess/access_eobs.php). The data provided are: daily mean temperature, daily minimum temperature, daily maximum temperature, daily precipitation sum and daily averaged sea level pressure.

3.3 European maps of weather related hazards in current and future climate

Climate change is increasingly affecting Europe. Most impacts of climate change have been adverse, although some might be beneficial. Increases in sea and land temperatures vary between southern and northern regions, being more harmful in southern than in norther areas. Changes in precipitation pattern make wet regions of Europe wetter, particularly in winter, and dry regions drier particularly in summer. Yet, rises in sea level, more frequent high winds, and storm surges can be directly dangerous for natural and built environments and human health.

Projections of climate change are supported by changes in European ground temperatures, precipitation levels, occurrences of windstorms, and rise in sea levels in northern regions. Rationale for review of the above meteo-and-climatic parameters rests on the fact that their variability has short, medium and long-term implications for functionality, serviceability and safety of overland transport (road and rail) infrastructures.

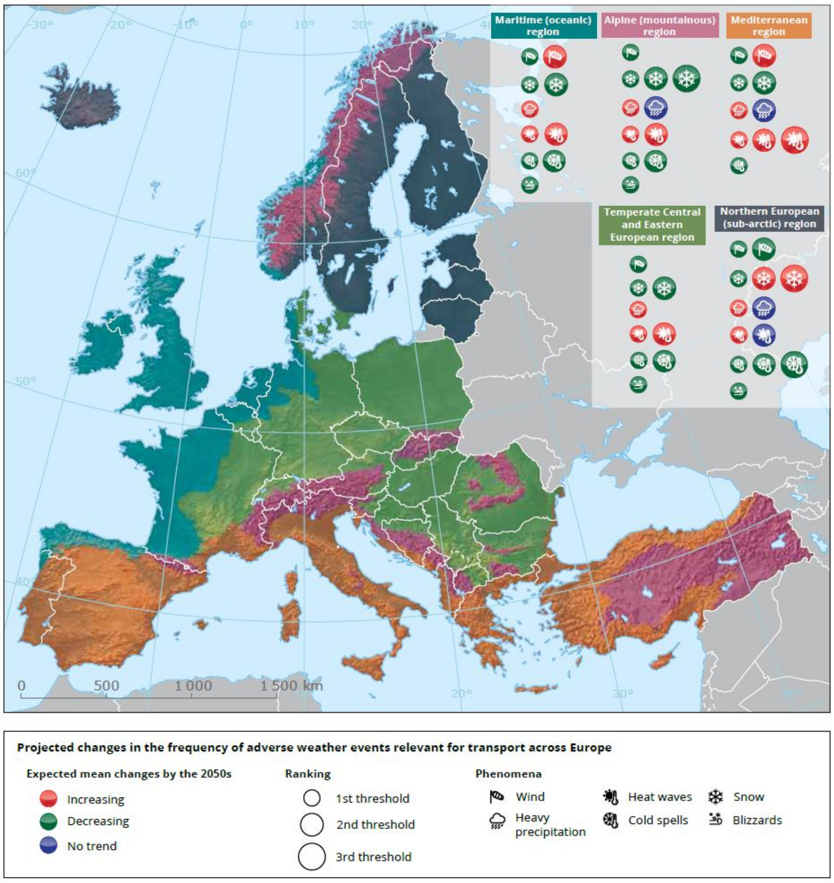

Figure 18: Projected changes in the frequency of adverse weather events relevant for transport across Europe. (Source: EEA (2017); adapted from Leviäkangas and Saarikivi (2012))

3.3.1 European Temperatures

Temperatures across Europe are expected to continue increasing throughout the 21st century. Projections from the EURO-CORDEX initiative suggest that European land will warm faster than global land areas (Jacob et al., 2014). According to the mean from multi-modal ensemble runs, European land areas are projected to warm in the range of 1 to 4.5°C for the RCP4.5 scenario and in the range of 2.5 to 5.5°C for RCP8.5 over the 21-century (2017-2100 as compared to 1971-2000). The strongest warming is projected in north-eastern Europe and Scandinavia during winter and in southern Europe during summer (EEA, 2017).

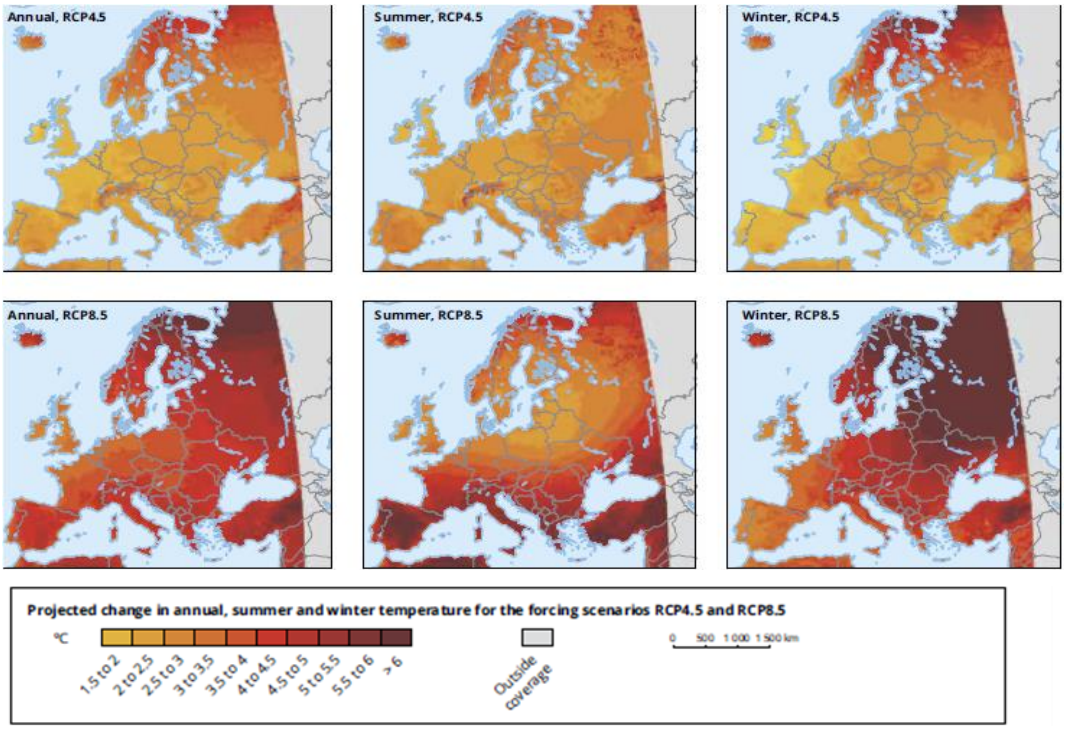

Figure 19: Projected Changes in Mean Annual Summer and Winter Temperature under Two Radiative Forcing Scenarios RCP4.5 and RCP8.5[2]. (Source: EEA; 2017)

Periods with extreme high temperature are projected to become more frequent and to last longer across Europe during the 21-century (Fischer and Schär, 2010; Russo et al., 2014; Schoetter et al., 2014). Projections based on multi-model ensemble agree on increases in heat wave frequency and magnitude for most European regions during the 21-century under RCP scenarios[3]. Extreme summer heat waves, such as the ones experienced in different parts of Europe in 2003 and 2010, will become much more common in the future. Under the RCP8.5 scenario, very extreme heat waves[4] are projected to occur as often as every two years in the second half of 21-century (see maps in the following). The projected frequency of heat waves is greatest in southern and south-eastern Europe (Russo et al., 2014). According to a different analysis, at the end of the 21-century, 90% of summers in southern, central and north-eastern Europe will be warmer than any summer in the period 1920-2014 under RCP8.5 scenario (Lehner et al., 2016). The most severe risks are projected for low altitude river basins in southern Europe, and for the Mediterranean coasts where many densely populated urban centres are located (Fischer and Schär, 2010).

[2] *Note: This map shows mean annual (left) summer and winter (right) near surface temperature (°C) over the period 2017-2100 compared with the baseline period 1971-2000 for the radiative forcing scenarios RCP4.5 (top) and RCP8.5 (bottom). Model simulations are based on the multi-model ensemble average of many different combined GCM-RCM simulations from the EURO-CORDEX initiative.*

[3] *The RCP (Representative Concentration Pathway) scenarios are projecting the radiative forcing which is determined not only by direct anthropogenic greenhouse emissions, but also by the future development of the global carbon cycle and other processes. Moreover, the process of RCP development has been separated from the socio-economic storyline development, which means that the different RCPs are not directly associated with a specific socio-economic scenario (EEA, 2017 p.38).*

[4] *To assess changes in heat waves, HWMI (Heat Wave Magnitude Index) has been used. The HWMI is defined based on the magnitude and length of heat waves in a year where the heat waves are periods of three consecutive days with a maximum temperature above the threshold of the reference period 1981-2010 (EEA, 2017, p.77).*

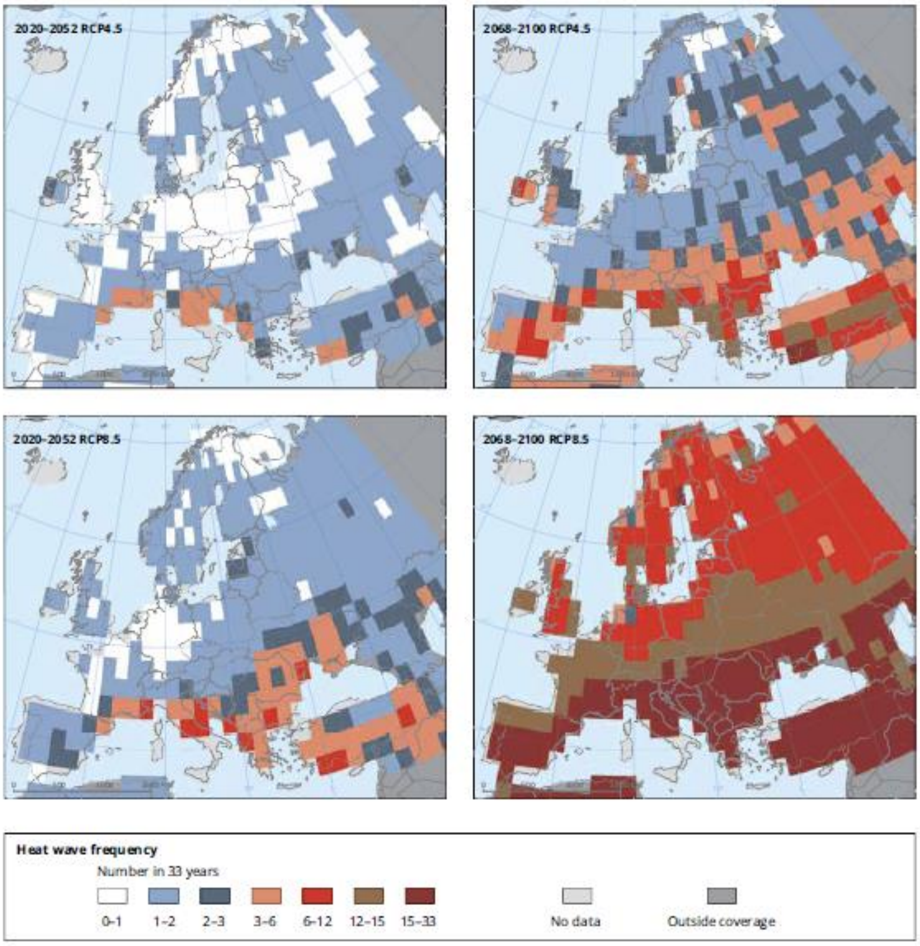

Figure 20: Number of Very Extreme Heat Waves in Europe's Future Climates under Two Different Emissions Scenarios[5]. (Source: Adopted from Russo et al., 2014 and reproduced from EEA, 2017 p.79)

3.3.2 Mean Precipitation

For a high emissions scenario, RCP8.5, the models (ensemble mean) do project a statistically significant increase in annual precipitation in large parts of central and northern Europe (up to about 30%), and a decrease in southern Europe (of up to 40%) from 1971-2000 to 2071-2100 (see maps in the following). In summer, though, the precipitation decrease extends northwards (Jacob et al., 2014). A zone with small changes that are not significant (but are however, partially robust in the direction of change), shows where the precipitation pattern (as presented in the ensemble mean) varies. For a medium emission scenario (RCP4.5) the magnitude of change is smaller, but the pattern is very similar to the pattern for the RCP8.5 scenario. The range of projected changes in precipitation from the

[5] *Note: Very extreme heat waves are defined as having HWMI (Heat Wave Magnitude Index) above 8. For comparison, the 2003 western European heat wave had an average of around 3, and the 2010 western European heat wave had an average HWMI of around 5. The upper maps show the median number of very extreme heat wave that derives from a multi-modal ensemble of GCMs of the near future (2020-2052) and later half of the century (2068-2100) under RCP4.5 scenario. The lower maps reflect the same time-period projections but under RPC8.5 scenario.*

multi-model ensemble are generally the same between RCP4.5 and RCP8.5, or larger in RCP8.5, especially at the end of 21-century (Jacob et al., 2014)[6] .

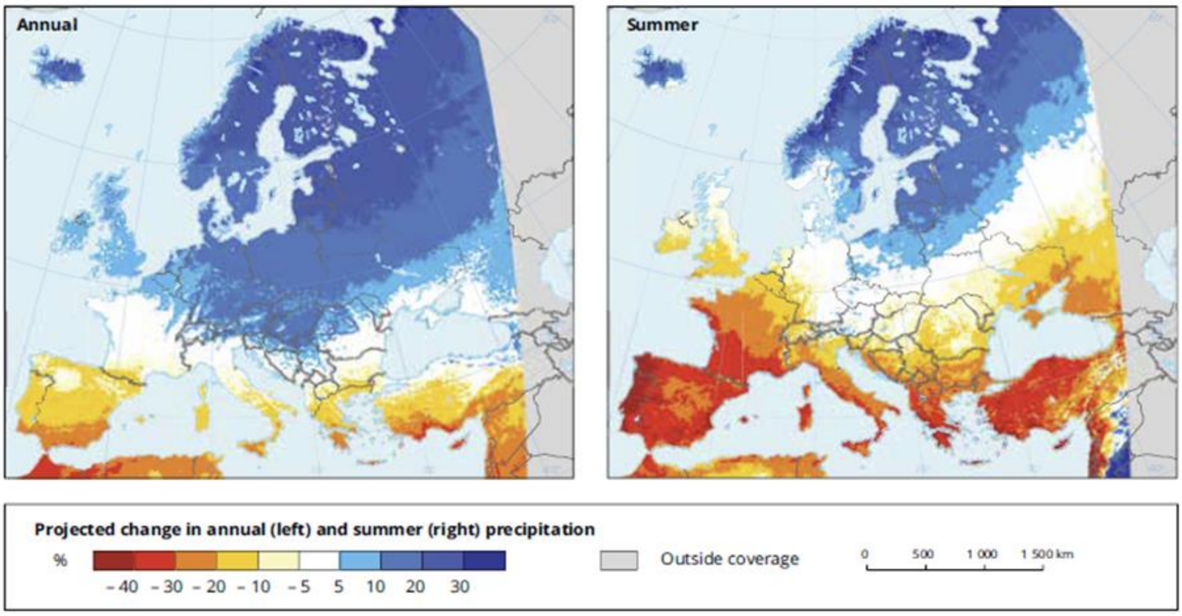

Figure 21: Projected Change in Annual and Summer Precipitation in Europe (EEA; 2017)[7]. (Source: EURO-CORDEX (Jacob et al., 2014), and reproduced from EEA, 2017, p.81)

3.3.3 Heavy Precipitation

Global warming is projected to lead to higher intensity of precipitation and longer dry periods in Europe (IPCC, 2012; Hov et al., 2013). Projections show an increase in heavy daily precipitation in most parts of Europe in winter, by up to 35% during the 21st century. Heavy precipitation in winter is projected to increase over most of Europe with increases up to 30% in north-eastern Europe (see left map below). In summer, an increase is also projected in most parts of Europe, but decreases are projected for some regions in southern and south-western Europe (see Figure 22b) (Jacob et al., 2014). Similar pattern was found for other heavy precipitation indices (Rajczak et al., 2013, Sillmann et al, 2013: Giorgi, Coppola and Raffaele, 2014).

---

[6] *Despite that daily precipitation records have been systematically collected since 1950s, still acclimate change signal cannot be detected with certainty in all European regions owing to the high spatial and temporal variability in precipitation. Difficulties in detecting trends can also arise from the small sampling area of rain gauges, calibration errors in instrumentation and erroneous measurement during snow and gales (e.g. Hofstra et al.., 2009 quoted in EEA, 2017 p.81.*

[7] *Note: The maps show projected changes in annual (left) and summer (right) precipitation (%) in the period 2071-2100 compared with the baseline period 1971-2000 for the radiative forcing scenario RCP8.5. Model simulations are based on a multi-model ensemble average of many different RCM simulations from the EURO-CORDEX initiative.*

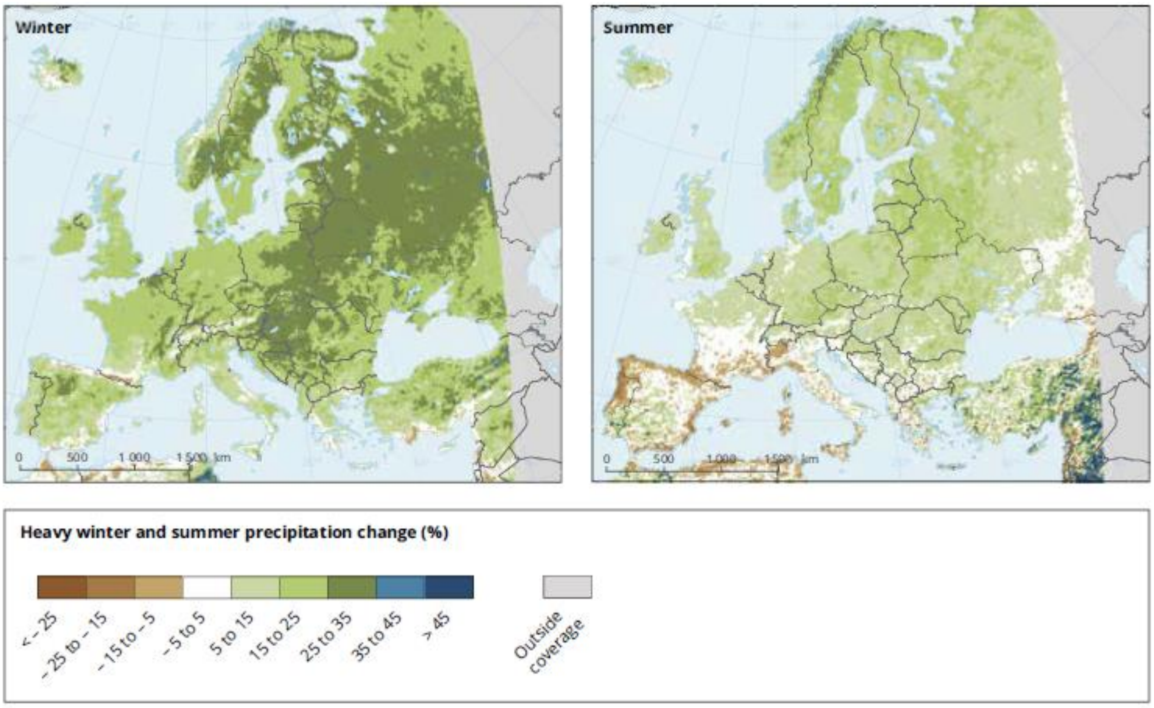

Figure 22: Projected Changes in Heavy Precipitation in Winter and Summer in Europe[8]. (Source. EURO-CORDEX (Jacob et al., 2014) and reproduced from EEA, 2017, p.84)

3.3.4 Wind Storms

Modelling studies show diverging results on changes in number of storms across Europe, but they generally agree on increases in the strongest, most damaging storms in most European regions. A study using a multi-model ensemble runs projects a small increase in the wind speed of the strongest winter storms over northern parts of central and western Europe, and a decrease in southern Europe (see map below) (Donat, Leckenusch et.al., 2011).

A comprehensive review study covering the North Atlantic and the northern, north-western and central Europe shows large agreement that the intensity of winter storms will increase in all these regions over the 21-century (Feser et al., 2014). Another recent study focusing on central Europe concluded that models consistently projected an increased frequency and intensity of severe storms over central Europe. Under SRES A1B conditions[9] , increases in frequency towards the end of the 21-century range between -11% and + 44% with an ensemble average of 21% (Pardowitz, 2015). The intensity of storms affecting central Europe once a year was found to increase by about +30%, with individual models projecting changes between -28% and up to +96%. These results are largely consistent with those of a recent study based on the GCM projections underlying the IPPC AR5 (Zappa et al., 2013). One recent study with a single, very high resolution (~25km) GCM indicates that the frequency and intensity in Europe of severe autumn storms

[8] Note: The map shows projected changes in heavy daily precipitation (%) in winter and summer for 2071-2100 compared with the baseline periods 1971-2000 for the RCP8.5 scenario based on the ensemble mean of different RCMs nested in different GCMs.

[9] The range of SRES (The Special Report on Emissions Scenarios) scenarios (from E1-low, A1B -medium to A1F1 – very high) provide a trajectory of anthropogenic greenhouse emissions coupled with the underlying storyline of socio-economic development. (EEA, 2017, p.38)

originating in the tropical Atlantic will increase in a warmer future climate as will the area affected (Baatsen et al., 2015). However, this result cannot be considered robust, as it has not been yet confirmed by other studies.

In summary, the risk of severe winter storms, and possibility of severe autumn storms is projected to increase in many regions in Europe, particularly in the Northern Atlantic and northern, north western and central Europe.

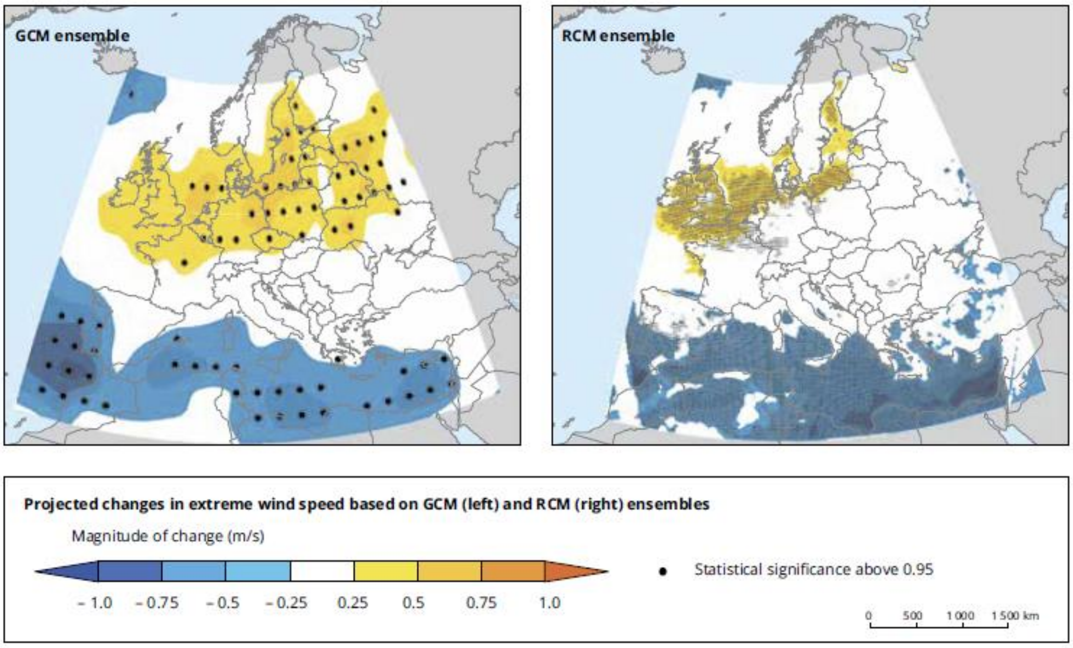

Figure 23: Projected Changes in Extreme Wind Speed Based on GCM and RCM Ensembles for 2071-2011 (EEA; 2017)[10]. (Source: Adopted from Donat, Leckebusch et al.,2011 and reproduced from EEA, 2017. p.87)

3.3.5 Flooding

Figure 24 shows the change in the level of one-in-a-century (Q100) floods between the reference period and three future time periods based on the hydrological model LISFLOOD and an ensemble of seven climate models (Alfieri, Burek et al., 2015). Blue rivers indicate an increase in flood level and red rivers indicate a decrease. For the end of the 21st century, the greatest increase in Q100 floods is projected for the British Isles, north-west and south-east France, northern Italy and some regions in south-east Spain, the Balkans and the Carpathians. Mild increases are projected for central Europe, the upper section of the Danube and its main tributaries. In contrast, decreases in Q100 floods are projected in large parts of north-eastern Europe owing to a reduction in snow accumulation, and hence melt-associated floods, under milder winter temperatures.

[10] Note: The above map shows the ensemble mean of changes in extreme wind speed (defined as the 98-the percentile of daily maximum wind speed) for AIB scenario (2071-2100) relative to 1961-2000. Left: based on nine GCMs. Right: based on 11 RCMs. Coloured areas indicate the magnitude of change (unit: m/s) and statistical significance at the 5% level is shown in black dots.

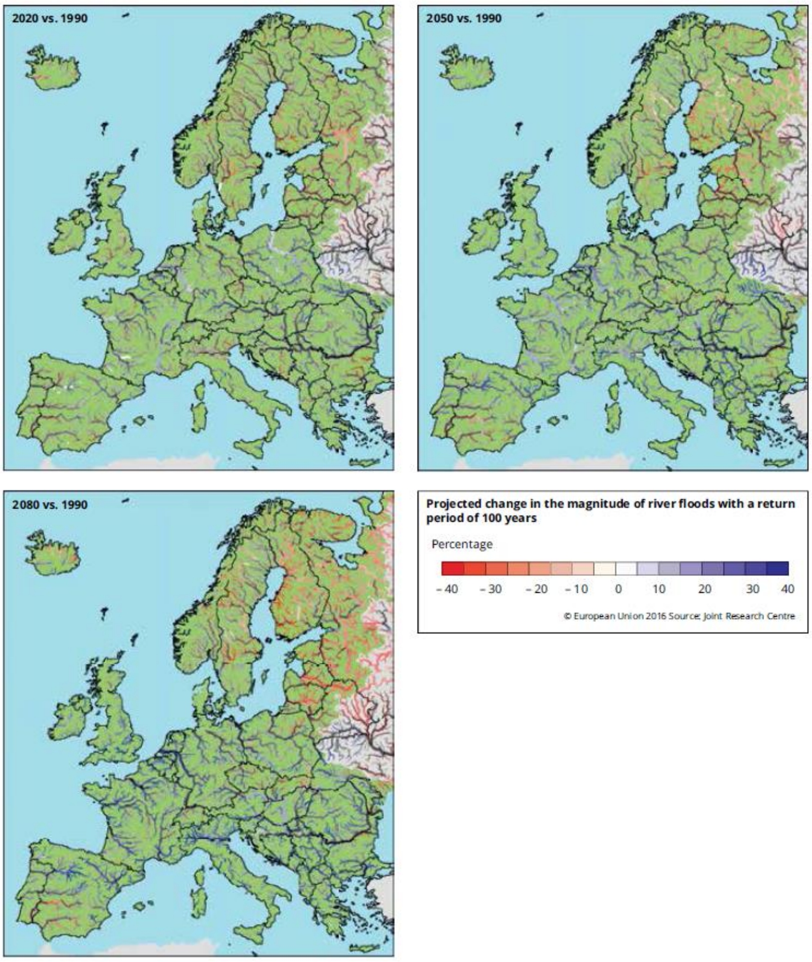

Figure 24: Projected change in river floods with a return period of 100 years (EEA; 2017)[11].
(Source: Adapted from Alfieri, Burek et al., 2015)

3.3.6 Forest fires

Climate change projections suggest substantial warming and increases in the number of droughts, heat waves and dry spells across most of the Mediterranean area and more generally in southern Europe (EEA; 2017). These projected changes would increase the length and severity of the fire season, the area at risk and the probability of large fires, possibly enhancing desertification (Moreno, 2014).

Figure 25 also includes fire danger projections for projected climate conditions in 2071–2100 (upper right map: projected state; lower right map: projected change). The results suggest that climate change would lead to a marked increase of fire potential in south-eastern and south-western Europe; in relative terms, the increase in SSR would be particularly strong in western-central Europe (Khabarov et al., 2014). Similar results were obtained for other forest fire indices, such as the FWI (Bedia et al., 2013).

---

[11] Note: This map shows the projected change in the level of one-in-a-century river floods (Q100). The relative changes for the time slices 2006–2035 (2020), 2036–2065 (2050) and 2066–2095 (2080) are compared with the ensemble mean of the baseline (1976–2005), based on an ensemble of seven EURO-CORDEX simulations forced by the RCP8.5 scenario and the LISFLOOD hydrological model. The consistency of the model projections is evaluated through the use of the coefficient of variation (CV) of the relative change. Smaller CVs indicate better model agreement of the projected mean change. Data points with CV > 1 are greyed out.

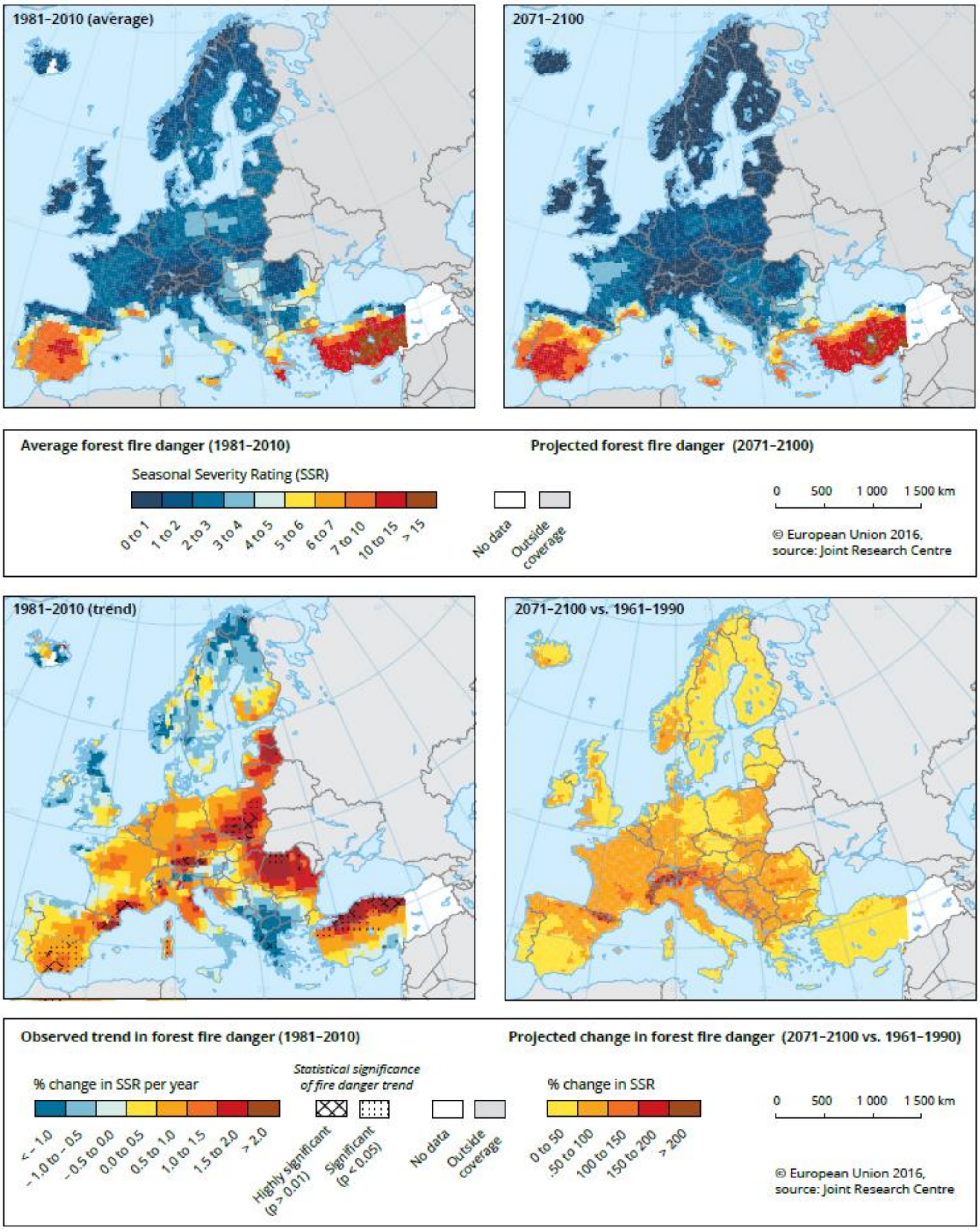

Figure 25: Current state, past trend and projections for forest fire danger (EEA; 2017)[12]. (Source: Camia, 2012 (personal communication), based on Camia et al., 2008)

3.4 European dynamic hazard maps used for monitoring and forecasting

This section gives a short overview of sources for dynamic hazard maps and forecasting products. The use of such products could be included into the contingency plans of the infrastructure owners, especially to support decisions

[12] *Note: Fire danger is expressed using the SSR. Daily severity values can be averaged over the fire season using the SSR index, which allows for objective comparison of fire danger from year to year and from region to region. The coarse scale of the map does not allow specific conditions of given sites to be accounted for, as, for example, in the Alpine region, where the complex topography may strongly affect local fire danger.*

regarding when to increase the preparedness and if possible to perform preventive actions.

3.4.1 ANYWHERE

ANYWHERE (EnhANcing emergencY management and response to extreme WeatHER and climate Events) is a program funded within EU's Horizon 2020 research and innovation programme, ongoing until August 31, 2019. The principal objective is to enable society as a whole and the main civil protection agencies to respond more rapidly than today to extreme climate and weather events, and to better cope with the high social, environmental and economic impacts related to these extremes.

The project aims to establish a pan-European platform on extreme climate risks, where identification of and early warning systems should improve protection measures as well as ameliorate the coordination of rescue operations.

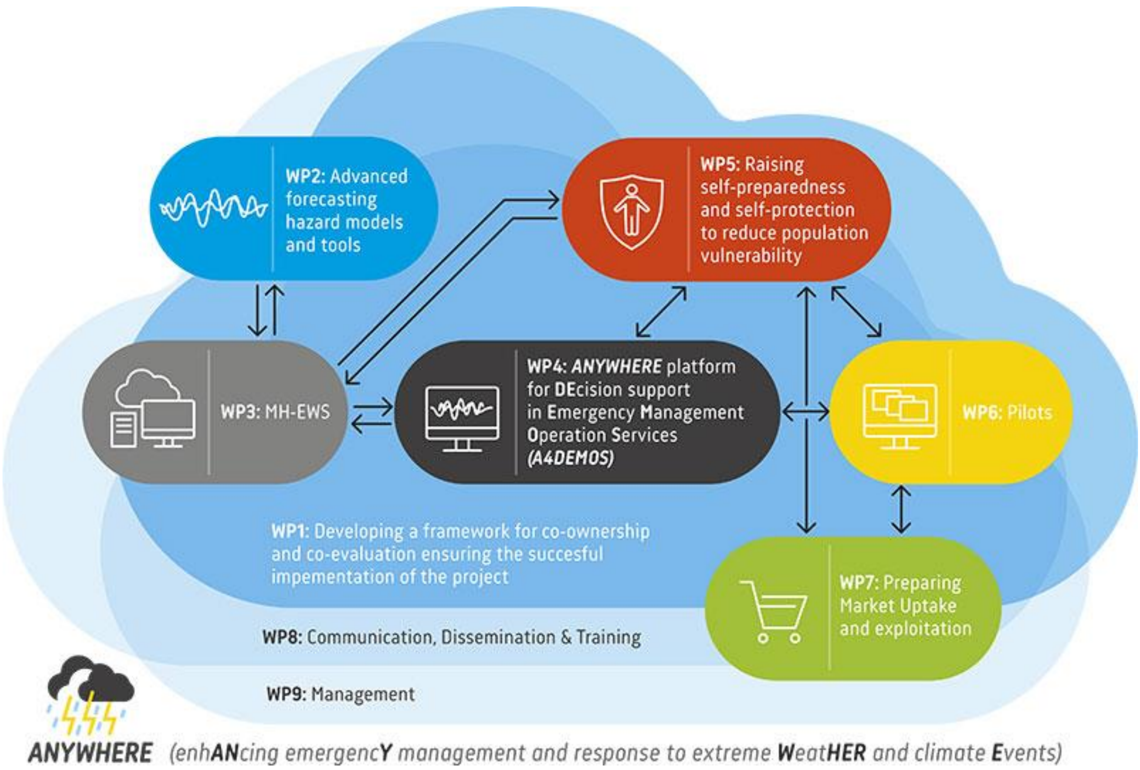

Figure 26: Structure of Anywhere Work packages (Source: ANYWHERE; 2017)

Products from the work packages aim to establish tools to forecast hazards induced by weather and climate events (WP2) and integrating these tools into a multi-hazard operational early warning system (WP3). In WP4 a prototype of a platform for decision support in emergency management operation services will be built. WP5 and -6 are focused on end-users and improved communication and awareness.

From the website, these are/will be available services (WP2/WP3/WP4):

- Hydro meteorological forecasts
- Floods, flash floods, debris flow and landslides
- Weather-induced forest fires
- Droughts
- Heatwaves and weather-induced health impacts
- Convective storms, severe winds
- Storm surges
- Snowfall

Each service category includes several products pertaining to the service. For floods, as an example, these products include (but are not limited to) observations of rainfall and temperatures, accumulated forecasts (rainfall), forecasts on flash floods and river flood impact as well as probabilistic river flood hazard forecasts.

3.4.2 COPERNICUS Emergency Management service

COPERNICUS Emergency Management service is a system for monitoring and forecasting floods across Europe (EFAS).

The aim of EFAS is to support preparatory measures before major flood events strike, particularly in the large trans-national river basins and throughout Europe in general. EFAS is the first operational European system monitoring and forecasting floods across Europe.

It provides complementary, added-value information (e.g. probabilistic, medium range flood forecasts, flash flood indicators or impact forecasts) to the relevant national and regional authorities. Furthermore, EFAS keeps the Emergency Response Coordination Centre (ERCC) informed about ongoing and possibly upcoming flood events across Europe.

The data is accessible for all users, but real-time products are restricted to EFAS partners only. Products older than one month are universally accessible.

3.4.3 I-REACT

I-REACT is aiming to be the first European-wide platform to integrate emergency management data coming from multiple sources, including that provided by citizens through social media and crowdsourcing (I-REACT, 2019). This way, information is produced faster and allow citizens, civil protection services and policy makers to effectively prevent and/or react against disasters. Their aim is to give flood early warning information up to 10 days in advance.

The platform aims to integrate emergency management data from multiple sources, among others crowdsourcing. As of now, an Android app is available on Google Play.

3.4.4 UrbanAdapt

The European Environment Agency (EEA) has compiled UrbanAdapt map layers for Urban forest fire and flood projections (EEA, 2019), sourcing maps from several sources including the EEA (https://www.eea.europa.eu/data-and-maps). This is presented via ESRI's ArcGIS Online map viewer.

This is an interactive map viewer, for climate adaptation of European cities, open and accessible for anyone. The service consists of 8 interactive maps plus city fact sheets for the cities included in Eurostat's Urban Audit (City Statistics). Data is received from different sources (or data source, European Environment Agency, Eurostat, Joint research Centre (JRC), Copernicus Urban Atlas, E-OBS via European Climate Assessment & dataset (ECA&D), EU-funded research projects (e.g. RESIN, RAMSES) and other research, etc.).

The aim of the map viewer is to provide an overview of the current and future climate hazards facing the European cities, the vulnerability of the cities to these hazards and their adaptive capacity. The map viewer collates information from various sources on the observed and projected spatial distribution and intensity of high temperatures, flooding, water scarcity and wild fires. It also provides some information on the causes of cities' vulnerability and exposure to these hazards, linked to the characteristics of cities and their population. Finally, the map viewer provides information on adaptation planning and actions of European cities.

The information contained in the maps, combined with the Urban Audit city factsheets allows gaining understanding about the current and projected climate impacts in European cities. It is also possible to compare individual cities to each other, and to identify other cities in similar situations. Additional sources of information, illustrative case studies and relevant indicators are suggested for learning more about the climate risks to European cities.

3.4.5 EFFIS

The European Forest Fire Information System (EFFIS) supports the services in charge of the protection of forests against fires in the EU countries and provides the European Commission services and the European Parliament with updated and reliable information on wildland fires in Europe (EFFIS, 2019). They offer services on current fire situation in Europe and the Mediterranean as well as a news service on wildland fires in Europe, updated daily.

Since 1998, EFFIS is supported by a network of experts from the countries in what is called the Expert Group on Forest Fires, which is registered under the Secretariat General of the European Commission. Currently, this group consists on experts from 40 countries in European, Middle East and North African countries. In 2015, EFFIS became one of the components of the Emergency Management Services in the EU Copernicus program.

Among the applications offered are monthly and seasonal fire weather forecasts, current situation view and a service for downloadable data.

4. National hazard maps for the Pilot study areas

4.1 Portugal

4.1.1 Flood

There are several flood hazard maps available for Portugal. Some of them derive by European or Worldwide database, such as: Joint Research Centre Data Catalogue; The Global Risk Data Platform; Global Assessment Report on Disaster Risk Reduction; The Socioeconomic Data and Applications Center (see section 3.1 and 3.2 for details). Even if the information of these databases is valid and reliable, some detailed datasets are available for Portugal at a bigger scale. In fact, detailed maps are provided by the *Sistema Nacional de Informacao Geografica* (SNIG). It is a national agency, created in 1990, dealing with the catalogue and analysis of geographical datasets for public and private institutions. The publication of the EU directive 2007/60/CE INSPIRE[13] and its transposition was an important step in the development and access to geographic information in Portugal and in the development of SNIG. Since then, SNIG made a lot of effort to gather data and produce maps of natural hazards. Several detailed datasets are freely available at the following website[14]. Hazard, consequence and risk maps (figure 27) for several return periods (20, 100, 1000 years) have been produced. Four levels for both hazard and risk classes have been defined. Other noteworthy datasets available are: the water depth, flux velocity and inundation boundary maps. These maps have been evaluated for 3 different scenarios with return periods of 20, 100, 1000 years (an example of these datasets is provided in figure 28). Also, these datasets are provided in a shape format and are available on the SNIG website.

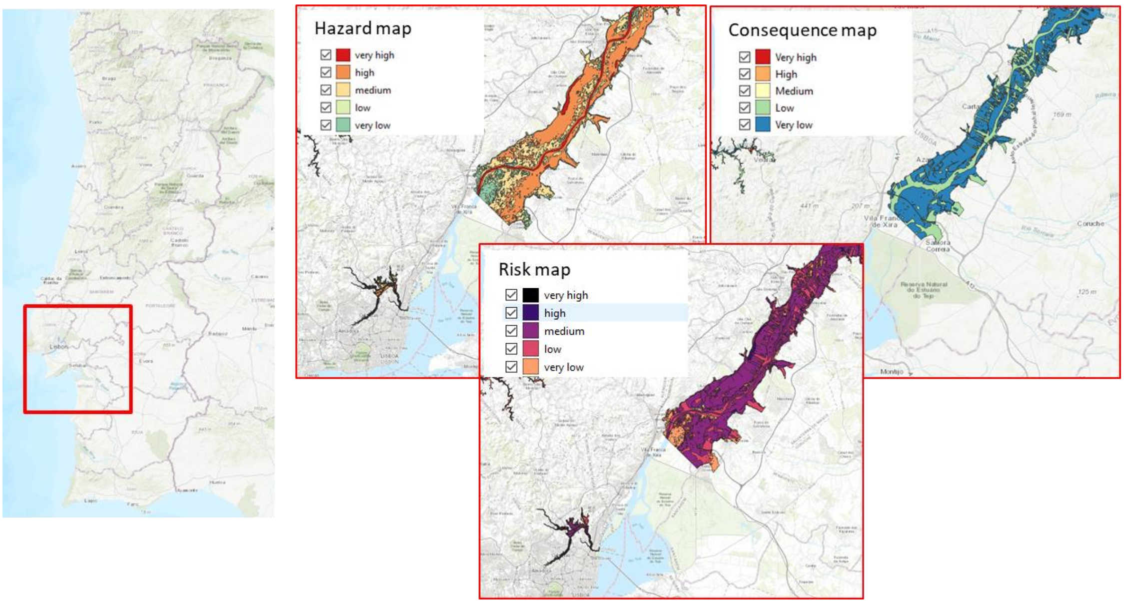

Figure 27: Example of a) hazard, b) consequence and c) risk map of flood available for Portugal.(Source: SNIG; http://snig.dgterritorio.pt/portal/index.php?option=com_wrapper&view=wrapper&Itemid=292&lang=pt)

[13] https://eur-lex.europa.eu/legal-content/EN/ALL/?uri=OJ:L:2007:108:TOC
[14] http://snig.dgterritorio.pt/portal/index.php?option=com_wrapper&view=wrapper&Itemid=292&lang=pt

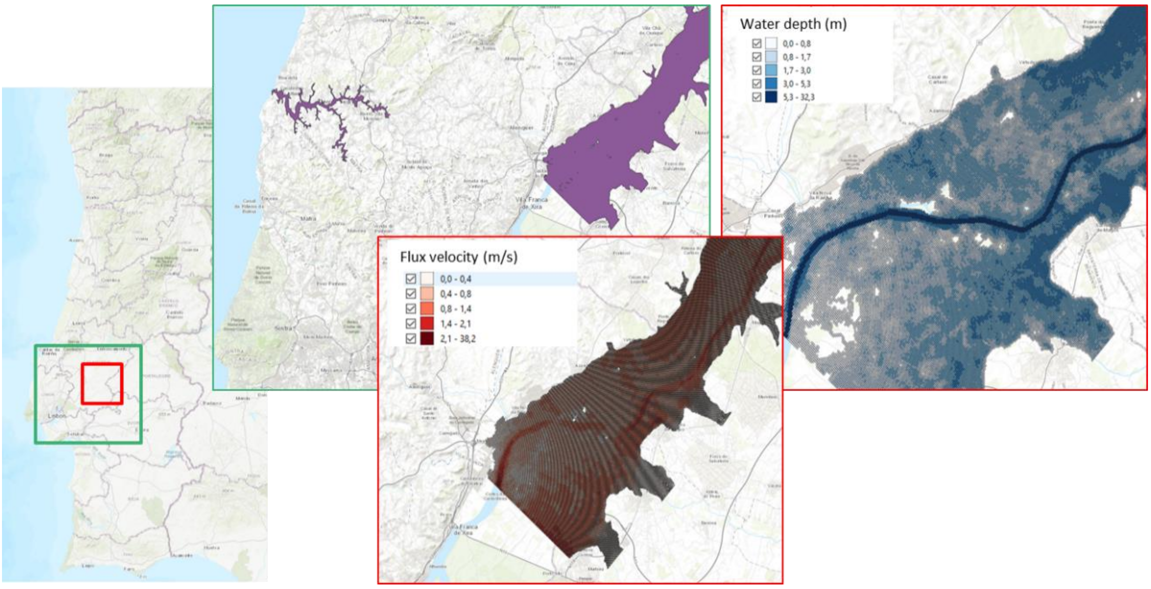

Figure 28: Example of the a) inundation areas, b) flood water depth, c) flux velocity maps available for Portugal. (Source: SNIG; http://snig.dgterritorio.pt/portal/index.php?option=com_wrapper&view=wrapper&Itemid=292&lang=pt)

4.1.2 Wildfire

The Global Risk Data Platform provides a global dataset for the fire density in the years 1997-2010. It can be also considered for risk analysis regarding Portugal. However, such information has a low level of detail and it gives just few insights about some possible fire susceptible areas in Portugal. A detailed dataset on wildfire is provided by "*Instituto de Conservaçao da Natureza e das Forestas*"(ICNF). ICNF is a public institute integrated in the indirect administration of the State, completely independent. The mission is to propose, monitor and ensure the implementation of nature conservation and forest policies, aiming at the conservation, sustainable use, valorisation and public recognition of the natural heritage, promoting the sustainable development of forestry and associated resources, fostering the competitiveness of forest ranks, and other activities directly associated with forestry. The ICNF provides detailed maps of the burned areas and a fire catalogue in Portugal (an elaboration is provided in figure 29 a). Those datasets, together with the map of the use of soil, have been used to derive the hazard map for wildfire (figure 29 b). Specifically, the hazard was produced based on the CSP methodology (Cover, Slope and Probability) developed at the National Forest Authority by Dr. João Verde (Verde and Zezere, 2011). The basic information used was: i) 2007 Soil Occupancy Chart Level 3 (COS2007); ii) slope chart produced from pan-European MDE, iii) cartography of burning areas (1997-2016). The map is available in a GeoTIFF format and it is freely available on the ICNF web site.

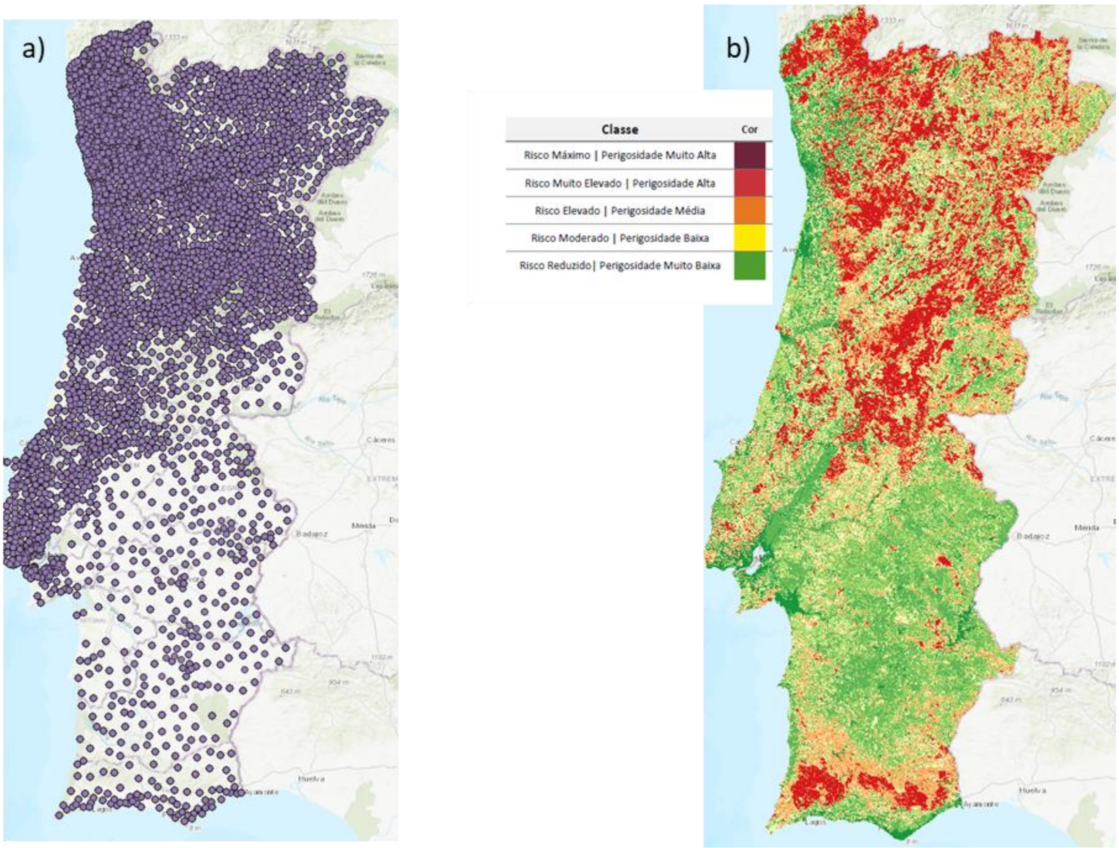

Figure 29: a) Wildfire events catalogue 1988-2015, b) hazard map for wildfires in Portugal. (Source: ICNF web site, https://www.icnf.pt/)

4.2 Spain

4.2.1 Flood

The Joint Research Centre Data Catalogue (see section 3.2.1) provides European flood hazard maps for different return periods: 10, 20, 50, 100, 200, 500 years. The database collection contains a set of flood hazard maps, based on streamflow data from the European and Global Flood Awareness System (EFAS and GloFAS) and computed using two-dimensional hydrodynamic models. Maps are in GeoTIFF format and can be used in any GIS program. Figure 30 shows the data available for Spain.

Another dataset collection, useful to describe the flood hazard in Spain, is provided by Global Assessment Report on Disaster Risk Reduction (GAR) (see section 3.2.6). A probabilistic approach for modelling the riverine flood of major river basins around the globe is used. This has been possible after compiling a global database of stream-flow data, merging different sources and gathering more than 8000 stations over the globe, in order to calculate the range of possible discharges from very low to the maximum possible scales at different locations along the rivers. Hazard maps for several return periods (25, 50, 100, 200, 500, 1000 years) were obtained. The hazard maps are developed at 1kmx1km resolution (figure 31).

The Global Risk Data Platform (see section 3.2.2) estimated a global risk index for floods worldwide. Four classes of risk are defined for each 7x9 km pixel (figure

32). This dataset is less detailed than the previous ones, in fact the minimum unit is coarser.

The Socioeconomic Data and Applications Center (SEDAC) produced global Flood Hazard Frequency and Distribution (see section 3.2.3) maps as a function of extreme flood events occurred between 1985 and 2003. However, also this grid is coarser than the previous first two datasets (i.e.: Joint Research Centre Data Catalogue, Global Assessment Report on Disaster Risk Reduction).

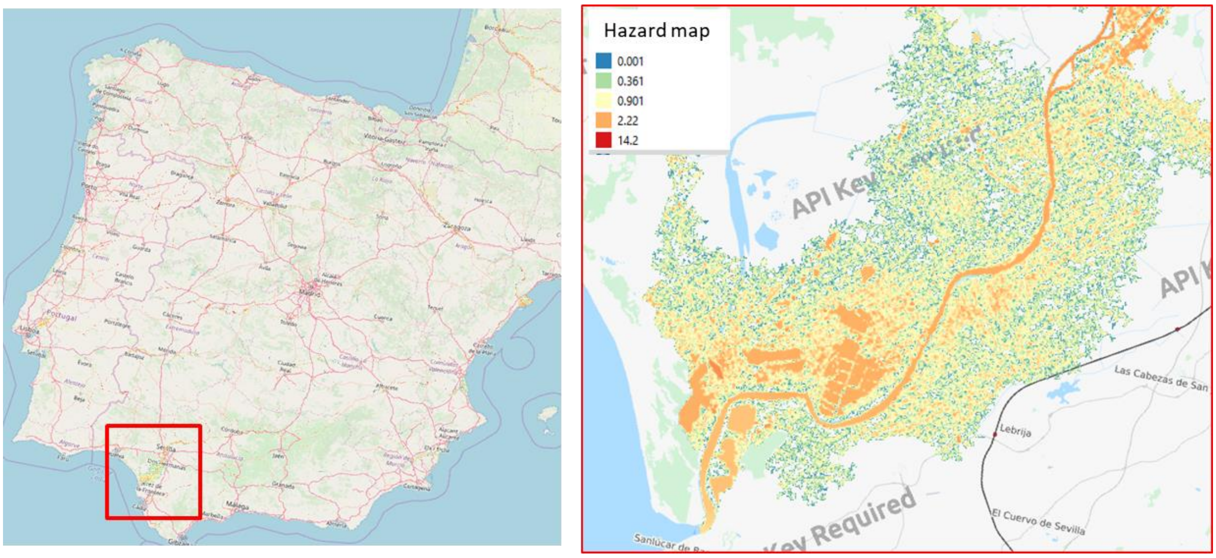

Figure 30: European flood hazard map for Spain. The map is expressed in terms of flood depth (m). (Source of the dataset: Joint Research Centre Data Catalogue)

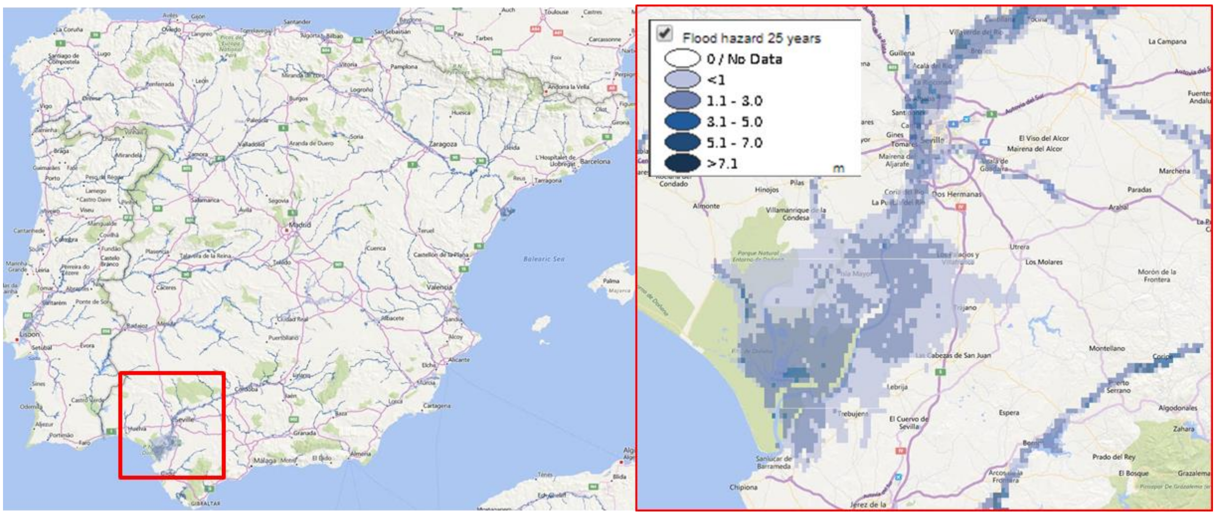

Figure 31: Flood hazard considering 100 years as return period. (Source: Global Assessment Report on Disaster Risk Reduction)

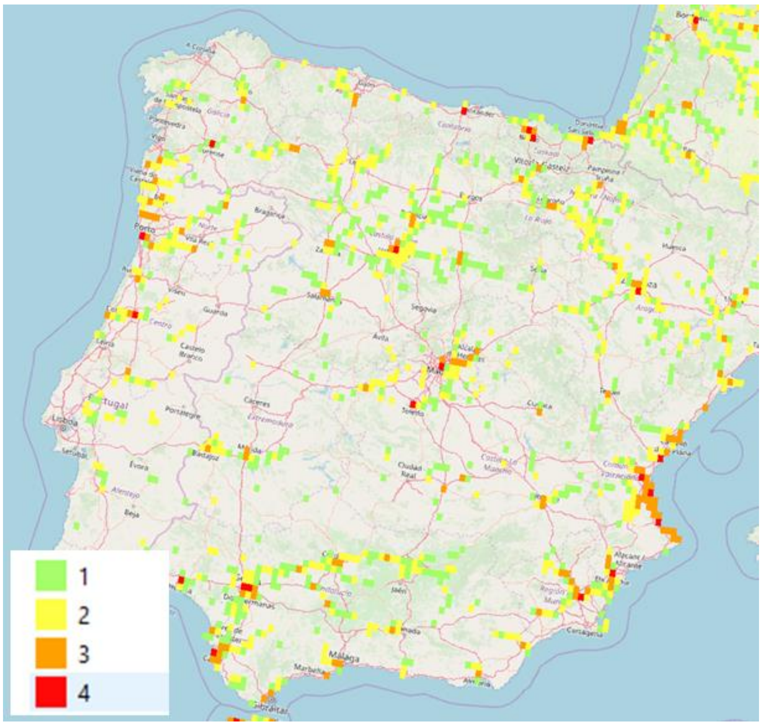

Figure 32: A global risk index for floods for Spain. (Source: Global Risk Data Platform)

More detailed hazard and risk maps for flood can be found on the website of the *Ministerio para la Transición Ecológica* (Ministry for the Ecological Transition[15]). Hazard maps for flooding, designed by River Basin Authorities, are available for each hydrographic basin within the framework of Directive 2007/60 on the assessment and management of flood risks. Hazard maps are prepared for scenarios with different flood probability: high, associated with a return period of 10 years; average, associated with a return period of 100 years; low, associated with a return period of 500 years. The maps represent, for each scenario, the foreseeable areas of the flood and the depth of the water in the flooded area.

4.2.2 Wildfire

Concerning maps of wildfire for Spain an estimation of the average fire density over the period 1997-2010 is provided by the Global Risk Data Platform. The map unit (figure 33) is the expected average number of event per 0,1 decimal degree pixel per year multiplied by 100 (e.g. 64 value means 0.64 events per year).

[15] https://www.miteco.gob.es/es/agua/temas/gestion-de-los-riesgos-de-inundacion/mapa-peligrosidad-riesgo-inundacion/

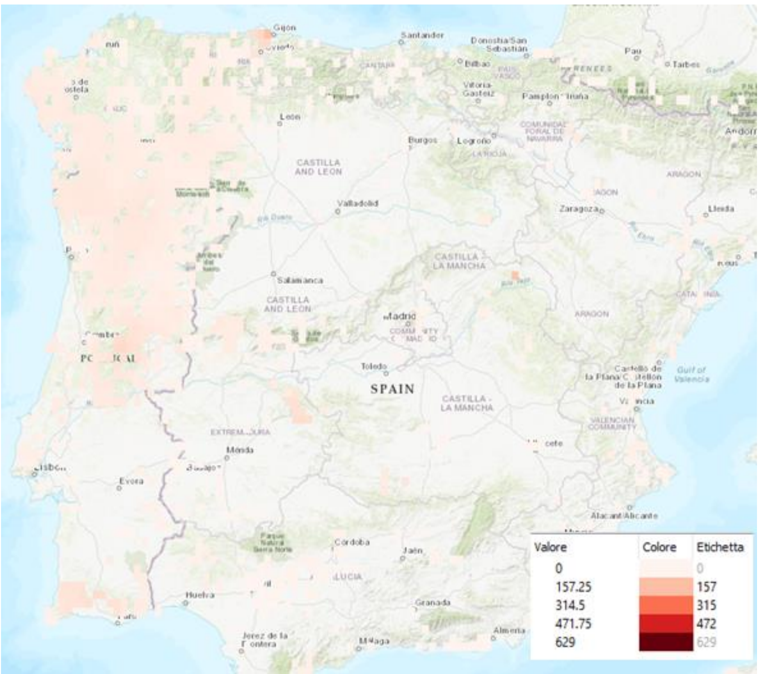

Figure 33: Fire density map for Spain and Portugal. (Source: Global Risk Data Platform)

4.2.3 Heatwave

In Spain the Agencia Estatal de Meteorología (AEMET), i.e., the Spanish meteorological agency, provides general meteorological information. It gathers climatological data, operates climate monitoring and seasonal and long-term forecasts. A summary of standard and extreme values of some meteorological indicators is provided for the period 1981-2010, for each meteorological station. Also, a summary of the values of rainfall and wind that exceeded the thresholds is provided for the latest four months. The regional projections of climate indicators give a forecast of several meteorological variables (such as: max and min temperatures, rainfall, wind velocity, soil moisture, humidity, 95th and 5th percentile of maximum and minimum temperatures, etc..) up to 2100 for different scenarios. Besides data on forecasts, historical data are also available for the mentioned variables for the period 1961-2005. The data are furthermore divided as a function of the global and regional models utilized. As an example, Figure 34 depicts the monthly average of daily maximum temperatures in August 2005 (C^0).

Other database providing information on meteorological variables are the NASA Earth Observations (see section 3.2.4) and the European Climate Assessment & Dataset project (see section 3.2.6) databases. The first provides information on: average land surface temperature [day], average land surface temperature [night], global temperature anomaly, land surface temperature anomaly [day], land surface temperature [day], etc... As an example of the type of data available, the land surface temperature (C^0) for July 2018 is depicted in figure 35. The colours on these maps represent temperature patterns of the top millimetre (or "skin") of the land surface as observed by MODIS in clear-sky conditions for the time period indicated. Yellow shows the warmest temperatures (up to 45°C) and light blue shows the coldest temperatures (down to -25°C). Black means "no data."

Finally, the European Climate Assessment & Dataset project (ECA&D) provides an accessible database of different meteorological variables[16]. The indices belonging to the "temperature" group are: mean of daily mean temperature; mean of daily minimum temperature; mean of daily maximum temperature; mean of diurnal temperature range; intra-period extreme temperature range; mean absolute day-to-day difference. The information is provided on a daily basis. Figure 36 displays an example of the dataset and it shows the maximum temperature for the 1rst July,2017.

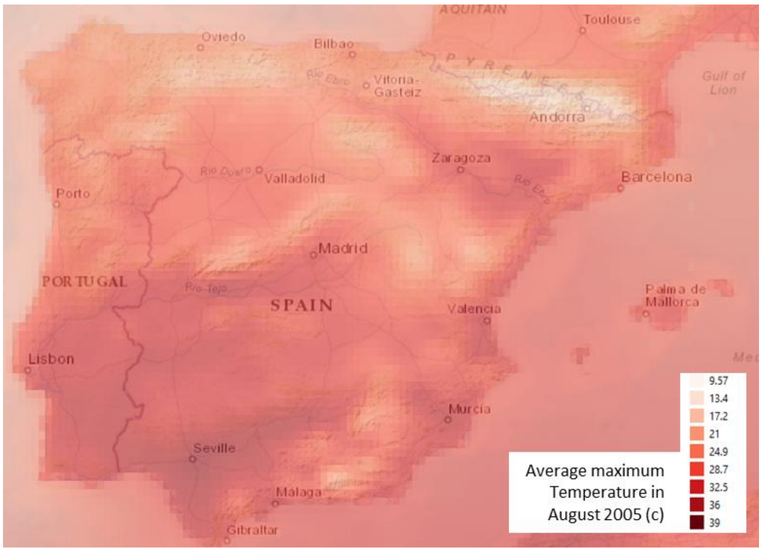

Figure 34: Monthly average of daily maximum temperatures in August 2005 (C0). (Source of the dataset: *Agencia Estatal de Meteorologia* (AEMET))

[16] https://eca.knmi.nl/download/millennium/millennium.php

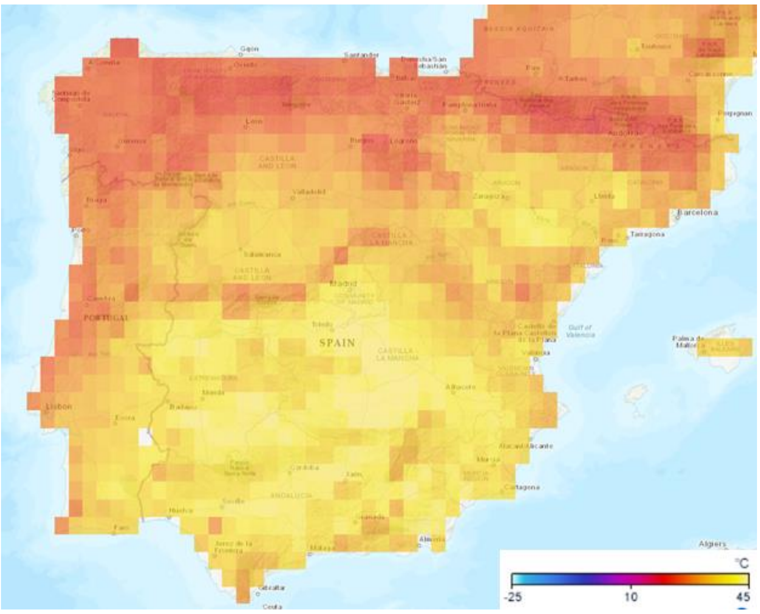

Figure 35: Land surface temperature (C0) in July 2017. Yellow shows the warmest temperatures (up to 45°C) and light blue shows the coldest temperatures (down to -25°C). (Source of the dataset: NASA Earth Observations (NEO))

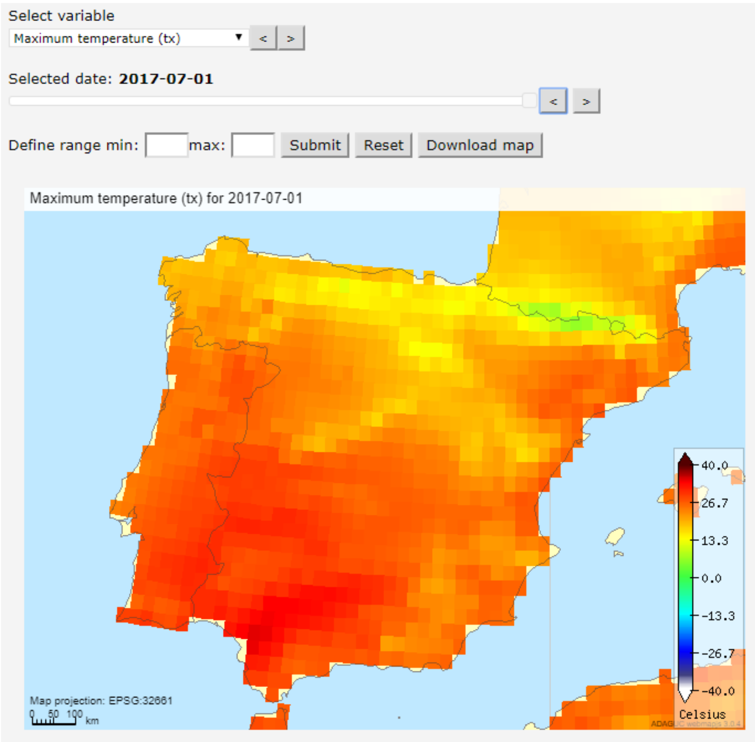

Figure 36: Maximum temperature for the 1rst July 2017. (Source: European Climate Assessment & Dataset project)

4.3 United Kingdom

4.3.1 Flood

The UK government publish several flood maps (https://flood-warning-information.service.gov.uk/long-term-flood-risk/map): flood risk from reservoirs, risk of flooding for land-use planning for England and development advisory map for Wales. There is also a 5-day flood risk map.

In addition to these, a new map (beta version) has been published on long-term flood risk. The map is a general indicator of an area's flood risk from rivers, the sea, surface water and some groundwater (The British Crown, 2019a).

Flood risk is classified as high (risk >3.3%), medium (1.1%> risk < 3.3%), low (0.1%> risk < 1%) or very low risk (risk <0.1%) for floods from rivers or the sea as well as from surface water, while flooding from groundwater or reservoirs do not have a risk classification (The British Crown, 2019a).

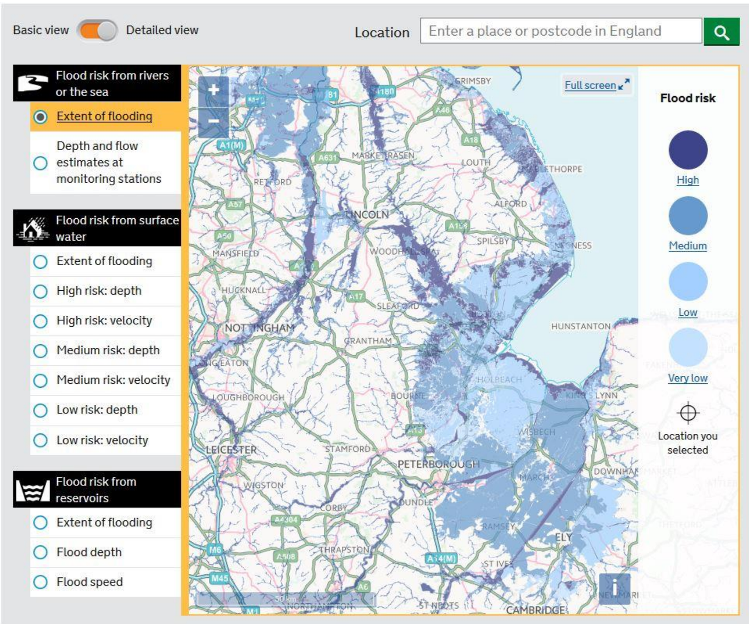

Figure 37: An example map from the long-term flood risk map provided by the UK government (Source: The British Crown, 2019a)

Flood maps for planning are published by the UK government as a useful tool for flood risk assessment for planning application. The maps include flood zones (classed from 1-3), flood defences, river and any flood storage areas (The British Crown, 2019a).

Here, the floods are modelled without any defences ("natural" flooding). Zone 1 is low probability, zone 2 medium probability and zone 3 high probability (Figure 39). The flood zones in the maps for planning do not take climate changes into account.

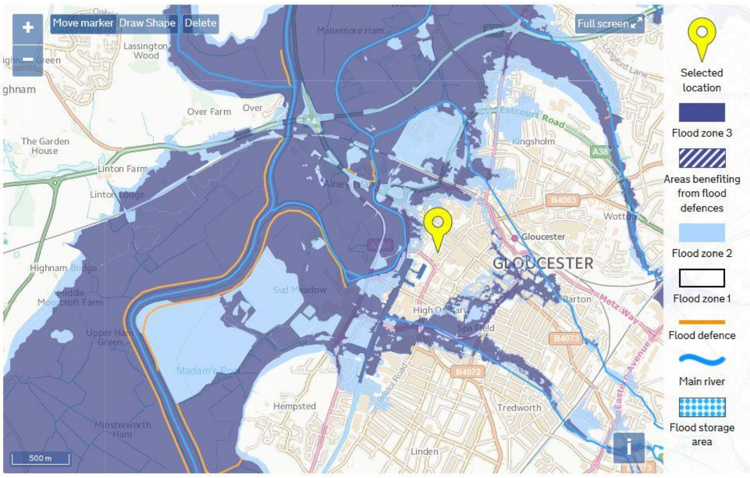

Figure 38: Flood map for planning tool from the UK government (Source: The British Crown, 2019a)

Flood Zone	Definition
Zone 1 Low Probability	Land having a less than 1 in 1,000 annual probability of river or sea flooding. (Shown as 'clear' on the Flood Map – all land outside Zones 2 and 3)
Zone 2 Medium Probability	Land having between a 1 in 100 and 1 in 1,000 annual probability of river flooding; or land having between a 1 in 200 and 1 in 1,000 annual probability of sea flooding. (Land shown in light blue on the Flood Map)
Zone 3a High Probability	Land having a 1 in 100 or greater annual probability of river flooding; or Land having a 1 in 200 or greater annual probability of sea flooding.(Land shown in dark blue on the Flood Map)
Zone 3b The Functional Floodplain	This zone comprises land where water has to flow or be stored in times of flood. Local planning authorities should identify in their Strategic Flood Risk Assessments areas of functional floodplain and its boundaries accordingly, in agreement with the Environment Agency. (Not separately distinguished from Zone 3a on the Flood Map)

Figure 39: Flood zone classification for planning (Source: The British Crown, 2019a)

4.3.2 Wind

The UK meteorological office publishes a wind map with up to 5 days forecast, but no hazard maps are freely available. However, the met office has a commercial service for the insurance industry (and other interested parties), where early alerts on windstorms are available, as well as a catalogue of windstorms used for hazard and risk modelling.

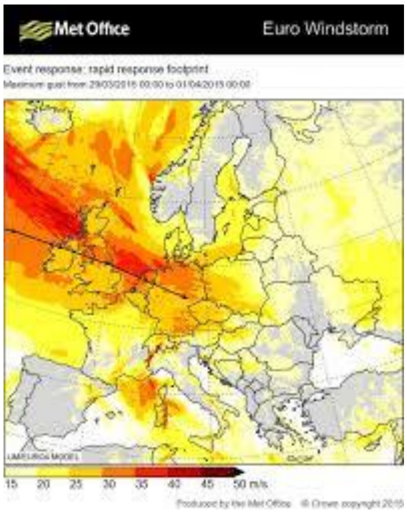

Figure 40: Windstorm modelling (Source: The British Crown, 2019b)

The Global Wind Atlas (Global Wind Atlas, 2019) is a free, web-based application developed to help policymakers and investors identify potential high-wind areas for wind power generation. The tool facilitates online queries and provides freely downloadable datasets based on the latest input data and modelling methodologies. Users can additionally download high-resolution maps showing global, regional, and country wind resource potential.

The current version of the Global Wind Atlas (GWA 2.0) is the product of a partnership between the Department of Wind Energy at the Technical University of Denmark (DTU Wind Energy) and the World Bank Group (consisting of The World Bank and the International Finance Corporation, or IFC). It is part of the global ESMAP initiative on Renewable Energy Resource Mapping that includes biomass, small hydropower, solar and wind.

5. Effect of climate change in the Pilot study areas

5.1 Central Portugal (Coimbra, Leiria and Santarém)

Particularly in summer the Mediterranean region is facing decreasing precipitation and increasing temperatures (Table 12). This trend has already been observed where annual precipitation has decreased by up to 90 mm per decade in the Iberian Peninsula, particularly in central Portugal. Decreasing precipitation leads to increasing risks of droughts, heat extremes and forest fires as well as adverse impacts on human health and well-being (EEA, 2017). Under the RCP8.5 scenario very extreme heat waves are projected to occur as often as every two years in the second half of 21st century, where the projected frequency of heat waves is greatest in the south and south eastern part of Europe. By 2080 central Portugal is projected to be affected by increases in the probability of hazard occurrence of at least 20% for three or even four out of the seven climate related hazards (heat waves, cold waves, droughts, wildfires, river floods, coastal floods and windstorms).

5.2 Southern Spain (Murcia and Malaga region)

Particularly in summer the Mediterranean region is facing decreasing precipitation and increasing temperatures (Table 12). The southernmost parts of the Iberian Peninsula could for the RCP8.5 scenario experience a decrease in precipitation by as much as 15-25% in the years 2017-2100. This leads to increasing risks of droughts, heat extremes and forest fires as well as adverse impacts on human health and well-being (EEA, 2017). Under the RCP8.5 scenario very extreme heat waves are projected to occur as often as every two years in the second half of 21st century, where the projected frequency of heat waves is greatest in the south and south eastern part of Europe. For the end of the 21st century, some of the greatest increases in Q100 floods in Europe are projected for some regions in the south-east of Spain. By 2080 southern parts of the Iberian Peninsula are projected to be affected by increases in the probability of hazard occurrence of at least 20% for three out of the seven climate related hazards (heat waves, cold waves, droughts, wildfires, river floods, coastal floods and windstorms).

5.3 United Kingdom (London and Manchester)

Low-lying coastal areas that already are exposed to coastal flooding will experience increased risk because of sea level rise and potentially stronger storm surges (Table 12). Areas especially vulnerable are those bordering the North Sea (EEA, 2017). Stronger extreme precipitation events, especially during winter, are projected to increase the frequency and intensity of winter and spring river flooding, urban floods and associated impacts. By the end of the 21st century, some of the greatest increases in Q100 floods in Europe are projected for the British Isles. The risk of severe winter storms, and possibly of severe autumn storms, is projected to increase (EEA, 2017). Projected changes in extreme wind speeds are estimated to increase with a magnitude of 0.25 to 0.75 m/s in large parts of UK (EEA, 2017). By 2080 UK is projected to be affected by increases in the probability of hazard occurrence of at least 20% for three or even four out of the seven climate related hazards (heat waves, cold waves, droughts, wildfires, river floods, coastal floods and windstorms).

Table 7: Projected climate change for the pilot sites (Source: modified from EEA, 2017)

Indicator/impact	Variable	Portugal	Spain	UK
Temperature	Temperature	Increase	Increase	Increase
Heat extremes	Frequency of warm days/heat wave magnitude index	Increase	Increase	Increase
Mean Precipitation	Annual Precipitation	Decrease	Decrease	Increase
Heavy precipitation	Intensity	Decrease	Decrease	Increase
Wind storms	Maximum wind speed	Decrease	Decrease	Increase
Hail	Potential hail index	Increases as well as decreases	Increases as well as decreases	Decrease
Sea level	Absolute sea level	Increase	Increase	Increase
	Relative sea level	Increase	Increase	Increase
	Coastal flooding frequency	Increase	Increase	Increase
River flows	Mean flow (near-natural rivers)	Decrease	Decrease	Increase
River floods	Frequency and magnitude	Increases as well as decreases	Increases as well as decreases	Increases as well as decreases
Meteorological and hydrological droughts	Frequency and severity of meteorological droughts	Increase	Increase	Increases as well as decreases
	Minimum river flow	Decrease	Decrease	Decrease
Forest fires	Area burnt	Increase	Increase	
	Forest fire risk index	Increase	Increase	Increase

Adverse Beneficial Both beneficial and adverse Neither / unspecified

6. Hot-spot maps for the Pilot study areas

This section provides hot-spot maps for the Pilot areas to better identify the most exposed parts of the infrastructure. The maps are obtained overlapping different natural hazard maps with the spatial distribution of road and railway tracks of the pilot areas. The aim is to highlight critical areas which need further investigations to mitigate dangerous situations.

The hazard maps used for the analyses were gathered from different sources, often from European research projects and agencies' web-sites (see Section 3). The spatial distribution of roads and railways is obtained by the Open Street Map database (http://download.geofabrik.de/europe.html), freely available on the internet. It is important to underline that, due to the databases and information available, the following analyses have been performed at a regional scale and can be considered as preliminary risk maps. The defined hot-spots, i.e. hazard prone areas of the infrastructure, should be investigated in detail through field surveys, in order to verify the actual risk level. The presence of various road and railway assets, together with their different vulnerabilities, may significantly modify the levels of risk. In fact, the risk could vary depending on the situation and type of asset (i.e., embankments, bridges, underpasses, etc…). This analysis only considers the spatial distribution of road and railway tracks.

6.1 Central Portugal (Coimbra, Leiria and Santarém)

The pilot area is the central part of Portugal, specifically the regions of Coimbra, Leiría and Santarem. This area includes 73.37 railway km and 5 European roads with 22'822 daily users; it can be considered an important connection network. Recently, many roads and railways have been affected by fires and floods. This section provides hot-spot maps to better identify the areas exposed at risk. The maps are obtained overlapping different natural hazard maps with roads and railway tracks for the pilot area. The aim is to highlight critical areas and dangerous situations to be mitigated. The following hazards have been considered for the pilot area in Portugal: flood, wildfire.

6.1.1 Flood

Detailed maps are provided by the *Sistema Nacional de Informacao Geografica* (SNIG). The hazard maps (see section 4.1.1) depict flood-prone areas for several return periods (20, 100, 1000 years). The flood hazard map is overlapped with road (Figure 41) and railway (Figure 42) tracks to highlight hot-spot areas exposed at risk. Figure 41 and Figure 42 highlight that the areas nearby Tago river can be affected by floods, specifically those close to Santarem, Tomar and Plombal. Consequently, the roads and railways passing through those areas are exposed to risk. However, a risk assessment analysis at a local scale could be necessary to evaluate the interaction of floods with different railway structures (i.e., embankments, bridges, underpasses, etc…).

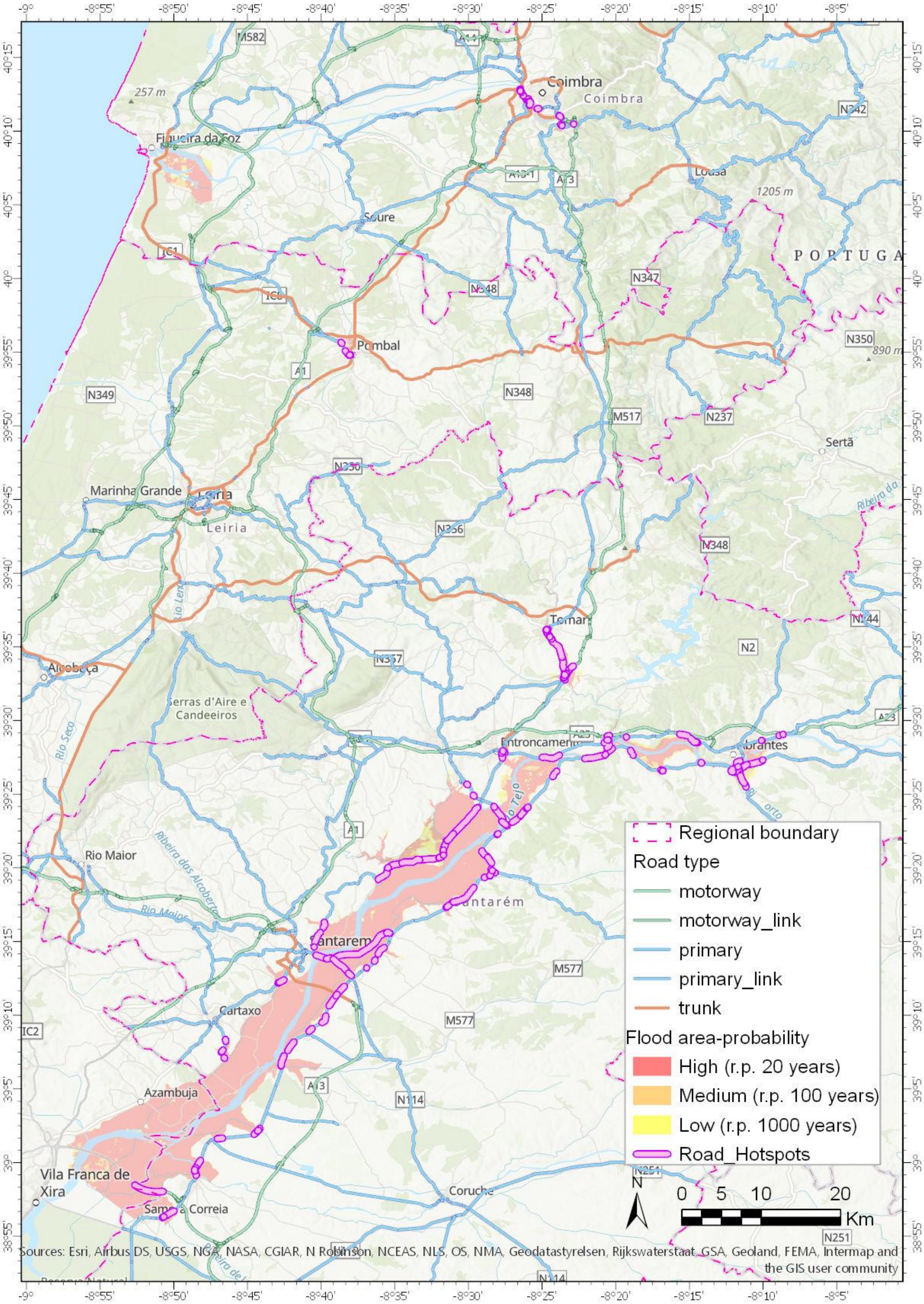

Figure 41: Risk map of possible roads affected by floods. (Source: SNIG)

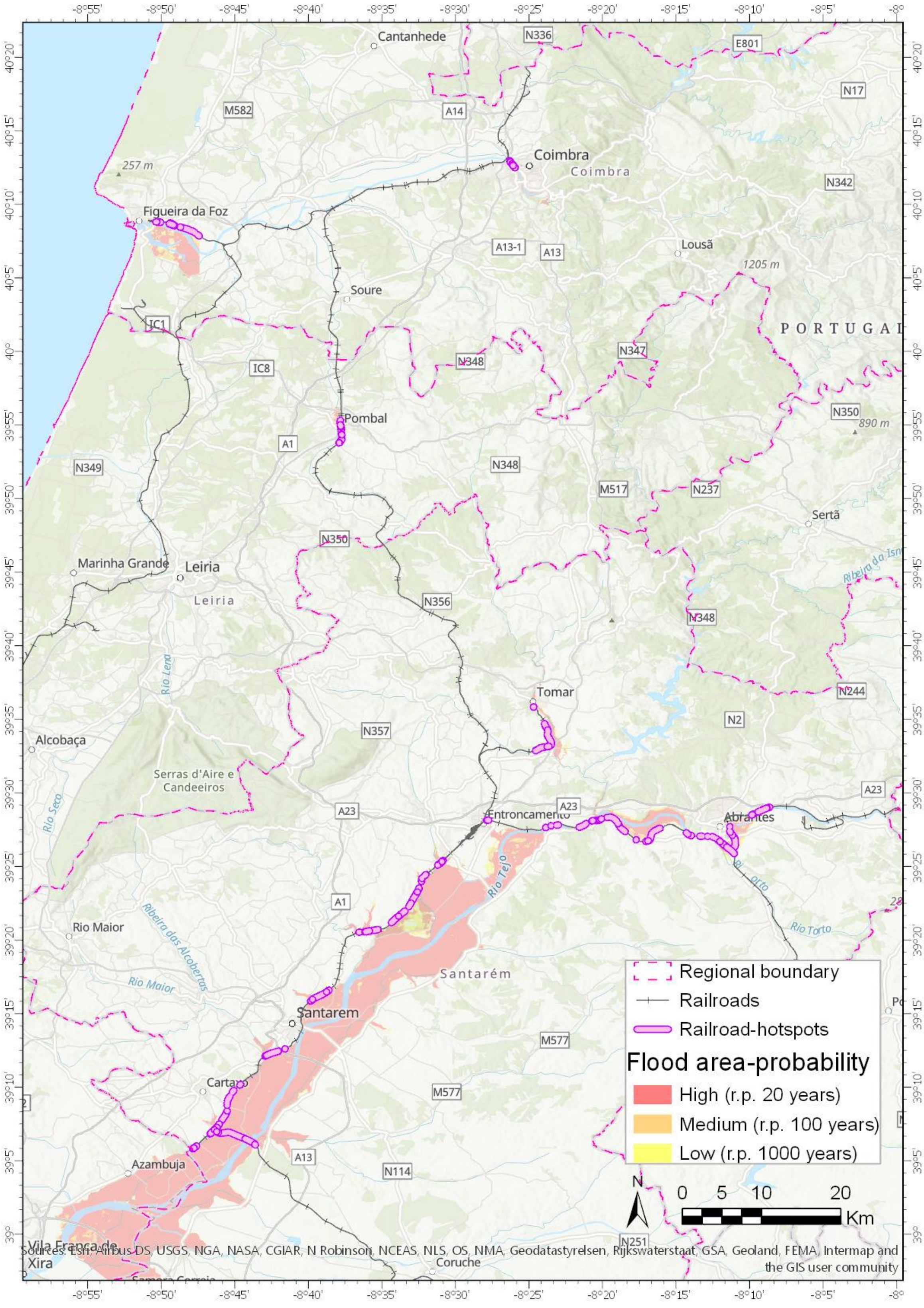

Figure 42: Risk map of possible railways affected by floods. (Source: SNIG)

6.1.2 Wildfire

The *Instituto de conservacao de natureza e das florestas* (ICNF) provides a detailed dataset on wildfire (see section 4.1.2). The maps of the burned areas and a fire catalogue in Portugal, together with the map of the use of soil, have been used to obtain the hazard map for wildfire. Five different levels of hazard are identified: very low, in green (level 1); low, in yellow (level 2); medium, in orange (level 3); high, in red (level 4); very high, in purple (level 5). The wildfire hazard map is overlapped with road (Figure 43) and railway (Figure 44) tracks to highlight hot-spot areas exposed at risk. Figure 43 depicts motorway and primary roads exposed to wildfire hazard levels "high" and "very high" (i.e., respectively levels 4 and 5). The roads nearby the city of Coimbra and in the east side of the Region seem to be the most exposed to wildfire. The region of Santarem also shows some roads at risk, both in the east and west side of the region (nearby Serras d'Aire e Candeeiros). Concerning the railways, Figure 44 depicts tracks exposed to wildfire hazard levels "high" and "very high" (i.e., respectively levels 4 and 5). The railway tracks between the regions of Santarem and Leiría are exposed to "very high" level of risk (Figure 44). However, this is a preliminary analysis carried out at a regional scale, and, the hot-spots highlighted, should be investigated more in detail with field surveys to verify and determine the actual level of risk.

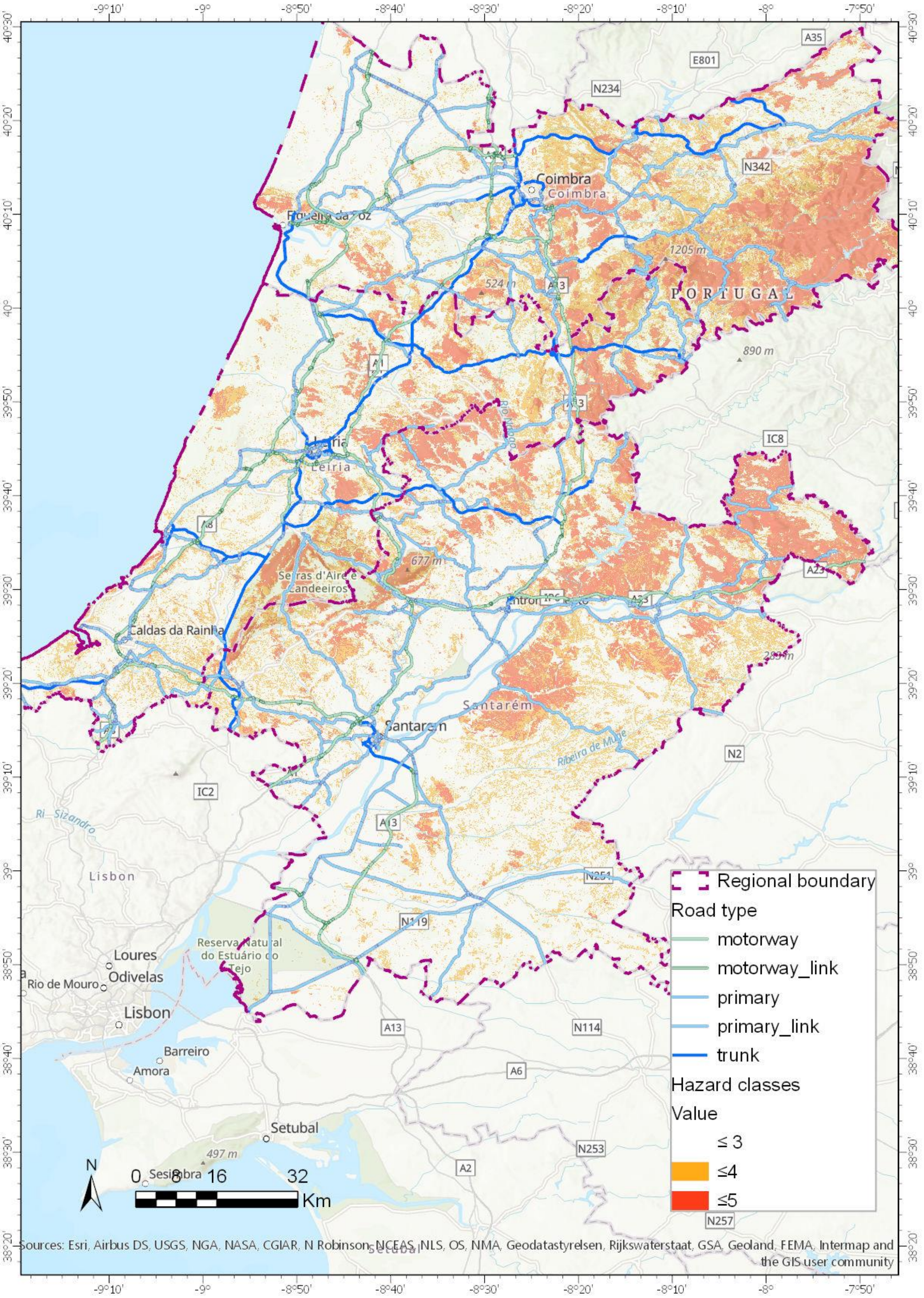

Figure 43: Risk map of possible roads affected by wildfire. (Source: ICNF)

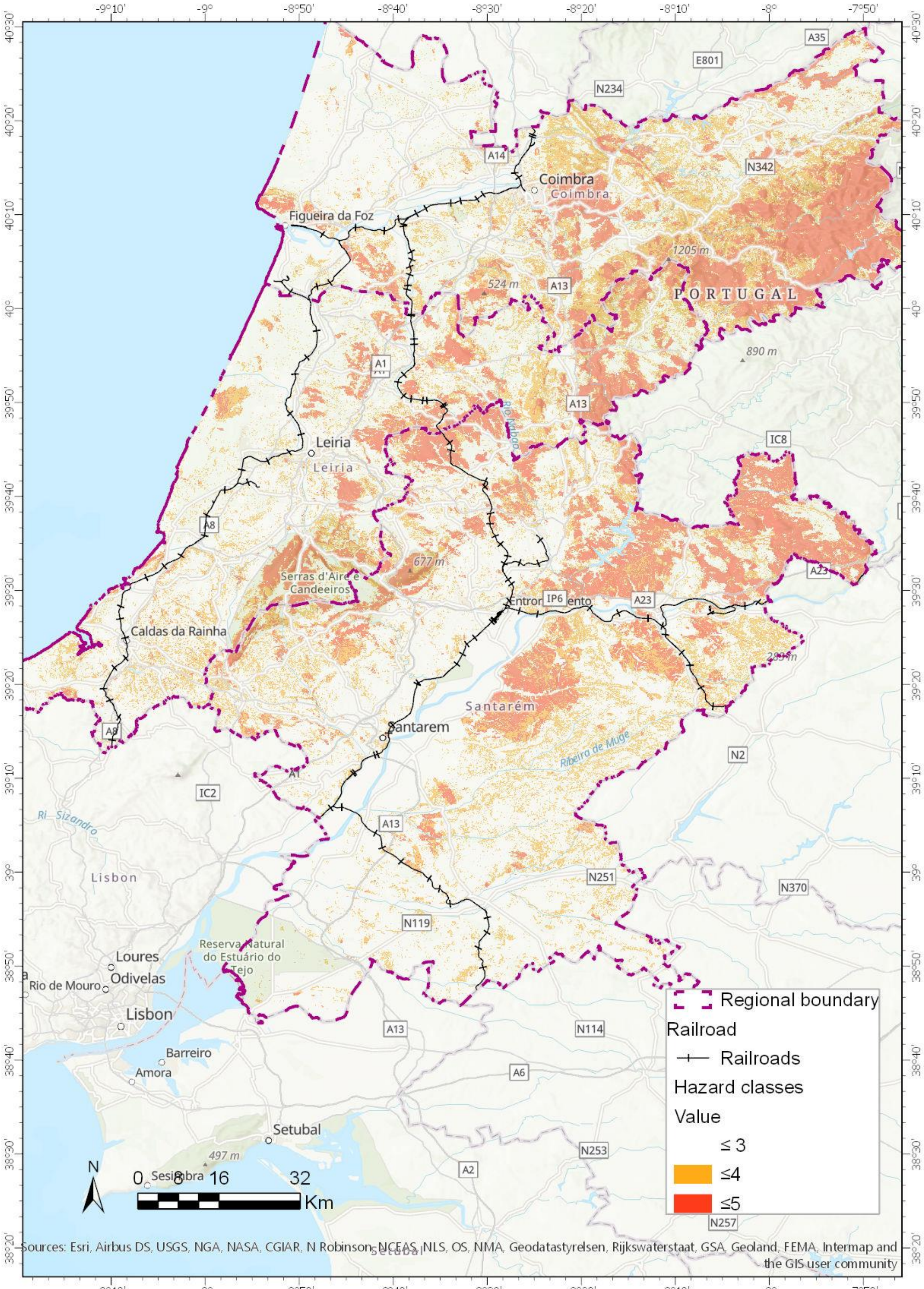

Figure 44: Risk map of possible railways affected by wildfire. (Source: ICNF)

6.2 Southern Spain (Murcia and Malaga region)

The pilot area in Spain is composed by two case studies and refer to the railway network. The case study areas are both located in the southern part of Spain, on the Mediterranean coast, within Andalucia (2a) and Murcia (2b) regions (Figure 45). The railway track of the case study 2a belongs to the high-speed network connecting Malaga to Cordoba (Andalucia region). The railway track under investigation, for case study 2b, belongs to the conventional network, and it connects Aguilas to Murcia (Murcia region).

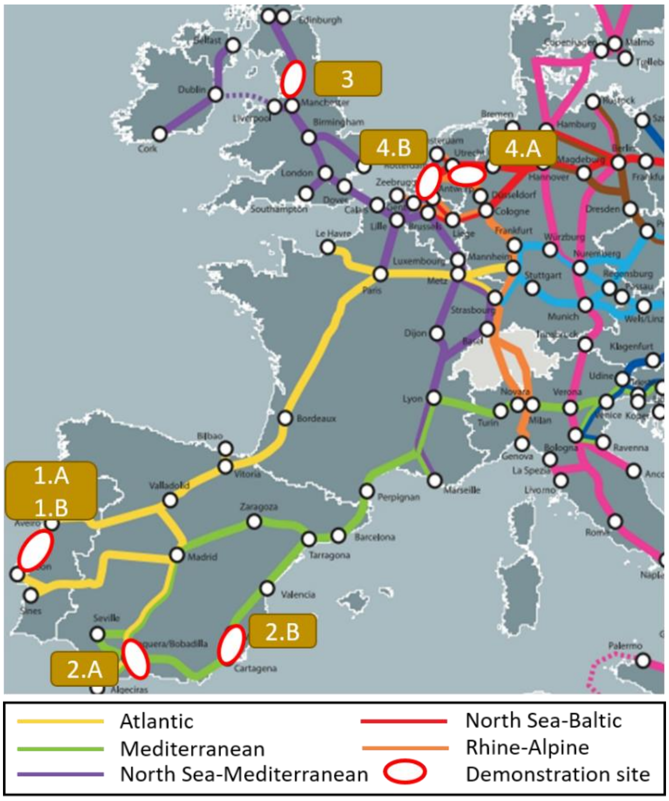

Figure 45: Location of the pilot areas in Spain

The southern part of Spain is exposed to different type of natural hazards that may damage or reduce the operability of the railway network, as well as threaten the users. This section provides hot-spot maps to better identify the areas exposed at risk. The maps are obtained overlapping different natural hazard maps with the railway tracks of the pilot area. The aim is to highlight critical areas and dangerous situations to be mitigated. The following hazards have been considered for the pilot area in Spain: flood, landslide, earthquake, heat-wave and rainfall.

6.2.1 Flood

The hot-spot maps are generated overlapping the hazard maps for flood available on the website of the Ministerio para la Transición Ecológica (Ministry for the Ecological Transition[17]) with the location of the railway tracks for the two pilot areas. The hazard flood maps show flood-prone areas at different flood probability:

[17] https://www.miteco.gob.es/es/agua/temas/gestion-de-los-riesgos-de-inundacion/mapa-peligrosidad-riesgo-inundacion/

"high", associated with a return period of 10 years; "average", associated with a return period of 100 years; "low", associated with a return period of 500 years.

Figure 46 and Figure 48 show the flood areas for different return periods respectively for case 2b, in Murcia, and case 2a, in Andalucia. The railway track, of case study 2b, is exposed to flood hazard in two extended areas, precisely, nearby the town of Torre-Pacheco and the city of Murcia (see Figure 47 for details). Concerning case study 2a, in Andalucia region, there are some hazardous areas close to: Malaga, Santa Ana, Cordoba (see Figure 49 for details). The railway tracks exposed to flood hazard and, specifically, the hot-spots highlighted (Figure 47 and Figure 49), should be investigated more in detail with field surveys to verify and determine the actual level of risk. A risk assessment analysis at a local scale is also needed to evaluate the risk due to the interaction of flood intensities with different railway structures (i.e., embankments, bridges, underpasses, etc…).

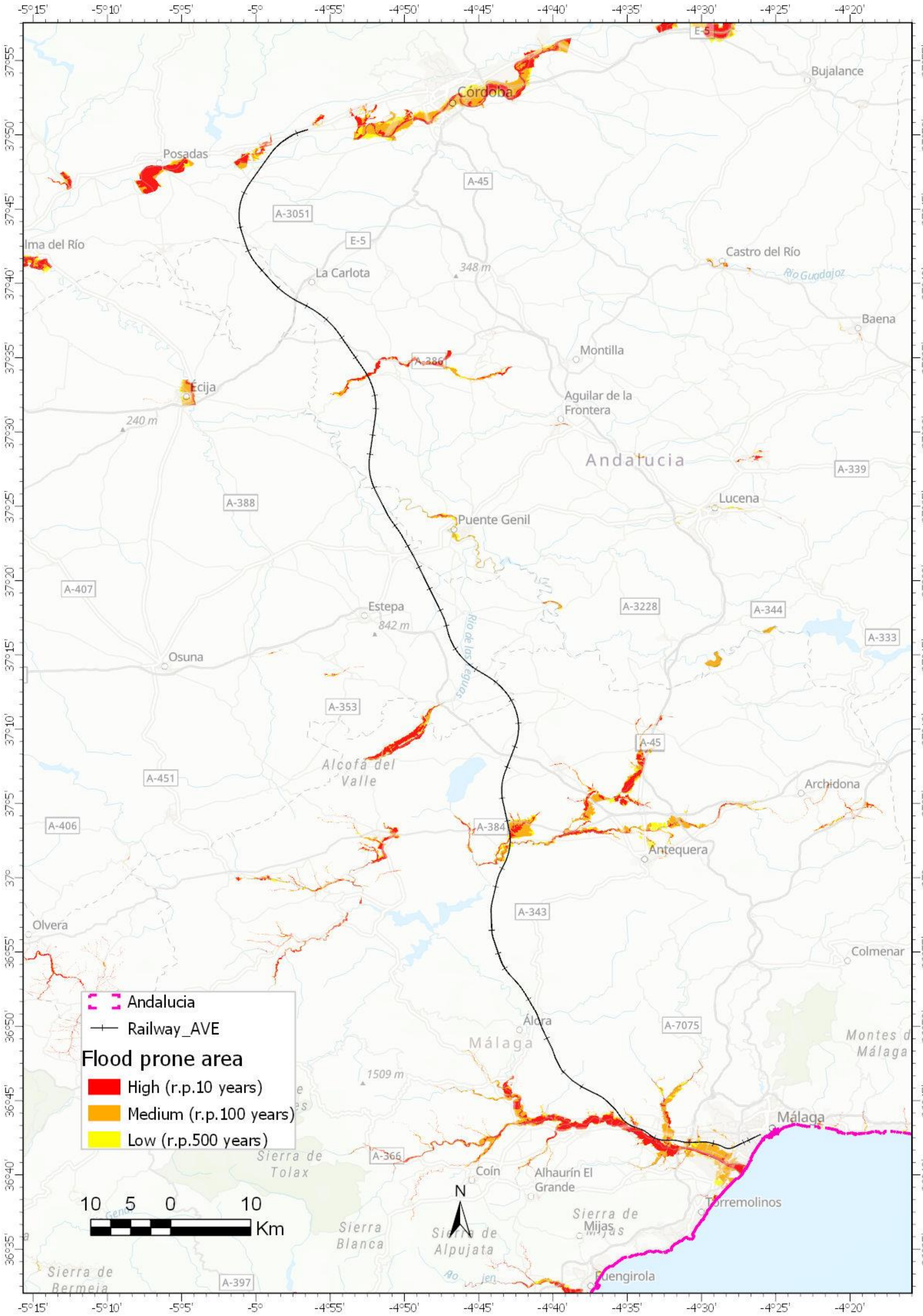

Figure 46: Different probability (high, medium, low) of flood-prone areas for case study 2a. (Source: *Ministerio para la Transición Ecológica*)

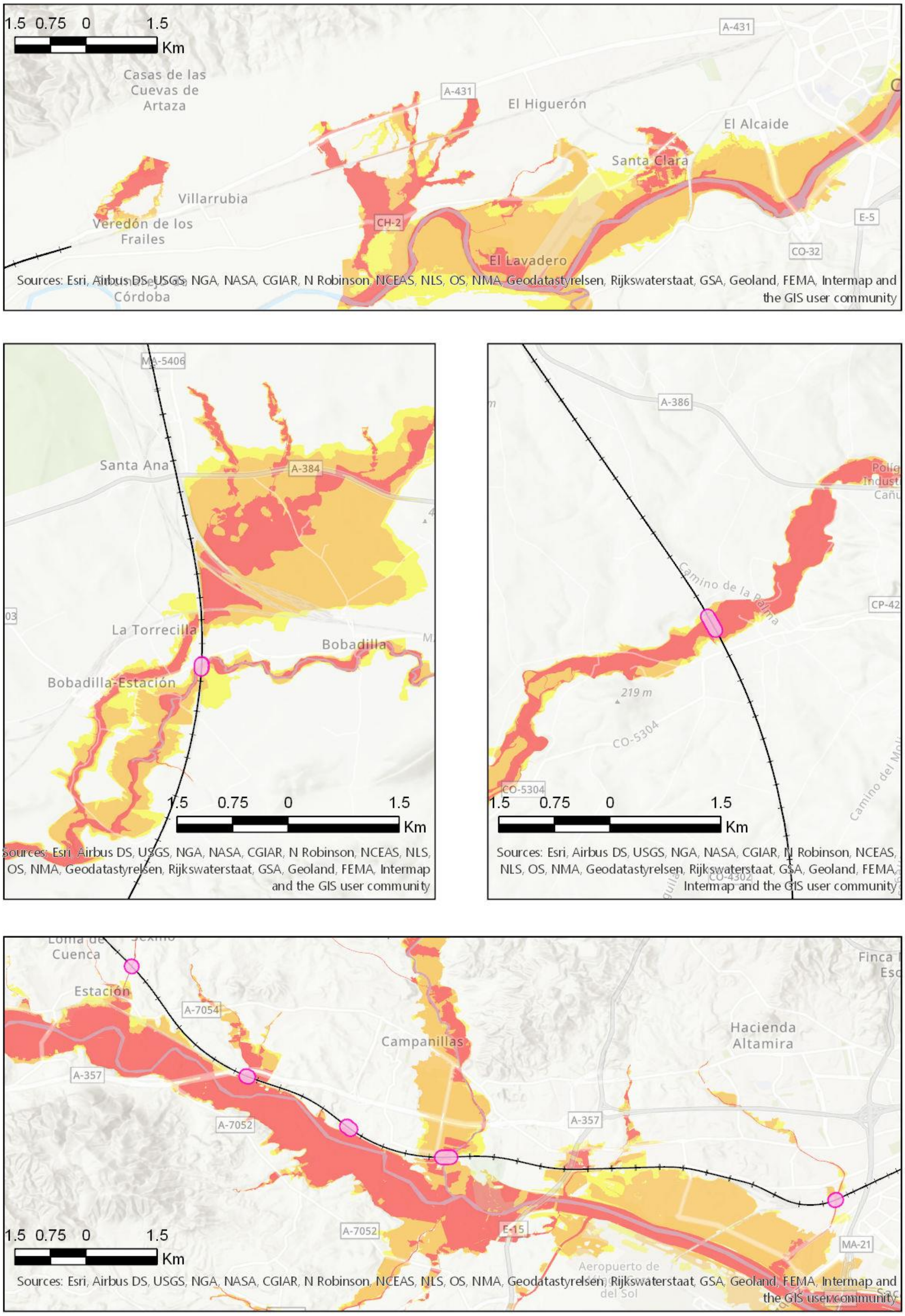

Figure 47: Detail of hot-spots for flood (in pink): case study 2a. (Source: *Ministerio para la Transición Ecológica*)

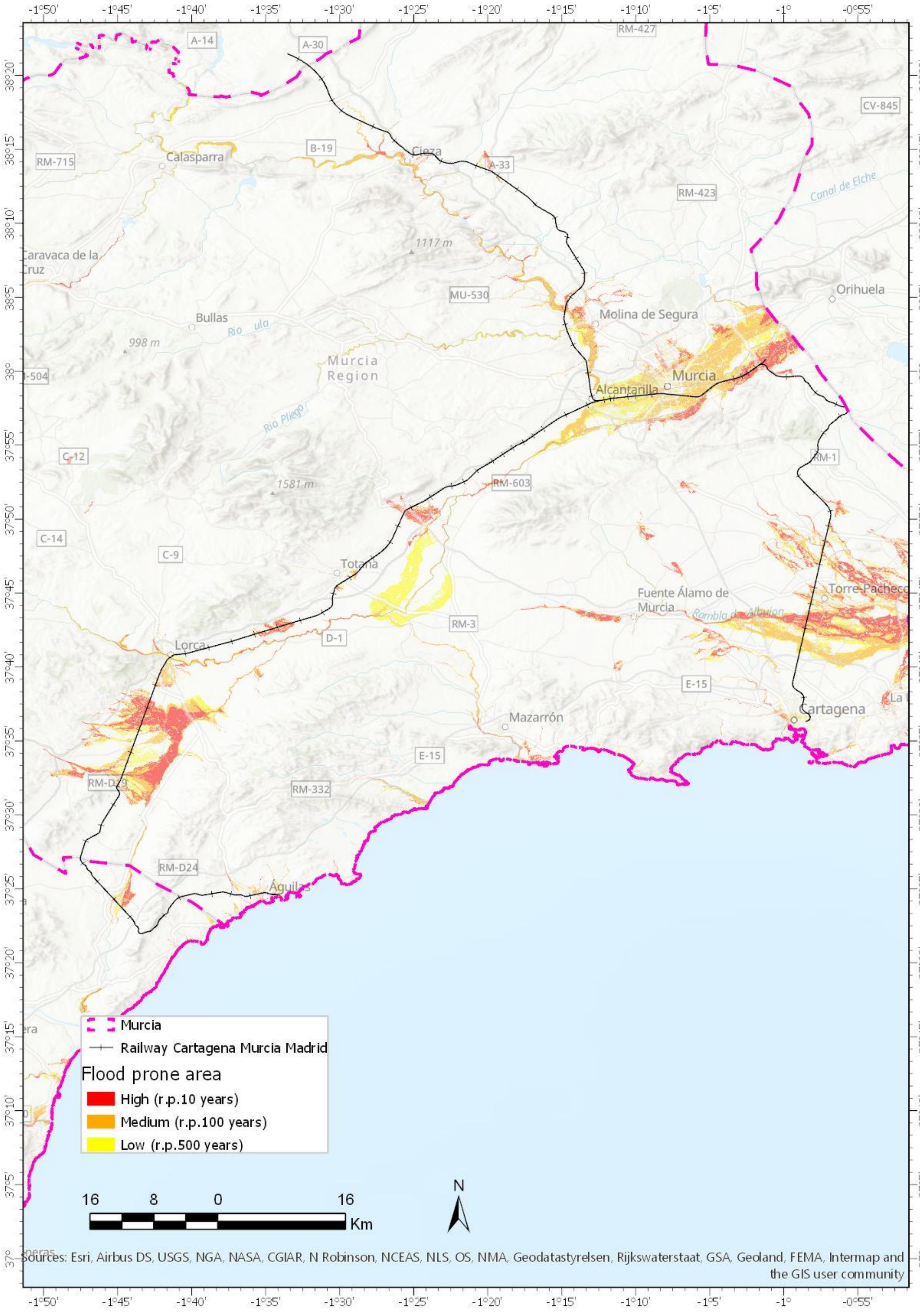

Figure 48: Different probability (high, medium, low) of flood-prone areas for case study 2b. (Source: *Ministerio para la Transición Ecológica*)

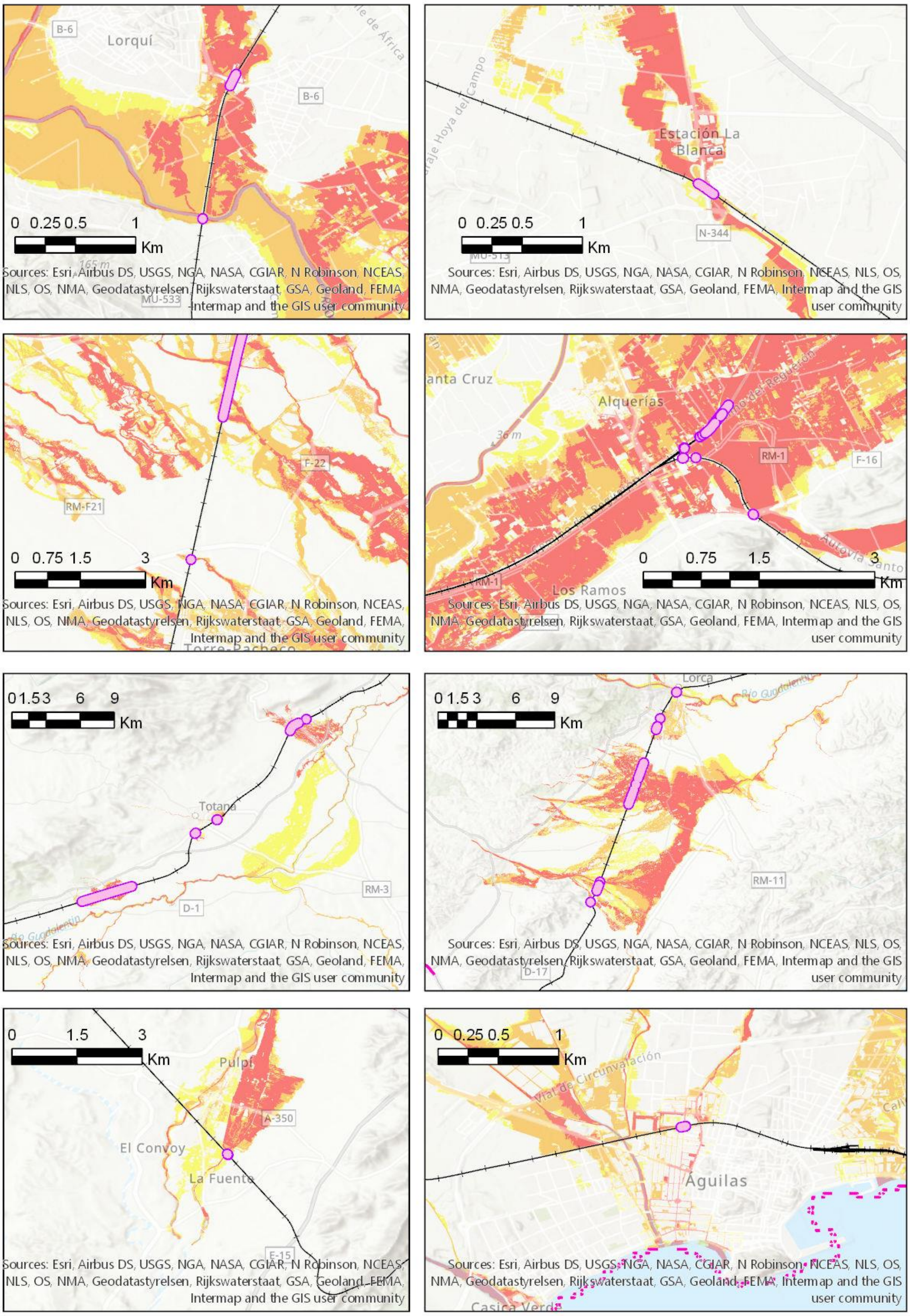

Figure 49: Detail of hot-spots for flood (in pink): case study 2b. (Source: *Ministerio para la Transición Ecológica*)

6.2.2 Landslide

The hot-spot maps are generated overlapping the spatial probability of landslide occurrence (landslide susceptibility) at European scale (ELSUS v2, Wilde et al., 2018), with the location of the railway tracks for the two case studies. The map on spatial probability of landslide shows 5 levels of landslide susceptibility: 5 = very high, 4 = high, 3 = medium, 2 = low. Figure 50 and Figure 51 show different levels of landslide susceptibility in a coloured scale. The railway tracks included into susceptibility levels "high" or very "high" (i.e., areas coloured in orange and red in Figure 50, Figure 51 and Figure 52) can be considered at high risk of landslide. On the other hand, the tracks passing through areas at medium level of susceptibility (i.e., coloured in yellow) can be considered exposed at a medium level of landslide risk. The railway tracks exposed at high and medium levels of landslide risk need to be investigated in detail. Field surveys can be useful to verify and determine the actual level of risk. Moreover, for a detail risk assessment analysis it is important to evaluate, at a local scale, the interaction between different railway structures (i.e., embankments, bridges, underpasses, etc…) and the expected runout and landslide intensities. It is important to mention that these analyses only consider the railway tracks and not the related functional structures (i.e., embankments, bridges, underpasses, etc…). Attention should be paid for case study 2b (Figure 52, b), north of the town of Cieza, where the railway track is passing through an area exposed to a very high landslide susceptibility level.

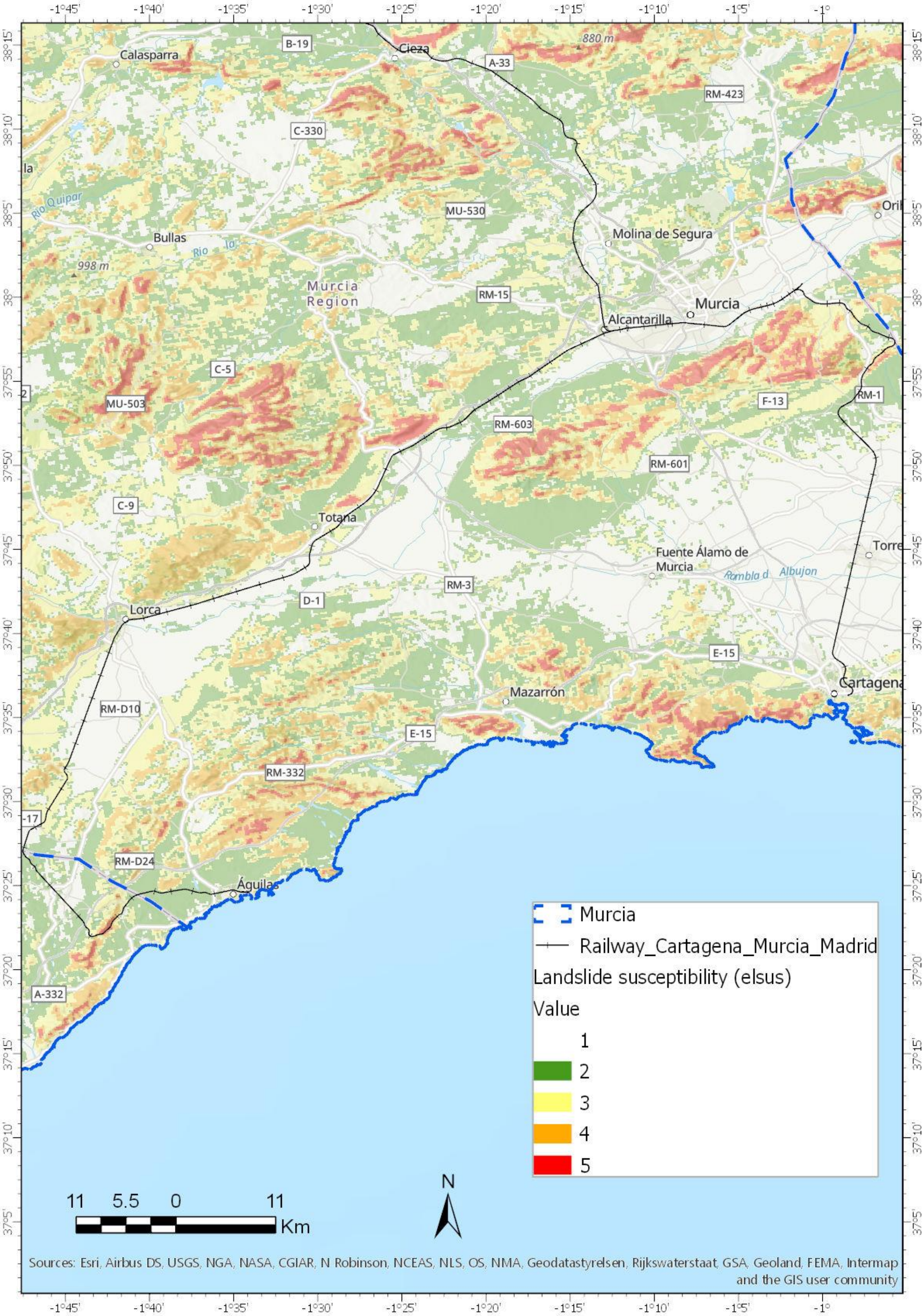

Figure 50: Different levels of landslide susceptibility and location of the railway track (case study 2b). (Source: ELSUS v2, Wilde et al., 2018)

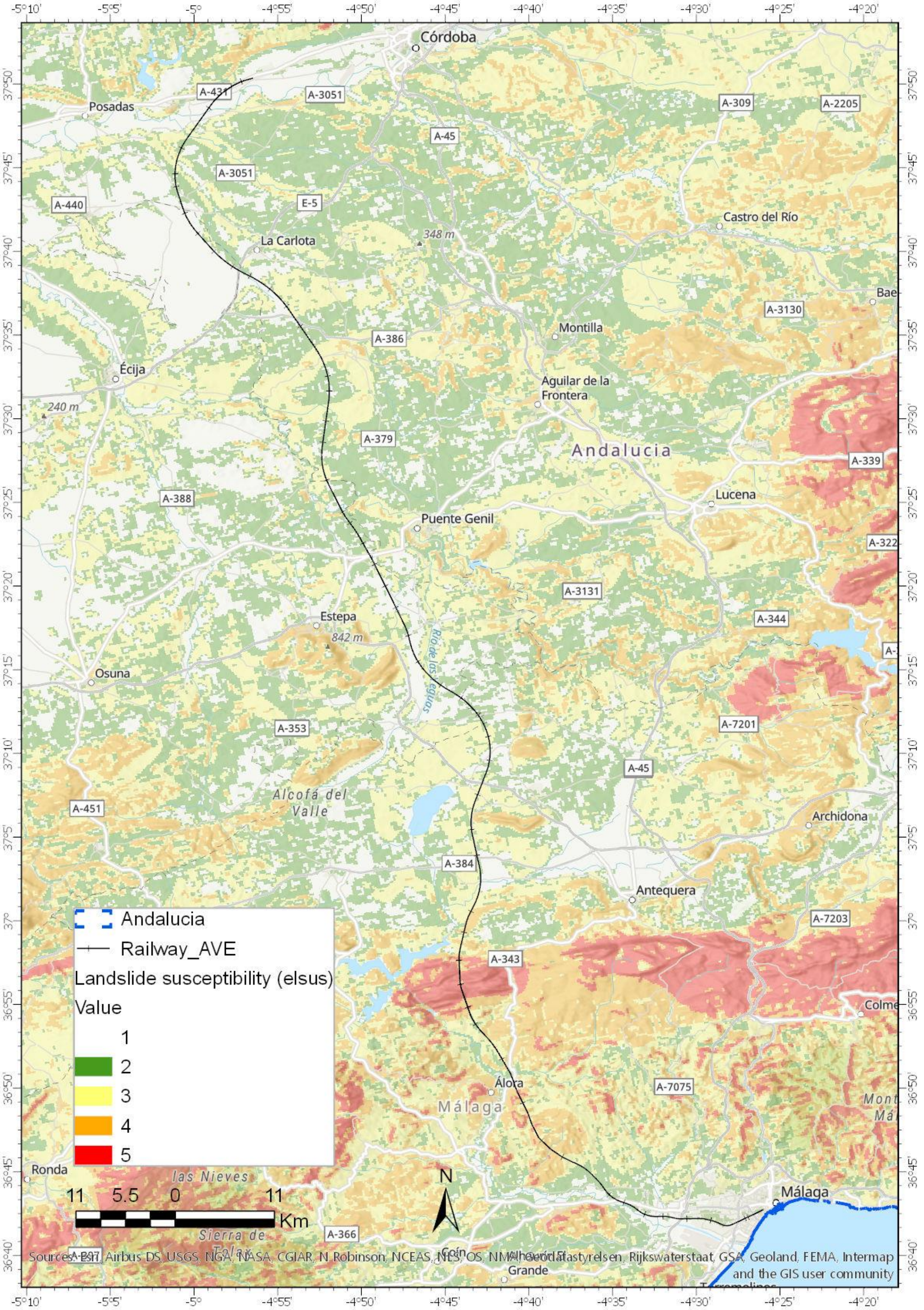

Figure 51: Different levels of landslide susceptibility and location of the railway track (case study 2a). (Source: ELSUS v2, Wilde et al., 2018)

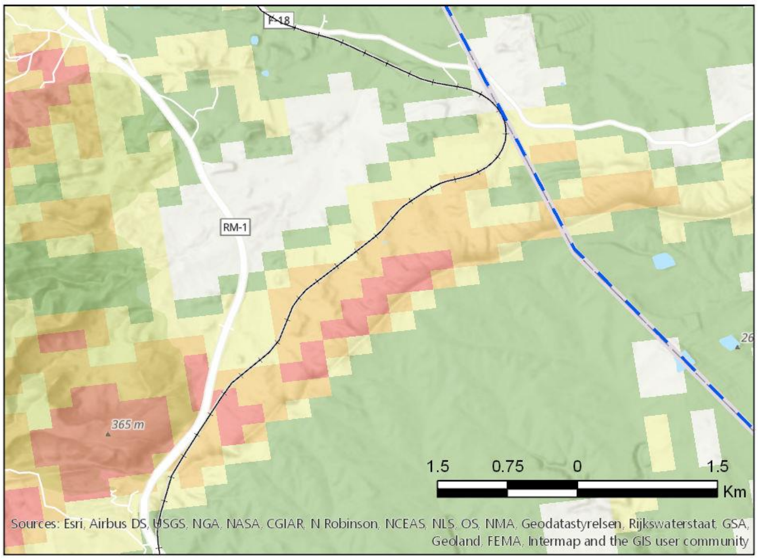

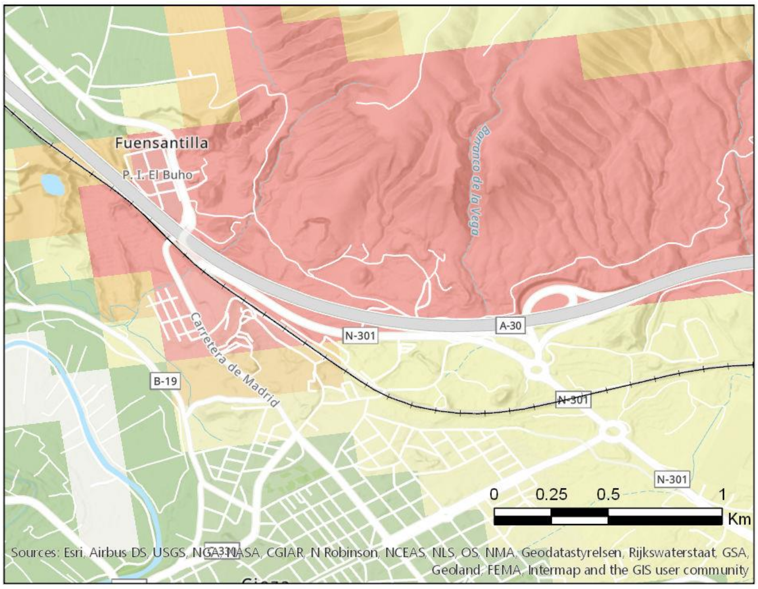

Figure 52: Detail of the railway tracks exposed at high and very high risk of landslide for the case study 2b, Murcia region. (Source: ELSUS v2, Wilde et al., 2018)

6.2.3 Heat-wave

The hot-spot maps for heat-wave are generated overlapping the NEO database (see section 3.2.4) with the position of the railway tracks for the two case studies. The NEO database provides several interesting indicators for describing the weather temperature and climate change. In the following, the land surface temperature maps have been used for analysing the heatwaves in summer time for the two case study areas. The land surface temperature is set of maps representing temperature patterns (in Celsius degrees) of the top millimetre (or “skin”), for both day-and night-time, of the land surface — including bare land, snow or ice cover, urban areas, and cropland or forest canopy — as observed by MODIS in clear-sky conditions for the period 2000-2018.

Figure 53-Figure 58 show the temperature patterns of the top millimetre (or “skin”) of the land surface in Celsius degrees in the month of August for the last three years (i.e., 2016, 2017 and 2018). August is chosen as reference month for heat-wave since it is, usually, the warmest month of the year in Spain. The Figure 53-Figure 58 show how the temperature in August is extremely high and above the 39 degrees in both case studies. However, the highest temperatures, around 45 degrees, have been registered, in the last three years (2016-2018), in Andalucia region, case study 2a. These analyses can be useful in order to prevent the possible deformation of the railway tracks due to the high temperatures. Particular attention should be focused on the high-speed railway track of case study 2a, in Andalucia region, where very high temperatures are usually reached during summer time (Figure 54, Figure 56 and Figure 58).

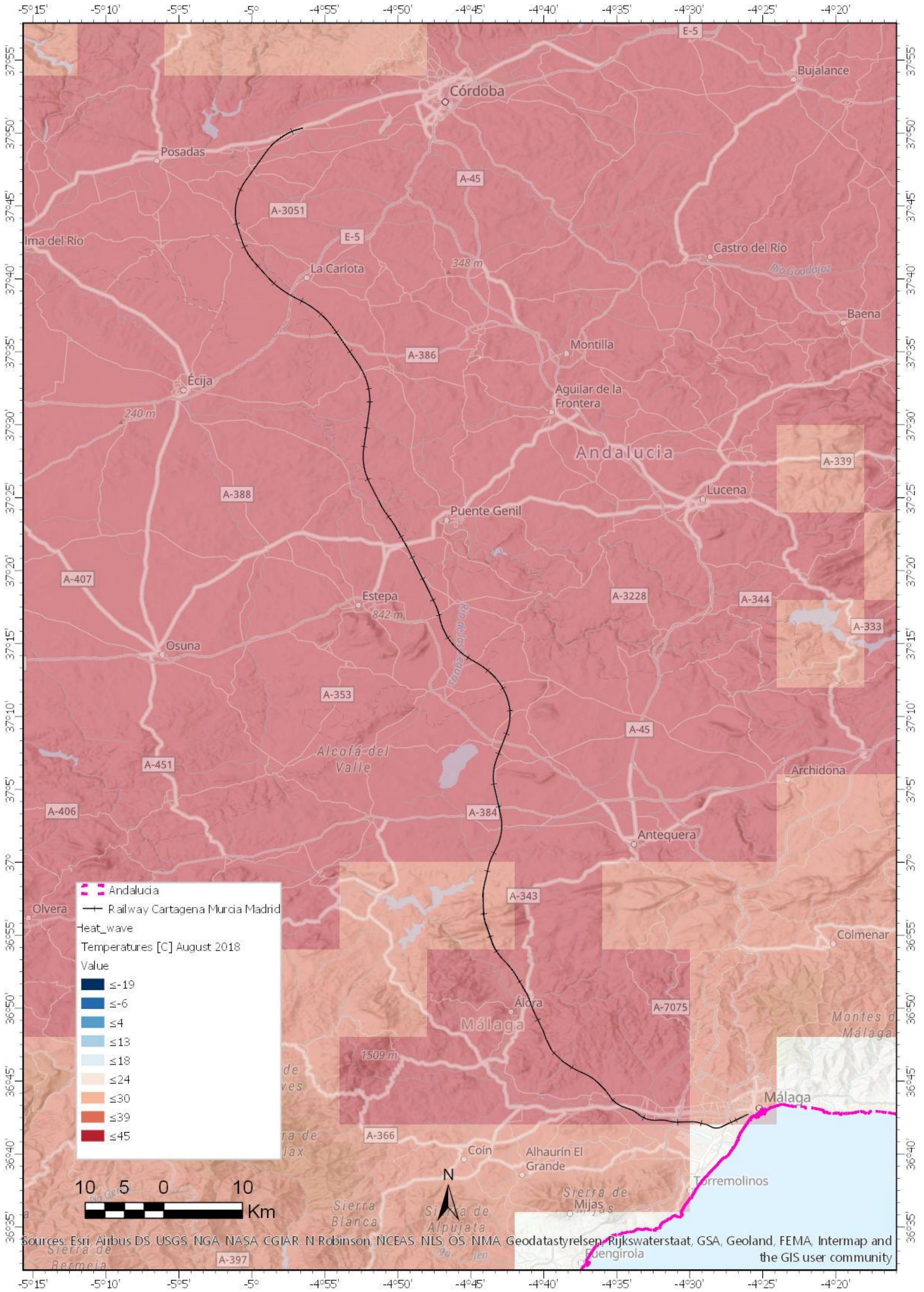

Figure 53: Case study 2a, Andalucia region: daytime land surface temperature (C) in August 2016. (Source: NEO database)

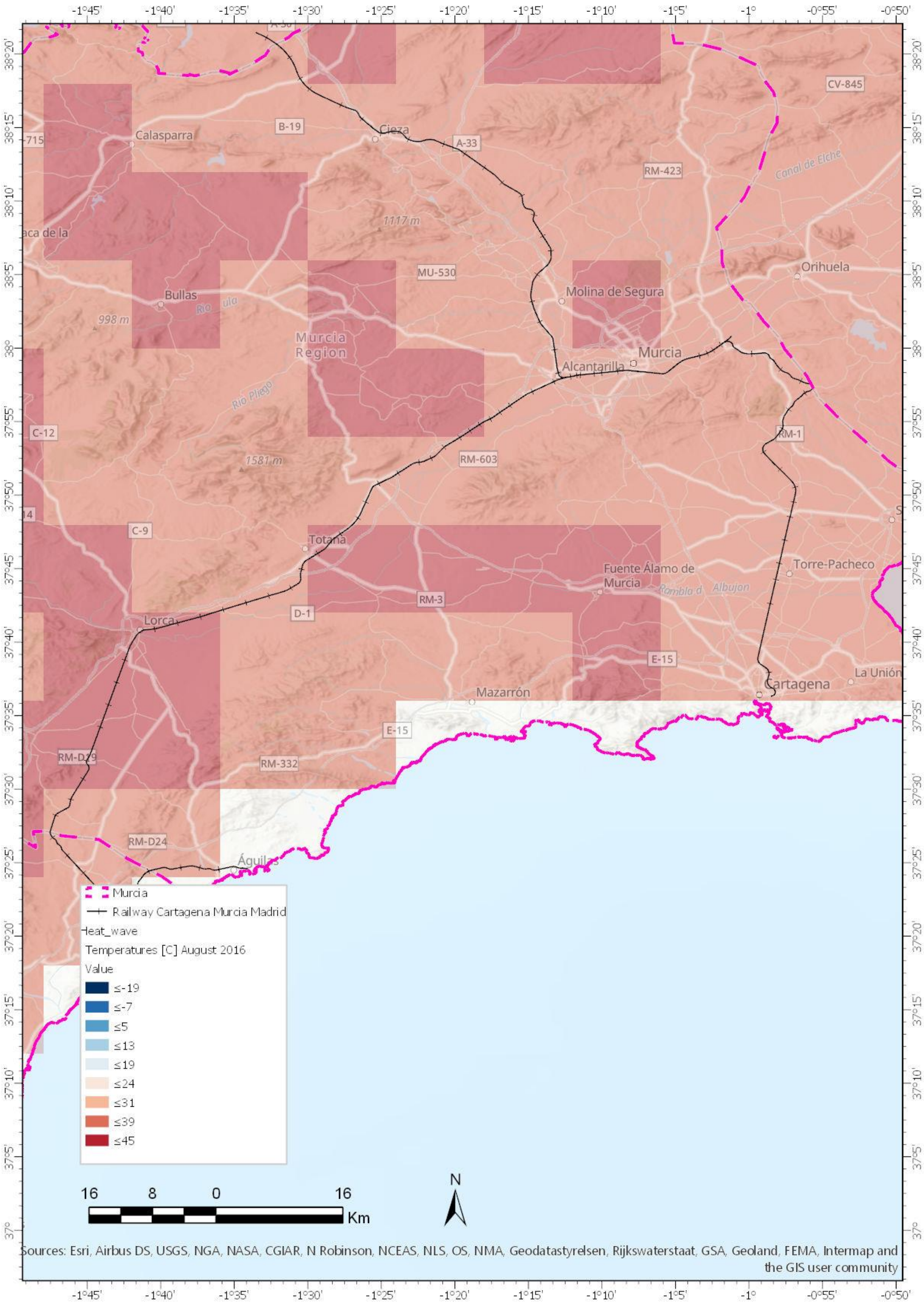

Figure 54: Case study 2b, Murcia region: daytime land surface temperature (C) in August 2016. (Source: NEO database)

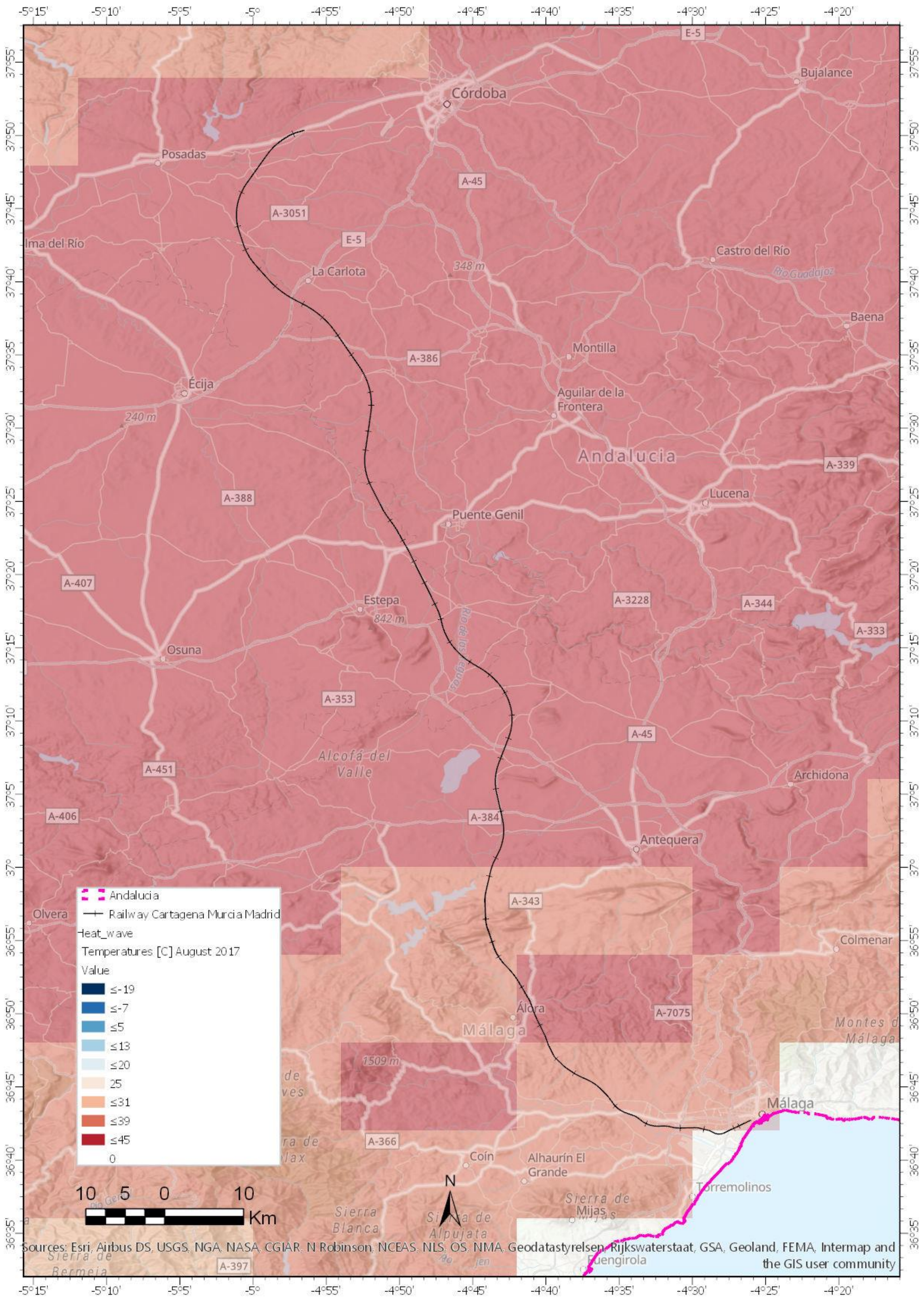

Figure 55: Case study 2a, Andalucia region: daytime land surface temperature (C) in August 2017. (Source: NEO database)

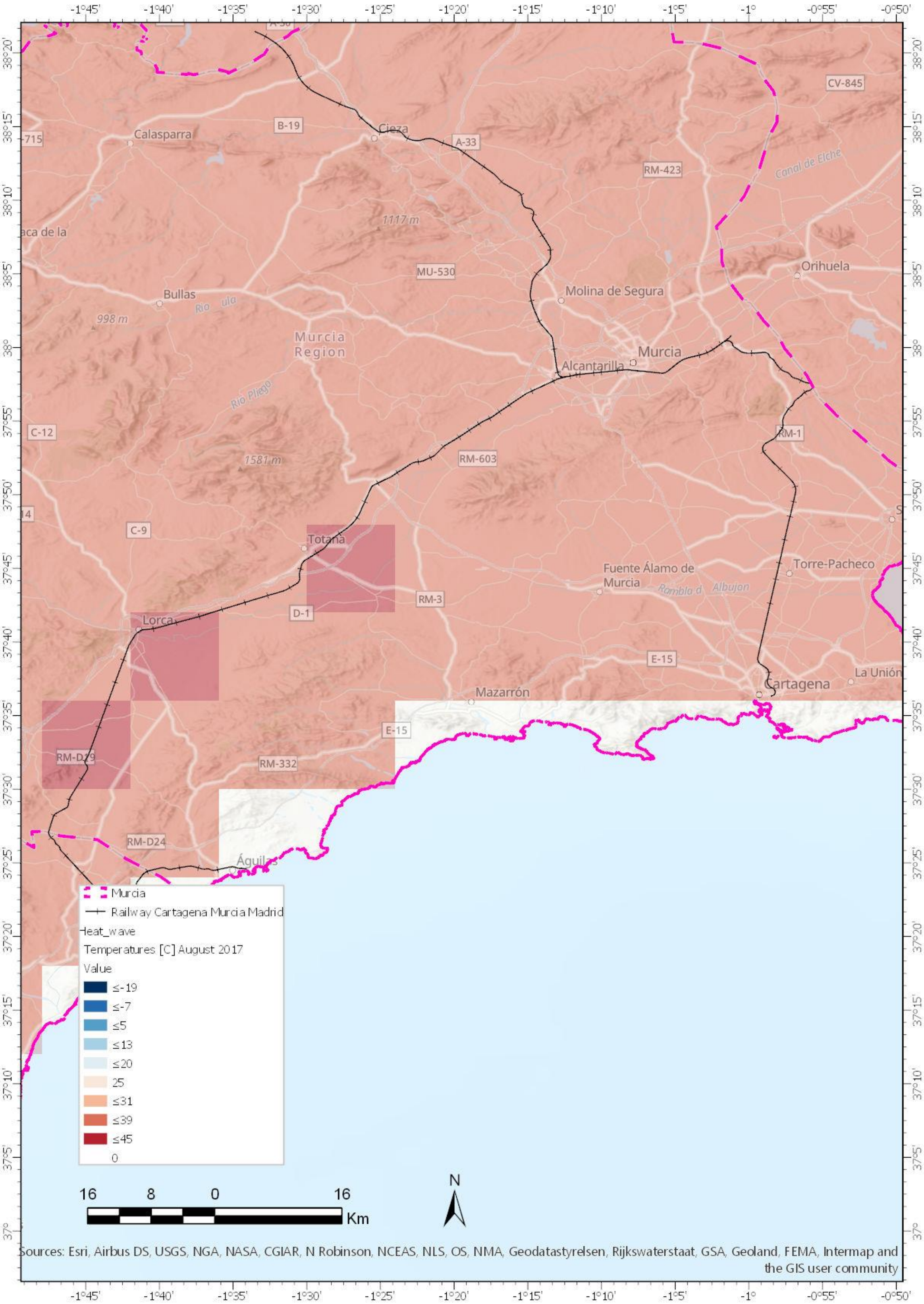

Figure 56: Case study 2b, Murcia region: daytime land surface temperature (C) in August 2017. (Source: NEO database)

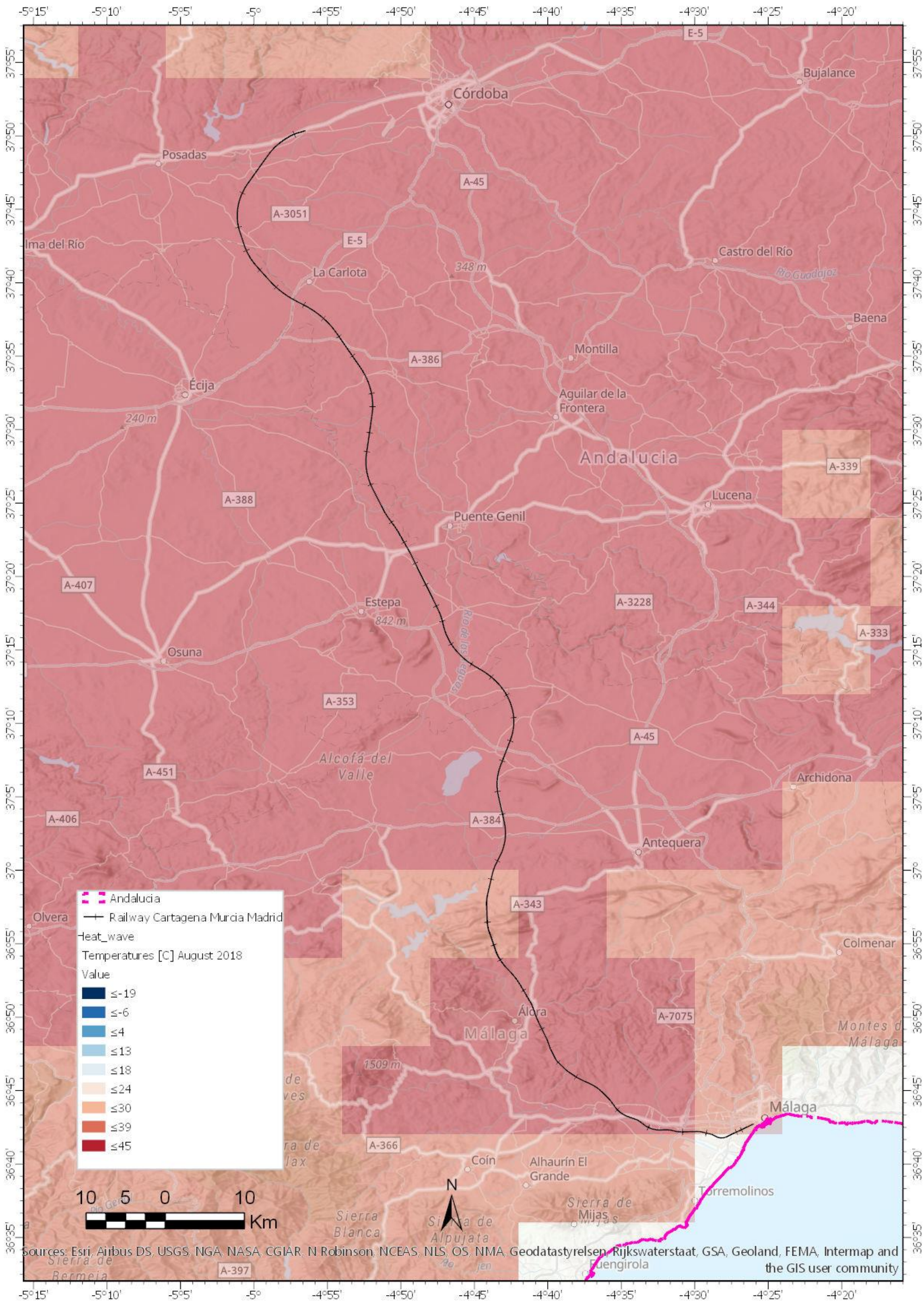

Figure 57: Case study 2a, Andalucia region: daytime land surface temperature (C) in August 2018. (Source: NEO database)

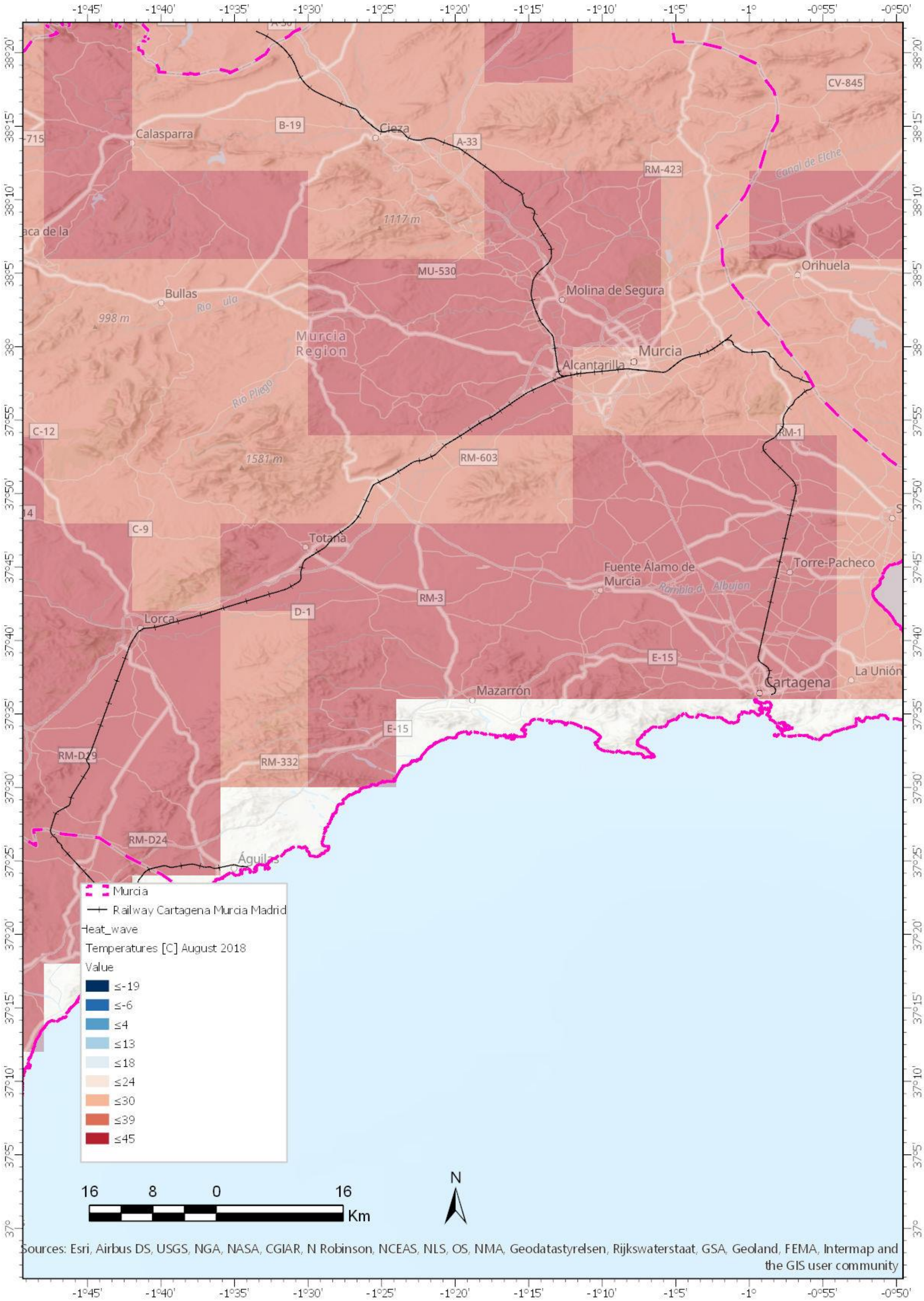

Figure 58: Case study 2b, Murcia region: daytime land surface temperature (C) in August 2018. (Source: NEO database)

6.2.4 Earthquake

For the analysis on the earthquake hazard the database GAR Atlas (see section 3.2.5) has been considered. The chosen variable for hazard intensity measure is the peak ground acceleration (PGA). Hazard maps considering different return periods have been considered. Specifically, hazard maps considering 475, 975 years, as return periods, have been analysed. Those values can represent a medium/high intensity event. The following Figure 59 and Figure 62 show the peak ground acceleration (PGA) in cm/s^2 for the two case studies for the two return periods selected. Considering the 475-years return period earthquake Spain has values of peak ground acceleration smaller than 100 cm/s^2 (Figure 59, Figure 60). Some PGA higher than that value can be reached in Southern Spain, between Malaga and Almeria. Differently, with a 975-years return period earthquake most of Andalucia and Murcia can have PGA between 100 and 200 cm/s^2 (Figure 61, Figure 62).

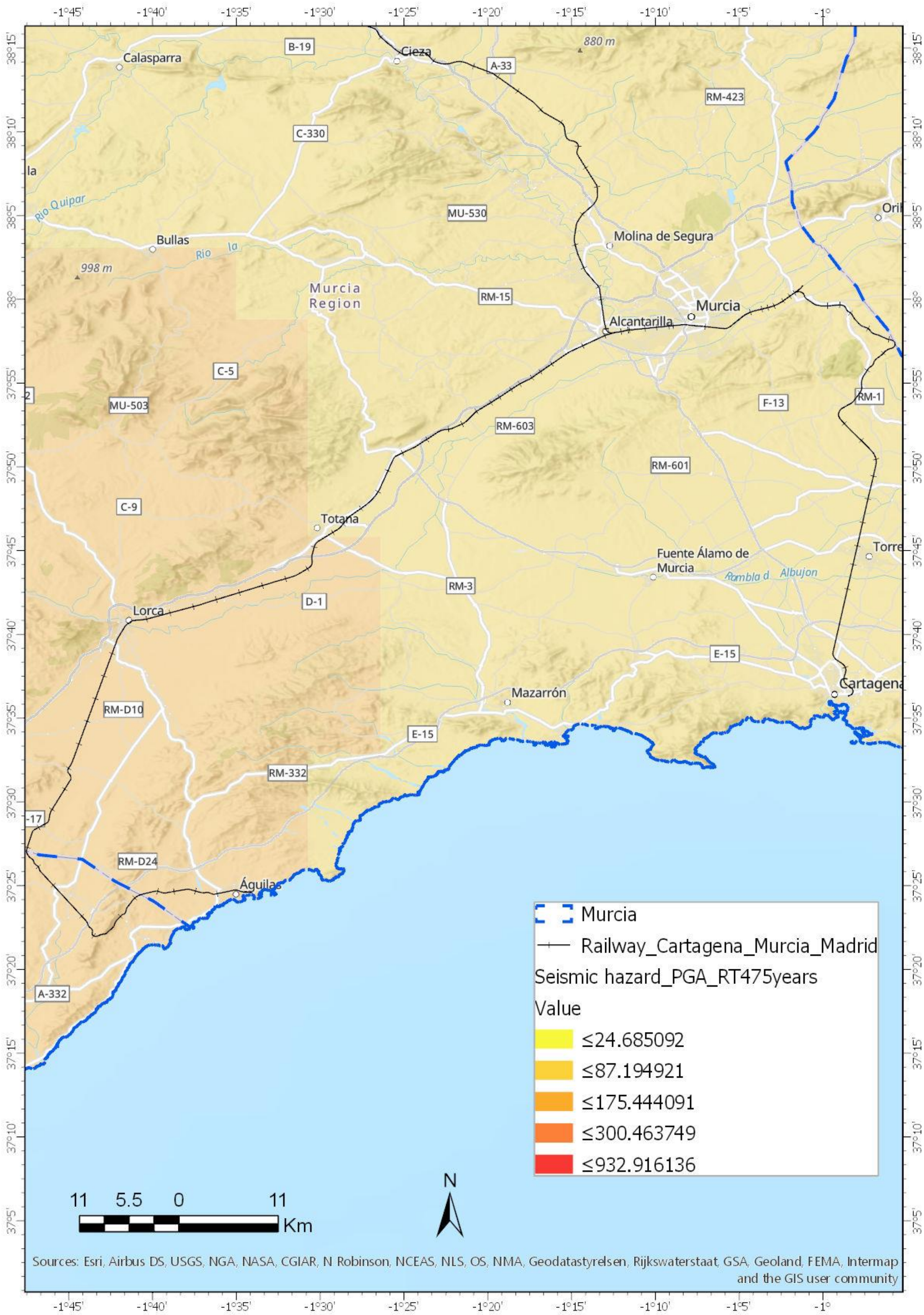

Figure 59: Case study 2b, Murcia region: peak ground acceleration (PGA) referred to horizontal ground with return period of 475 years. Values in cm/s^2. (Source: GAR Atlas database)

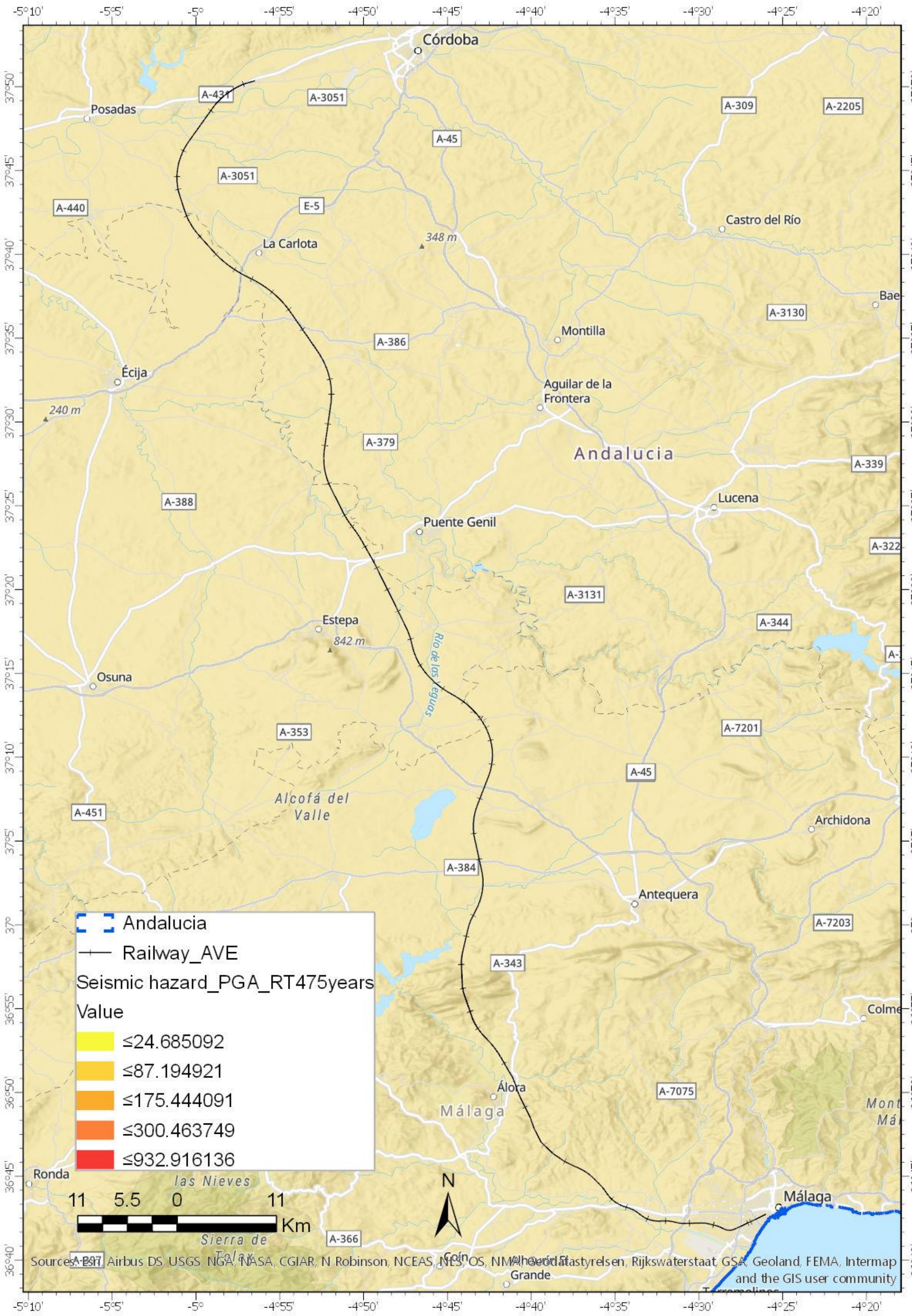

Figure 60: Case study 2a, Andalucia region: peak ground acceleration (PGA) referred to horizontal ground with return period of 475 years. Values in cm/s^2. (Source: GAR Atlas database)

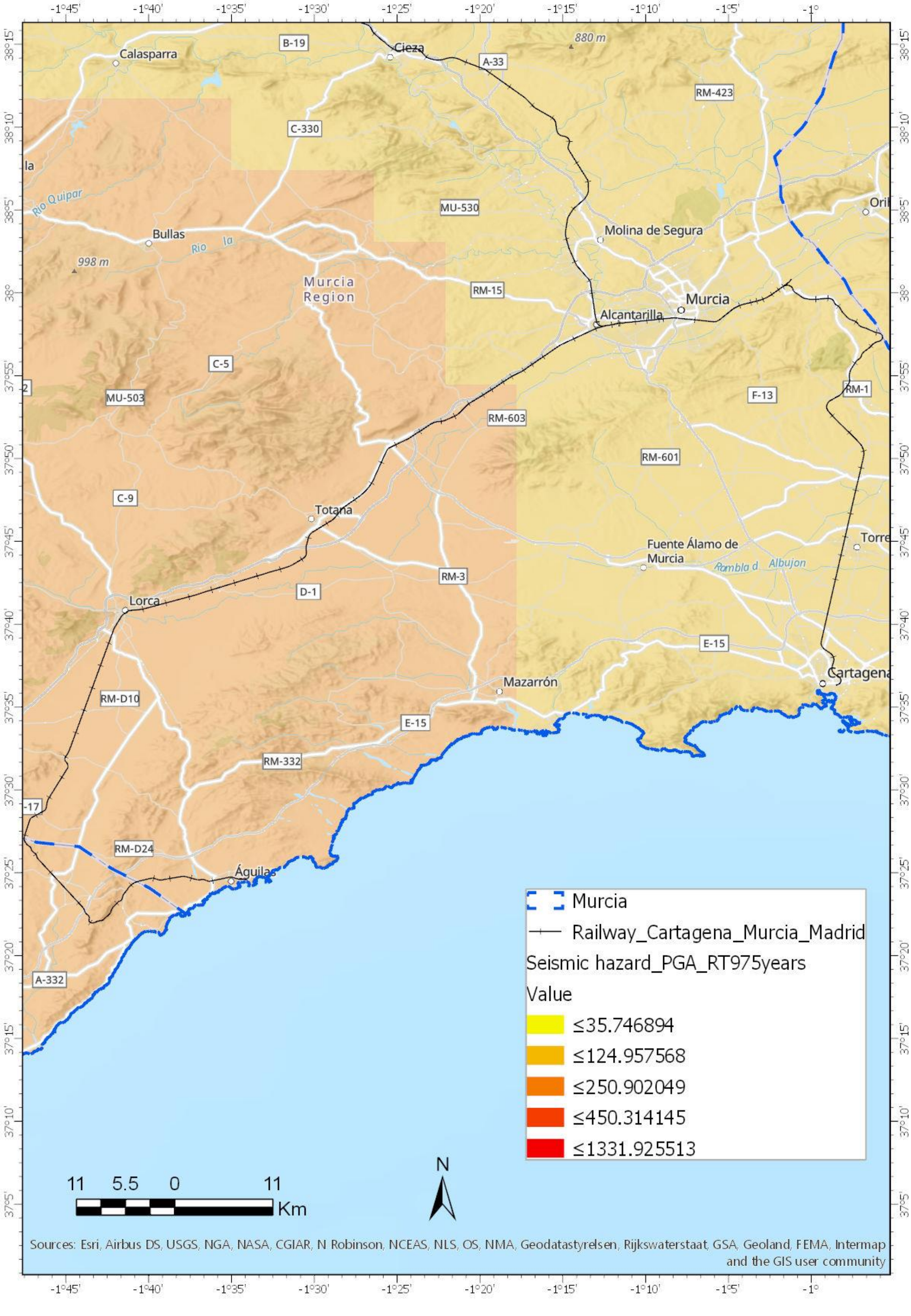

Figure 61: Case study 2b, Murcia region: peak ground acceleration (PGA) referred to horizontal ground with return period of 975 years. Values in cm/s^2. (Source: GAR Atlas database)

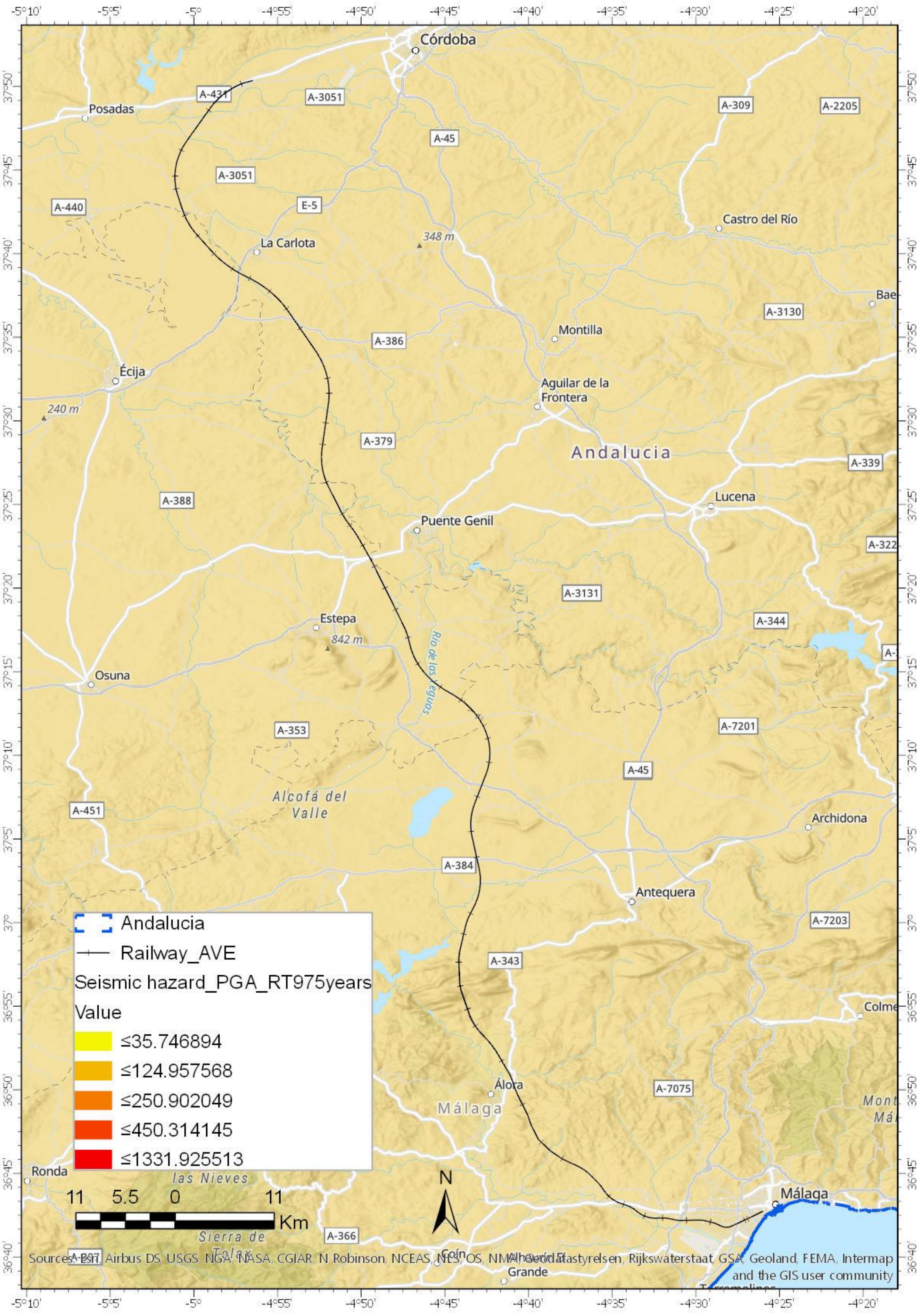

Figure 62: Case study 2a, Andalucia region: peak ground acceleration (PGA) referred to horizontal ground with return period of 475 years. Values in cm/s^2. (Source: GAR Atlas database)

6.2.5 Rainfall

The INTACT database (see section 3.2.7) has been used to produce the following maps on precipitation. The INTACT project provides different rainfall indicators, in particular, two of them can be considered as interesting and representative for our pilot area: R99p, the percentage of annual total precipitation due to events with precipitation higher than 99th percentile of the reference period; SDII, simple daily intensity index (annual precipitation divided by the number of wet days, defined as days with precipitation greater or equal to 1mm, in the year). The first indicator indicates the amount of rainfall due to extreme events (with precipitation higher than 99th percentile), the latter expresses the daily intensity and can be seen as an indicator of the average precipitation of the area. The case study 2b shows a high value for the R99p index (Figure 63). In this area between 8 and 11% of the total annual rainfall is due to extreme events. For case study 2a, the area around Malaga (Figure 64) has a high percentage of the R99p index, around 8%. The remain areas are around 6-7%. Concerning SDII indicator, the case study 2a, in the Andalucia region, has a higher daily intensity index than case 2b in the Murcia region, resulting in a higher piovosity in terms of mm of rainfall per day. The results for the SDII indicator cannot be displayed in a GIS environment but are showed, together with the other indicators, at the following webGis page of the INTACT project:
http://scm.ulster.ac.uk/~scmresearch/intactnew/index.php/Extreme_weather_maps.

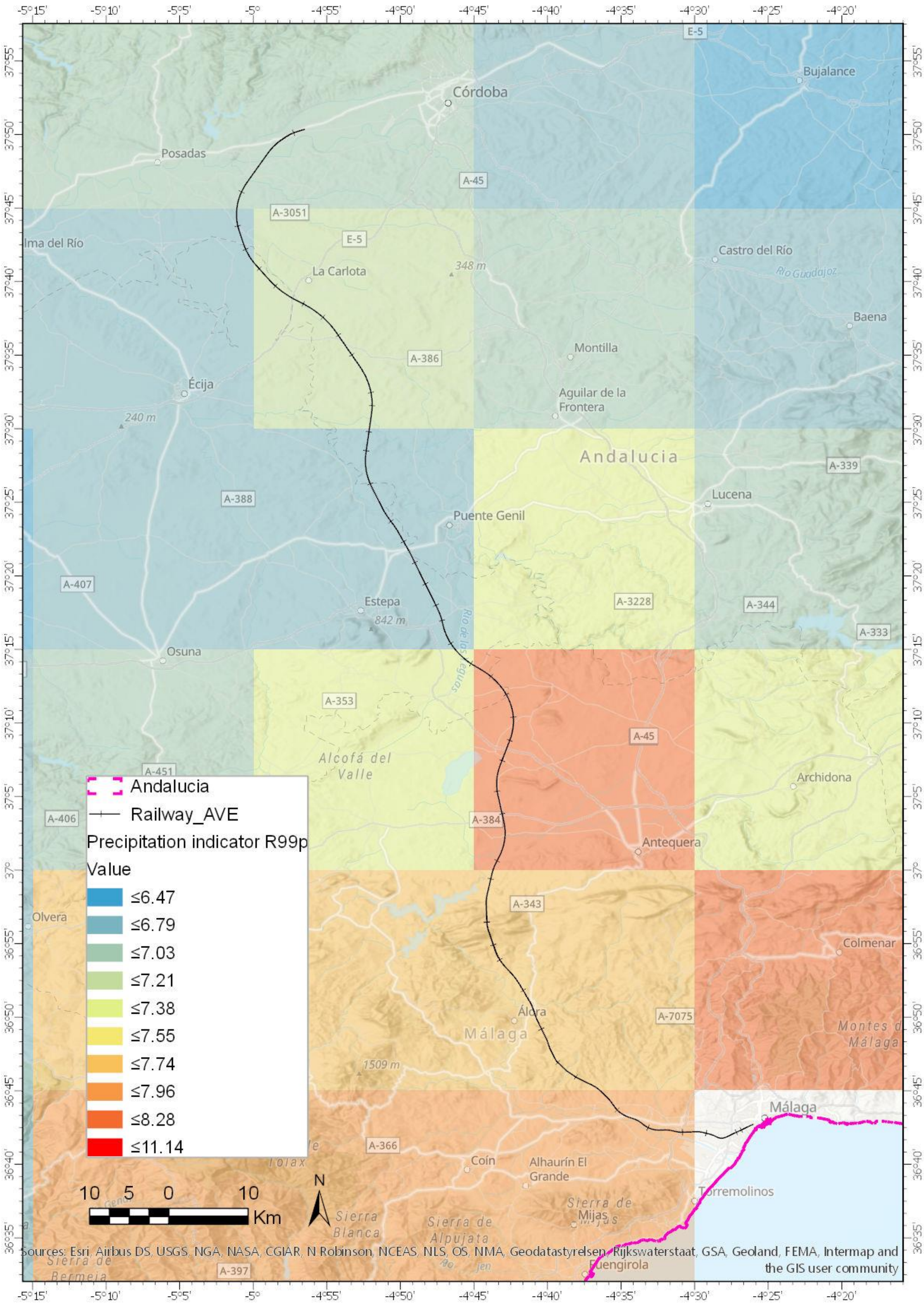

Figure 63: Case 2b, Andalucia region. R99p, the percentage of annual total precipitation due to events with precipitation higher than 99th percentile of the reference period. (Source: INTACT EWE database)

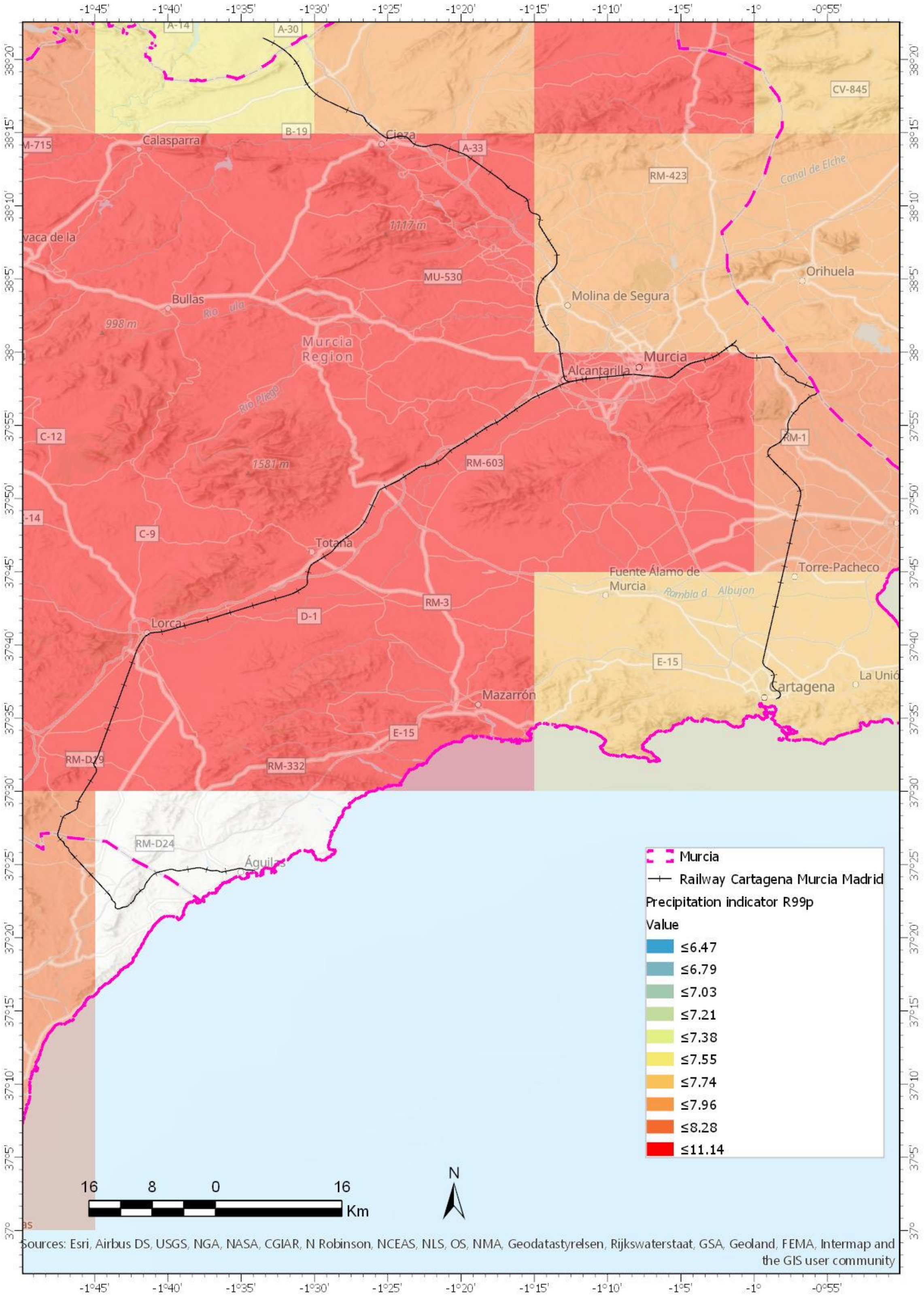

Figure 64: Case 2a, Murcia region. R99p, the percentage of annual total precipitation due to events with precipitation higher than 99th percentile of the reference period. (Source: INTACT EWE database)

6.3 United Kingdom (London and Manchester)

The pilot area in the UK is the North Sea - Mediterranean corridor. The Case study will be carried-out in the London-Manchester rail network including 337.3 railway km, 1'235 bridges, 13 tunnels, 846 retaining walls and 28 stations. This section provides hot-spot maps to better identify the areas exposed at risk. The maps are obtained overlapping different natural hazard maps with the railway tracks of the pilot area. The aim is to highlight critical areas to be mitigated. The following hazards have been considered for the pilot area in United Kingdom: flood, wind.

6.3.1 Flood

The JRC floods collection (see section 3.2.1) consists in 13 datasets about flood hazard maps at European and global scale. This collection contains pan-European flood hazard maps at 100-meter resolution for several return periods, from 10 to 500 years. The maps of Figure 65 and Figure 66 show the flood prone areas in UK for flood events with return periods respectively for 10 and 100 years. The cell values indicate water depth in meters. Tracks exposed to flood are located just before and after the city of Lichfield, North-east from Birmingham (Figure 65 and Figure 66).

6.3.2 Wind

The INTACT database on wind (see section 3.2.7) has been used to produce the following maps. The indicator describing the maximum of daily mean wind intensity has been considered for the analysis. The pilot area can be exposed to a maximum of daily mean wind intensity between 12-14,2 m/s (Figure 67).

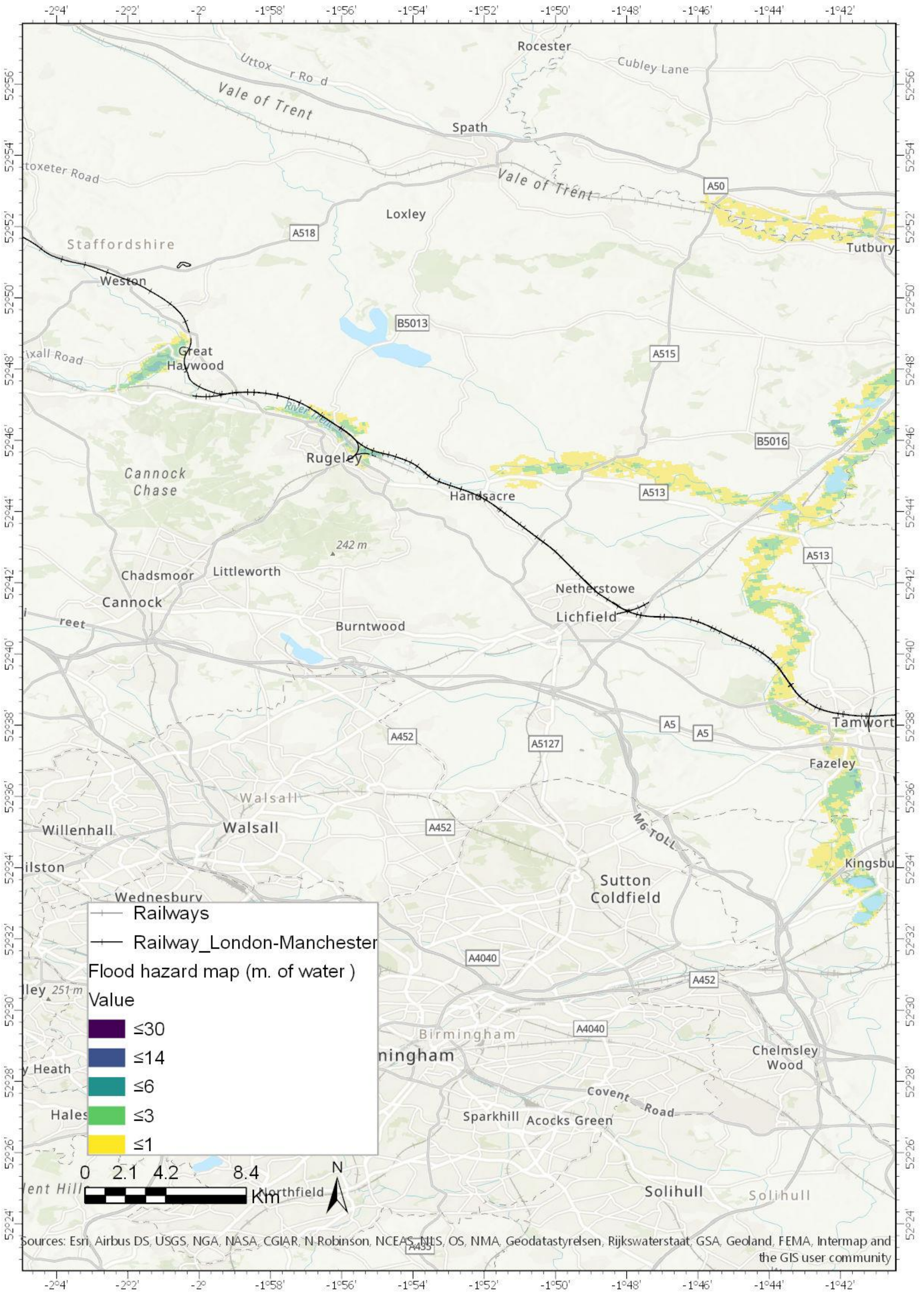

Figure 65: European flood hazard map 10 years return period. The map is expressed in terms of flood depth (m). (Source: JRC flood database)

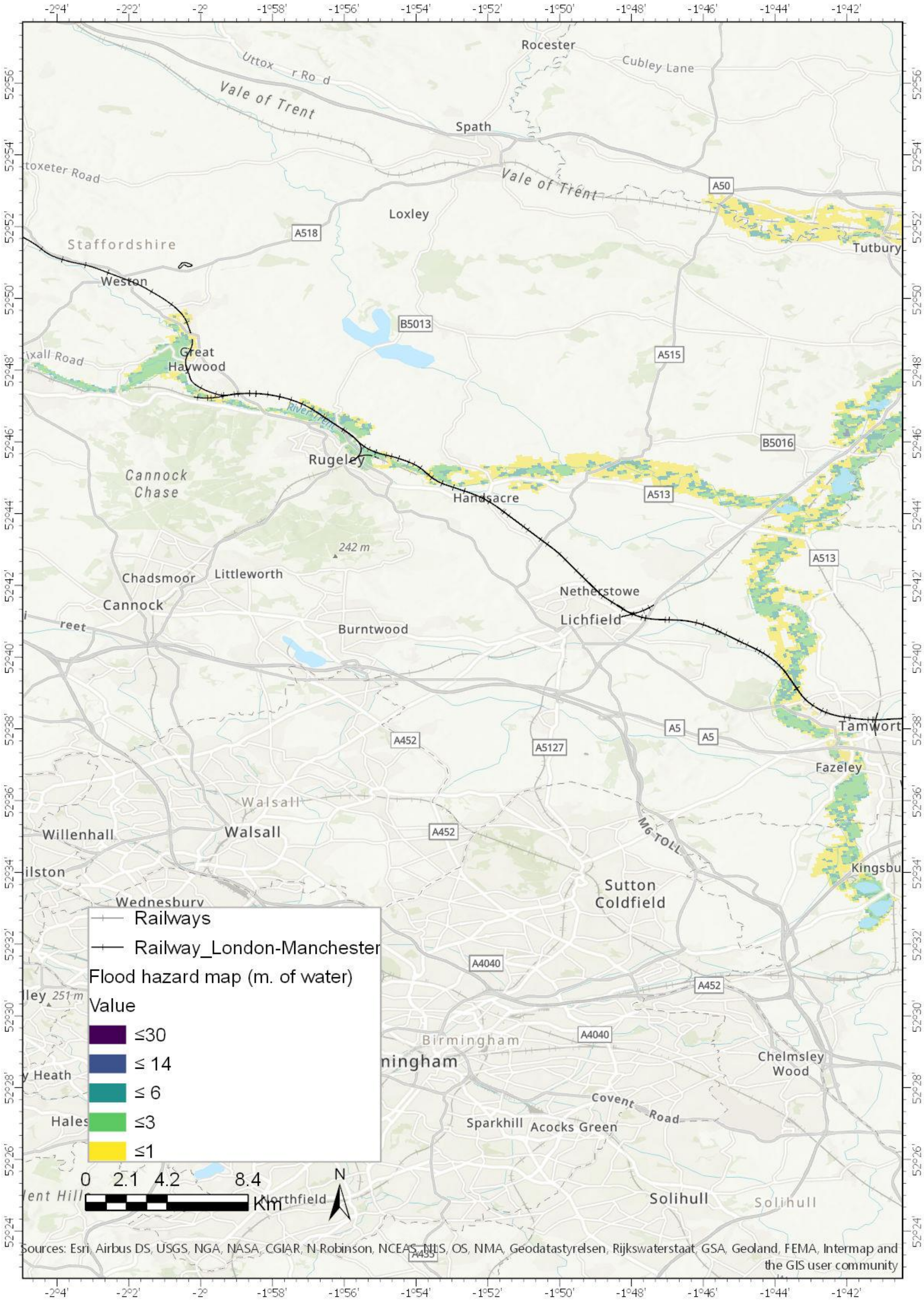

Figure 66: European flood hazard map 100 years return period. The map is expressed in terms of flood depth (m). (Source: JRC flood database)

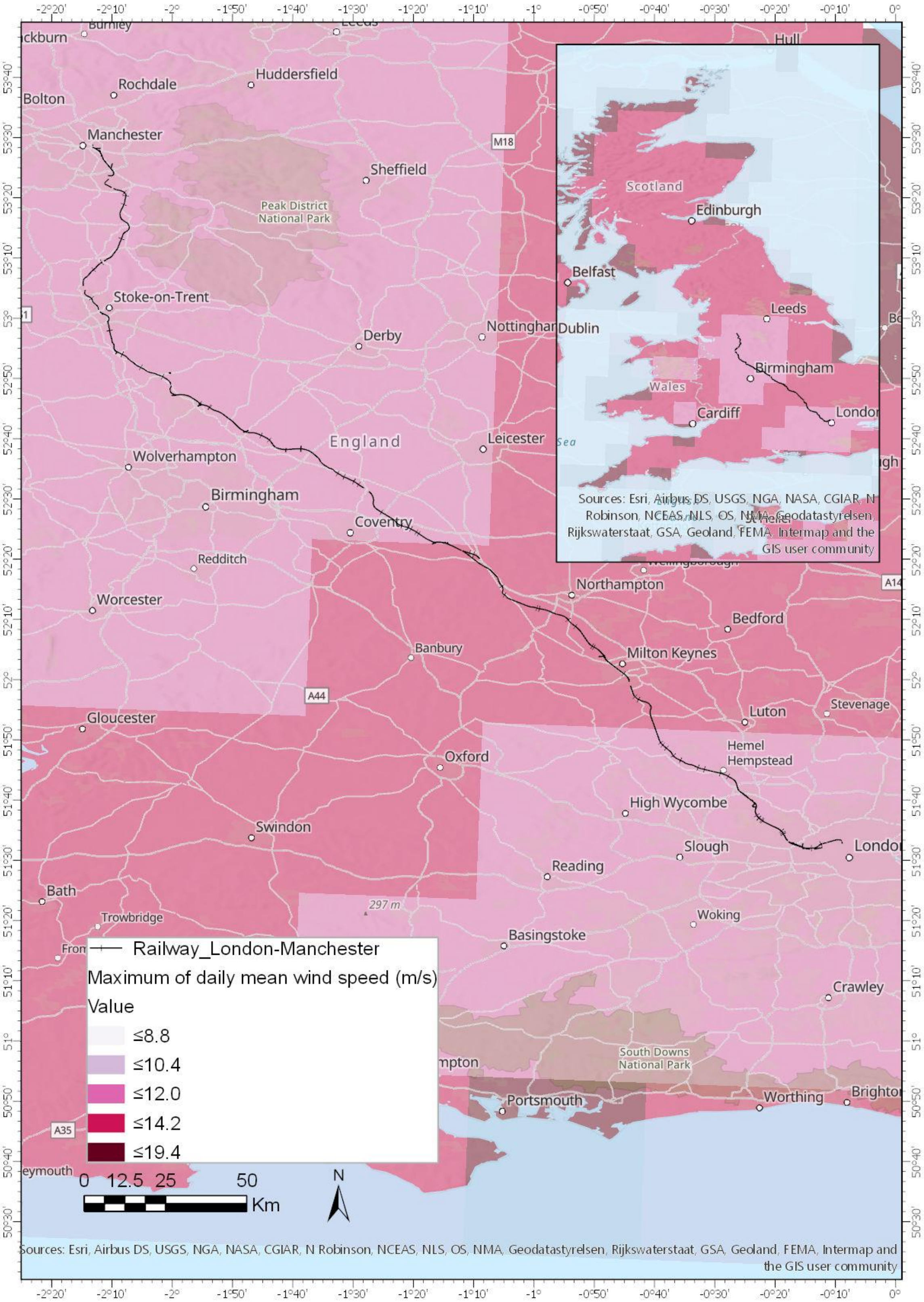

Figure 67: Maximum of daily mean wind speed in m/s. (Source: INTACT EWE database)

7. Conclusions

The number of natural disasters and the economic damage have dramatically increased in the last three decades. The reason can be ascribed to the increase in number and intensity of events due to climate change and continuous urbanization in areas often exposed to natural hazards. Roads and railways are important infrastructures ensuring social and commercial exchanges within and among different nations. In our changing environment the infrastructures are more often exposed to different types of natural hazards, such as: flood, landslide, heat-wave, earthquake, wildfire. The impacts generated may produce accidents, damages to the whole infrastructure or components, delays and malfunctioning of the transportation network, resulting in economic and social consequences. Natural hazards can lead to an escalation of such negative impacts if no counter-measures are taken.

The first step in risk reduction of natural and weather-related phenomena is to identify the infrastructures exposed and the different natural hazards threatening them. A review of the available natural hazards databases at Global and European scales has been carried out. An increased number of governmental and research institutions are involved, or have been involved in the last decade, with natural hazards analysis and mapping. Detailed hazard maps, as well as reliable forecasts of such events, are important parts of risk management of natural hazards. The list of databases for mapping natural hazards is reported in the Appendix tables. The tables gather information on different natural hazards: flood, wildfire, wind, heat, landslide, earthquake.

A detailed research has then been conducted to find databases specifically for our three Pilot areas: Spain, Portugal, United Kingdom. The databases at a national scale have been used to determine the natural hazards threatening the infrastructures. The information on the different infrastructures (railways and primary, secondary and tertiary roads) are provided by Open Street Map per each nation. Whenever a national database for a specific natural hazard was not available, global databases have been considered. Hot-spot maps have been produced by overlapping the hazard maps with road and railway tracks. The results in section 6 highlight the location of the infrastructures at risk and the different natural hazards threatening them. The most relevant data for the pilot areas will be integrated into the SAFEWAY Infrastructure Management System (WP7). In this report the impacts of the different events are described verbally in terms of failure modes. To each failure mode, the impact is classified as either reduction of mobility in the network or damage to infrastructure assets – or both. Strategies, tools and data for quantification of the impacts will be established in D2.2, D2.3 and applied within WP5.

Acknowledgements

This deliverable was carried out in the framework of the GIS-Based Infrastructure Management System for Optimized Response to Extreme Events of Terrestrial Transport Networks (SAFEWAY) project, which has received funding from the European Union's Horizon 2020 research and innovation programme under grant agreement No 769255.

References

Alfieri, L., Burek, P., Feyen, L. and Forzieri, G., 2015, 'Global warming increases the frequency of river floods in Europe', *Hydrology and Earth System Sciences* 19(5), 2 247–2 260 (doi: 10.5194/hess-19-2247-2015).

Alfieri, L., Salamon, P., Bianchi, A., Neal, J., Bates, P., Feyen, L., 2014. 'Advances in pan-European flood hazard mapping', Hydrological Processes 28(13), 4067-4077 (https://doi.org/10.1002/hyp.9947)

ANYWHERE (2017) "Workplan – Global view". Anywhere. Accessed February 20, 2019. http://anywhere-h2020.eu/workplan/#

The British Crown (2019a). "Floodmap for planning", service. Accessed February 25, 2019. https://flood-map-for-planning.service.gov.uk/

The British Crown (2019b). "Euro Windstorm Event Response", service. Accessed February 25, 2019. https://www.metoffice.gov.uk/services/industry/insurance/euro-windstorm

Bedia, J., Herrera, S., Camia, A., Moreno, J. M. and Gutiérrez, J. M., 2013, 'Forest fire danger projections in the Mediterranean using ENSEMBLES regional climate change scenarios', Climatic Change 122(1–2), 185–199 (doi: 10.1007/s10584-013-1005-z).

Copernicus (2019). "European flood awareness system, EFAS". Accessed February 20, 2019. https://www.efas.eu/en/european-flood-awareness-system-efas

Dilley, M., Chen, Robert S., Deichmann, U., Lerner-Lam, A. L., Arnold, M., Agwe, JM, Buys, P., Kjevstad, O., Lyon, B., Yetman, G., 2005. Natural disaster hotspots: A global risk analysis. Washington, DC: World Bank. http://documents.worldbank.org/curated/en/621711468175150317/Natural-disaster-hotspots-A-global-risk-analysis. ISBN 0-8213-5930-4.

EEA (2017) Climate change, impacts and vulnerability in Europe 2016, An indicator-based report, EEA Report No1/2017, ISSN 1977-8449, www.eea.europa.eu.

EEA (2019). "Datasets in Urban Adaptation Map Viewer", website. Accessed February 19, 2019. https://climate-adapt.eea.europa.eu/knowledge/tools/urban-adaptation/Urban-Adaptation-datasets

EFFIS (2019). "European Forest Fire Information System (EFFIS)". Accessed February 20, 2019. Updated February 1, 2019. http://effis.jrc.ec.europa.eu/

Ferrovial(2018) Internal Report Case Study 2 in Spain, Internal Delivery 9.1.SP, October 2018.

Cardona, O.D., Ordaz, M.G., Yamin, L.E., 2015. Update on the Probabilistic Modelling of Natural Risks at Global Level: Global Risk Model. Global earthquake and tropical cyclone hazard assessment. Disaster risk assessment of countries for seismic, cyclonic (wind and storm surge) and flood. The 2015 Global Assessment Report on Disaster Risk Reduction. Geneva, Switzerland: UNISDR.

Global Wind Atlas (2019), "The Global Wind Atlas", service. Accessed February 25, 2019. https://globalwindatlas.info/

Global and Regional Vegetation Fire Monitoring from Space. Planning and Coordinated International Effort (Eds. Ahern F, Goldammer JG, Justice C), pp 105-124, 2001

Gregoire, J.M., Cahoon, D.R., Stroppiana, D., Li, Z., Pinnock, S., Eva, H., Arino, O., Rosaz, J.M., and I. Csiszar, 2001. Forest fire monitoring and mapping for GOFC: current products and information networks based on NOAA-AVHRR, ERS-ATSR, and SPOT-VGT.

I-REACT (2019). Website. Accessed 19. February 2019. http://project.i-react.eu/

Khabarov, N., Krasovskii, A., Obersteiner, M., Swart, R., Dosio, A., San-Miguel-Ayanz, J., Durrant, T., Camia, A. and Migliavacca, M., 2014, 'Forest fires and adaptation options in Europe', Regional Environmental Change 16(1), 21–30 (doi: 10.1007/s10113-014-0621-0)

Leviäkangas, P. and Saarikivi, P., 2012, European extreme weather risk management — Needs, opportunities, costs and recommendations, EWENT project, Deliverable 6.

Moreno, J. M. (ed), 2014, Forest fires under climate, social and economic changes in Europe, the Mediterranean and other fire-affected areas of the world, FUME project.

NetworkRail (2019) Note on critical events and maps for LNW route, 14 January 2019.

NetworkRail (2014) Route weather resilience and climate change adaptation plans, London North West, September 2014.

Planetek (2019) Data Acquisition Report, SAFEWAY deliverable D3.1, August 2019.

Purdy,G. (2010) Perspective ISO 31000:2009—Setting a New Standard for Risk Management Risk Analysis, Vol. 30, No. 6, DOI: 10.1111/j.1539-6924.2010.01442.x ,2010.

Sachs, J. D., A. D. Mellinger, and J. L. Gallup. 2001. The geography of poverty and wealth. Scientific American 284(3): 70–75

Snelder M. and Calvert (2016) Quantifying the impact of adverse weather conditions on road network performance, European Journal of Transport and Infrastructure Research (EJTIR), Issue 16(1), 2016, pp. 128-149, ISSN: 1567-7141

UVIGO (2019) SAFEWAY Pilots, Internal SAFEWAY deliverable InD 3.1.1, June 2019.

Verde, J.C., Zezere, J.L., 2011. Avaliação e validação da susceptibilidade e perigosidade de incêndio florestal em Portugal Continental (in portuguese). In book: Trunfos de uma Geografia Activa: desenvolvimento local, ambiente, ordenamento e tecnologia. DOI: 10.14195/978-989-26-0244-8_91

VTT(2011) Extreme weather impacts on transport systems, VTT working papers 168, EWENT Project Deliverable D1, ISBN 978-951-38-7509-1, URL: http://www.vtt.fi/publications/index.jsp

Wald, D.J., Quintoriano, V., Heaton, T.H., Kanamori., H., 1999. Relationships between peak ground acceleration, peak ground velocity, and Modified Mercalli intensity in California. Earthquake Spectra, 15: 557-564.

Wilde, M., Günther, A., Reichenbach, P., Malet, J.-P., Hervás, J., 2018. Pan-European landslide susceptibility mapping: ELSUS Version 2. Journal of Maps, 14(2), 97-104 and supplemental map.

(19) (PDF) Relationship Between Peak Ground Acceleration and Modified Mercalli Intensity in Costa Rica. Available from: https://www.researchgate.net/publication/228755080_Relationship_Between_Peak_Ground_Acceleration_and_Modified_Mercalli_Intensity_in_Costa_Rica [accessed Feb 26 2019].

SAFEWAY

GIS-BASED INFRASTRUCTURE MANAGEMENT SYSTEM FOR OPTIMIZED RESPONSE TO EXTREME EVENTS OF TERRESTRIAL TRANSPORT

NETWORKS

Grant Agreement No. 769255

European critical hazards (natural) D2.1- Appendices

WP 2 Risk Factors and Risk Analysis

Deliverable ID	**D2.1**
Deliverable name	**GIS Map and identification of hot spots of sudden extreme natural hazard events, including database with impact and return periods**
Lead partner	NGI
Contributors	UMINHO, Ferrovial, Budimex, TØI, IMC, IP, NR

PUBLIC

Appendix 1 Natural hazard databases

Table A1.1: *Flood*

a) Hazard maps

Name	Description	Scale	Type of file	Variable	Descriptor	Database	Web-site
Joint Research Centre Data Catalogue (JRC)	flood hazard maps	Europe	Geotiff (1 tfw, 1 tif, 2 xml, 1 ovr) 13 datasets (6 for Europe)	water depth	(m)	10, 20, 50, 100, 200, 500-year return period	http://data.jrc.ec.europa.eu/collection/floods
Global Risk Data Platform	Physical exposure to floods	World	Geotiff (raster format) 1 folder with 3 files (xml,tfw.tif)	annual physical exposition	(people/ year)	Observed flood from 1999 to 2007. In area where no information was available, it was set to 50 years return period. A population grid for the year 2010, provided by LandScanTM Global Population Database	https://preview.grid.unep.ch/index.php?preview=data&events=floods&evcat=3&lang=eng
Global Risk Data Platform	Economical exposition to flood	World	Geotiff (raster format) 1 folder with 3 files (xml,tfw.tif)	economical exposure	($/year)	Observed flood from 1999 to 2007. In area where no information was available, it was set to 50 years return period. A population grid for the year 2010, provided by LandScanTM Global Population Database	https://preview.grid.unep.ch/index.php?preview=data&events=floods&evcat=4&lang=eng
Global Risk Data Platform	risk index for flood hazard	World	Geotiff (raster format) 1 folder with 4 files (xml,nfo,tfw.tif)	risk index	(from 1 to 5)		https://preview.grid.unep.ch/index.php?preview=data&events=floods&evcat=5&lang=eng
Global Assessment Report on Disaster Risk Reduction 2017	flood hazard maps (riverine flood)	World	Grid file From 'Download section' we can download capraViewer (sw) and	frequency	5 classes (<1, 1.1-3.0, 3.1-5.0, 5.1-7.0, >7.1)	25, 50, 100, 200, 500, 1000-year return period	https://risk.preventionweb.net/capraviewer/download.jsp?tab=9&map

Name	Description	Scale	Type of file	Variable	Descriptor	Database	Web-site
			files of all the layers of the maps through all the years (Flood hazard 25, 50, 100, 200, 500, 1000 years). We get a folder per country; the 4 countries are here (ESP, NLD, PRT, GBR) (1 grd). Going to 'Download Portal' we get a folder per hazard and then country (there's no Portugal). There's a folder per year range (2 grd files, 1 ame file)				center=0,1123252.698 2849&mapzoom=2; http://unisdr.envcomp.eu/browse/Hazard/Earthquake_Hazard_maps
Socioeconomic Data and Applications Center (SEDAC)	Global Flood Hazard Frequency and Distribution	World	asc.grid 2 files (asc, prj) or 3 (asc, dbf, prj) (raster, map, map service)	decile	decile	1985 - 2003 (poor or missing data in the early/mid 1990s)	http://sedac.ciesin.columbia.edu/data/set/ndh-flood-hazard-frequency-distribution/data-download
Socioeconomic Data and Applications Center (SEDAC)	Global Flood Proportional Economic Loss Risk	World	asc.grid 2 files (asc, prj) (raster, map, map service)	decile	decile	Calendar date: 2000	http://sedac.ciesin.columbia.edu/data/set/ndh-flood-proportional-economic-loss-risk-deciles/data-download
Socioeconomic Data and Applications Center (SEDAC)	Global Flood Total Economic Loss Risk Deciles		1 asc, 1 dbf, 1 prj	decile	decile	2000	https://sedac.ciesin.columbia.edu/data/set/ndh-flood-total-economic-loss-risk-deciles/data-download
Socioeconomic Data and Applications Center (SEDAC)	Global Flood Mortality Risks and Distribution		1 asc, 1 dbf, 1 prj			1981 - 2000	https://sedac.ciesin.columbia.edu/data/set/ndh-flood-mortality-risks-distribution/data-download

a) Catalogues

Name	Description	Time interval data	Method	Scale	Type of file	Variable	Descriptor	Web-site
Global Risk Data Platform	flood events	1999-2007		World	Shape ESRI GRID (7 adf, 1 xml, 1 log) ArcInfo (1 xml, 1 nfo, 2 rtf) ERDAS (1 xml, 1 nfo, 2 rtf)	flood events		*http://floodobservatory.colorado.edu/Archives/index.html* *https://preview.grid.unep.ch/index.php?preview=data&events=floods&evcat=1&lang=eng*

Table A1.2*: Wildfire Catalogues*

Name	Description	Time interval data	Method	Scale	Type of file	Variable	Descriptor	Web-site
Global Risk Data Platform	Fires events	1995-2011	t is based on the modified algorithm 1 product of World Fire atlas (WFA, ESA-ESRIN) dataset	world	gif(monthly map), ASCII (.fire; monthly fire location; 1 line per file : [Date (YYYYMMDD) Orbit (9999) Time (SS.MMM) Latitude (s999.999) Longitude (s999.999)])	Fire events	(event/pixel)	*https://preview.grid.unep.ch/index.php?preview=data&events=fires&evcat=1&lang=eng* *http://due.esrin.esa.int/page_wfa.php*
Global Risk Data Platform	Fires density	1997-2010	t is based on the modified algorithm 1 product of World Fire atlas (WFA, ESA-ESRIN) dataset		Geotiff 2 xml, 1 tfw, 1 tiff	Fire events	(event/pixel)	https://preview.grid.unep.ch/index.php?preview=data&events=fires&evcat=3&lang=eng
NASA earth observations	Fires density	24/02/2000-25/06/2019	Up to date information and satellite images on fires, storms, floods, volcanoes, earthquakes, and droughts	world	Geotiff, CSV, , CSV for Excel, Jpeg,png, GeoTIFF (floating point), GeoTIFF (raster), GoogleEarth 1.0 degrees (360x180) 0.5 degrees (720x360) 0.25 degrees (1440x720) 0.1 degrees (3600x1800)	Fire pixels	(event/pixel)	https://neo.sci.gsfc.nasa.gov/view.php?datasetId=MOD14A1_M_FIRE

Name	Description	Time interval data	Method	Scale	Type of file	Variable	Descriptor	Web-site
Socioeconomic Data and Applications Center (SEDAC)	Global Fire Emissions Indicators	1997-2015	Satellite-Derived Environmental Indicators.		CSV Excel file Pdf file	Burned area (hectares) and total carbon content (tons)	(hectares, tons)	http://sedac.ciesin.columbia.edu/data/set/sdei-global-fire-emissions-indicators-country-level-1997-2015/data-download#close
European Forest Fire Information System (EFFIS)	Burned area indicator	2008-2018			csv per country. Interactive map can be seen too in second link	Burned areas and number of fires		http://effis.jrc.ec.europa.eu/static/effis_stats/ http://effis.jrc.ec.europa.eu/static/effis_current_situation/public/index.html

Table A1.3: Wind

Name	Description	Time interval data	Method	Scale	Type of file	Variable	Descriptor	Database	Web-site
INTACT project	wind prediction	short (2011-2040), medium (2040-2070), long (2070-2100)		World	ascii grid map and grid are showed directly on the website	http://scm.ulster.ac.uk/~scmresearch/intactnew/index.php/Extreme_weather#Extreme_indicators_based_on_wind	m/s	Absolute, trend or Delta	http://scm.ulster.ac.uk/~scmresearch/intactnew/index.php/Extreme_weather_maps
The Global Wind Atlas	wind speed	unknown	from mesoscale to microscale (250 m)	World	tiff 1 pdf, 3 csv, 3 json, 1 geojson	velocity	m/s		https://globalwindatlas.info/area/Norway/Hordaland
European Monthly wind speed (MAPPE model)	wind speed	2002-2006	aggregated station indices data for all stations within ECA&D.	Europe	adf 1 folder per month (5 adf,1 xml). 1 info folder (1 dir, several dat, several nit)	velocity	m/s		http://data.jrc.ec.europa.eu/dataset/jrc-mappe-europe-setup-d-11-wind-speed
European Climate Assessment (ECAD)	Maximum value of daily maximum wind gust (FXx)	1939 – 2018 (year is seen inside the txt files, 2nd column of the data; indexFXx000123.txt - indexFXx016617.txt)	aggregated station indices data for all stations within ECA&D.	aggregated station indices data for all stations within ECA&D.	txt (1 txt per station and 1 with stations info)			yearly/ daily	https://eca.knmi.nl//download/millennium/millennium.php
European Climate Assessment (ECAD)	Days with FG <= 2 m/s (calm days) (FGcalm)	1923 – 2018 (year is seen inside the txt files, 2nd column of the data; indexFGcalm000035.txt - indexFXx016617.txt)	aggregated station indices data for all stations within ECA&D.	aggregated station indices data for all stations within ECA&D.	txt (1 txt per station and 1 with stations info)			yearly/ daily	https://eca.knmi.nl//download/millennium/millennium.php

Name	Description	Time interval data	Method	Scale	Type of file	Variable	Descriptor	Database	Web-site
European Climate Assessment (ECAD)	Days with southerly winds (DDsouth)	1939 – 2018 (year is seen inside the txt files, 2nd column of the data; indexDDsouth000123.txt - indexDDsouth016617.txt)	aggregated station indices data for all stations within ECA&D.	World	txt (1 txt per station and 1 with stations info)			yearly/ daily	https://eca.knmi.nl//download/millennium/millennium.php
European Climate Assessment (ECAD)	Days with easterly winds (DDeast)	1939 – 2018 (year is seen inside the txt files, 2nd column of the data; indexDDeast000123.txt - indexDDeast016617.txt)	aggregated station indices data for all stations within ECA&D.	World	txt (1 txt per station and 1 with stations info)			yearly/ daily	https://eca.knmi.nl//download/millennium/millennium.php
European Climate Assessment (ECAD)	Days with FG >= 6 Bft (10.8 m/s) (FG6Bft)	1920 – 2018 (year is seen inside the txt files, 2nd column of the data; indexFG6Bft000034.txt - indexFG6Bft016617.txt)	aggregated station indices data for all stations within ECA&D.	World	txt (1 txt per station and 1 with stations info)			yearly/ daily	https://eca.knmi.nl//download/millennium/millennium.php
European Climate Assessment (ECAD)	Days with northerly winds (DDnorth)	1939 – 2018 (year is seen inside the txt files, 2nd column of the data; indexDDnorth000123.txt - indexDDnorth016617.txt)	aggregated station indices data for all stations within ECA&D.	World	txt (1 txt per station and 1 with stations info)			yearly/ daily	https://eca.knmi.nl//download/millennium/millennium.php

Name	Description	Time interval data	Method	Scale	Type of file	Variable	Descriptor	Database	Web-site
European Climate Assessment (ECAD)	Days with westerly winds (DDwest)	1939 – 2018 (year is seen inside the txt files, 2nd column of the data; indexDDwest000123.txt - indexDDwest016617.txt)	aggregated station indices data for all stations within ECA&D.	World	txt (1 txt per station and 1 with stations info)			yearly/ daily	https://eca.knmi.nl//download/millennium/millennium.php
European Climate Assessment (ECAD)	Mean of daily mean wind speed (FG)	1920 – 2018 (year is seen inside the txt files, 2nd column of the data; indexFG000034.txt - indexFG016617.txt)	aggregated station indices data for all stations within ECA&D.	World	txt (1 txt per station and 1 with stations info)			yearly/ daily	https://eca.knmi.nl//download/millennium/millennium.php

Table A1.4: Heat

Catalogues

Name	Description	Time interval data	Method	Scale	Type of file	Variable	Descriptor	Database	Web-site
INTACT project	temperature prediction	short (2011-2040), medium (2040-2070), long (2070-2100)		world	ascii grid map and grid are showed directly on the website	http://scm.ulster.ac.uk/~scmresearch/intactnew/index.php/Extreme_weather#Extreme_indicators_based_on_wind	°C, day	Absolute, Trend or Delta	http://scm.ulster.ac.uk/~scmresearch/intactnew/index.php/Extreme_weather_maps
NASA EARTH OBSERVATIONS	Land surface temperature anomaly	18/02/2000-25/06/2019	Up to date information and satellite images on fires, storms, floods, volcanoes, earthquakes, and droughts	world	Geotiff, CSV, CSV for Excel, Jpeg,png, GeoTIFF (floating point), GeoTIFF (raster), GoogleEarth 1.0 degrees (360x180) 0.5 degrees (720x360) 0.25 degrees (1440x720) 0.1 degrees (3600x1800)	°C	°C/pixel	monthly	https://neo.sci.gsfc.nasa.gov/view.php?datasetId=MOD_LSTAD_M
NASA EARTH OBSERVATIONS	global temperature anomaly	01/1880-04/2019 (per year or per month)			Geotiff, CSV, CSV for Excel, Jpeg,png, GeoTIFF (floating point), GeoTIFF (raster), GoogleEarth 1.0 degrees (360x180) 0.5 degrees (720x360)		°C/pixel	monthly, yearly	https://neo.sci.gsfc.nasa.gov/view.php?datasetId=GISS_TA_Y&date=2018-02-01

Name	Description	Time interval data	Method	Scale	Type of file	Variable	Descriptor	Database	Web-site
NASA EARTH OBSERVATIONS	Land Surface Temperature	24/02/2000-26/06/2019 (per day, or per month)	Up to date information and satellite images on fires, storms, floods, volcanoes, earthquakes, and droughts	world	Geotiff, CSV, CSV for Excel, Jpeg,png, GeoTIFF (floating point), GeoTIFF (raster), GoogleEarth 1.0 degrees (360x180) 0.5 degrees (720x360) 0.25 degrees (1440x720) 0.1 degrees (3600x1800)	°C	°C/pixel	monthly	https://neo.sci.gsfc.nasa.gov/view.php?datasetId=MOD_LSTD_M
NASA EARTH OBSERVATIONS	Average land surface temperature [day], average land surface temperature [night],	24/02/2000-26/06/2019 (per day, or per month)		World	Geotiff, CSV, CSV for Excel, Jpeg,png, GeoTIFF (floating point), GeoTIFF (raster), GoogleEarth 1.0 degrees (360x180) 0.5 degrees (720x360) 0.25 degrees (1440x720) 0.1 degrees (3600x1800)	°C	°C/pixel	monthly	https://neo.sci.gsfc.nasa.gov/view.php?datasetId=MOD_LSTD_M
NASA EARTH OBSERVATIONS	Average land surface temperature [day], average land surface temperature [night],	24/02/2000-26/06/2019 (per day, or per month)		world	Geotiff, CSV, CSV for Excel, Jpeg,png, GeoTIFF (floating point), GeoTIFF (raster), GoogleEarth 1.0 degrees (360x180) 0.5 degrees (720x360) 0.25 degrees (1440x720) 0.1 degrees (3600x1800)	°C	°C/pixel	monthly	https://neo.sci.gsfc.nasa.gov/view.php?datasetId=MOD_LSTAN_M

Name	Description	Time interval data	Method	Scale	Type of file	Variable	Descriptor	Database	Web-site
European Climate Assessment (ECAD)	Heating degree days	1756-2018 (year is seen inside the txt files, 2nd column of the data; indexHD17000010.txt - indexHD17017289)	aggregated station indices data for all stations within ECA&D.	world	txt (1 txt per station and 1 with stations info)	°C	°C/year	yearly/daily	https://eca.knmi.nl//download/millennium/millennium.php
European Climate Assessment (ECAD)	Minimum value of daily maximum temperature	1775-2018 (year is seen inside the txt files, 2nd column of the data; indexTXn000027.txt - indexTXn017289)	aggregated station indices data for all stations within ECA&D.	world	txt (1 txt per station and 1 with stations info)	°C	°C/year	yearly/daily	https://eca.knmi.nl//download/millennium/millennium.php
European Climate Assessment (ECAD)	No. of summer days (SU)*	1775 - 2018 (year is seen inside the txt files, 2nd column of the data; indexSU000027.txt - indexSU017289)	aggregated station indices data for all stations within ECA&D.	world	txt (1 txt per station and 1 with stations info)	days		yearly/daily	https://eca.knmi.nl//download/millennium/millennium.php
European Climate Assessment (ECAD)	Warm spell duration index (WSDI)*	1775 - 2018 (year is seen inside the txt files, 2nd column of the data; indexWSDI000027.txt - indexWSDI017289)	aggregated station indices data for all stations within ECA&D.	world	txt (1 txt per station and 1 with stations info)	WSDI		yearly/daily	https://eca.knmi.nl//download/millennium/millennium.php

Name	Description	Time interval data	Method	Scale	Type of file	Variable	Descriptor	Database	Web-site
European Climate Assessment (ECAD)	No. of warm nights (TN90p)*	1767 - 2018 (year is seen inside the txt files, 2nd column of the data; indexTN90p000017.txt - indexTN90p017289.txt)	aggregated station indices data for all stations within ECA&D.	world	txt (1 txt per station and 1 with stations info)	days		yearly/daily	https://eca.knmi.nl//download/millennium/millennium.php
European Climate Assessment (ECAD)	Maximum of daily maximum temperature (TXx)*	1775 - 2018 (year is seen inside the txt files, 2nd column of the data; indexTXn000027.txt - indexTXn017289.txt)	aggregated station indices data for all stations within ECA&D.	world	txt (1 txt per station and 1 with stations info)	°C		yearly/daily	https://eca.knmi.nl//download/millennium/millennium.php
European Climate Assessment (ECAD)	Consecutive summer days (CSU)	1775 - 2018 (year is seen inside the txt files, 2nd column of the data; indexCSU000027.txt - indexCSU017289.txt)	aggregated station indices data for all stations within ECA&D.	world	txt (1 txt per station and 1 with stations info)	days		yearly/daily	https://eca.knmi.nl//download/millennium/millennium.php
European Climate Assessment (ECAD)	No. tropical nights (TR)*	1767 - 2018 (year is seen inside the txt files, 2nd column of the data; indexTR000017.txt - indexTR017289.txt)	aggregated station indices data for all stations within ECA&D.	world	txt (1 txt per station and 1 with stations info)	days		yearly/daily	https://eca.knmi.nl//download/millennium/millennium.php

Name	Description	Time interval data	Method	Scale	Type of file	Variable	Descriptor	Database	Web-site
European Climate Assessment (ECAD)	No. of warm days (TG90p)	1756 - 2018 (year is seen inside the txt files, 2nd column of the data; indexTG90p000010.txt - indexTG90p017289.txt)	aggregated station indices data for all stations within ECA&D.	world	txt (1 txt per station and 1 with stations info)	days		yearly/daily	https://eca.knmi.nl//download/millennium/millennium.php
European Climate Assessment (ECAD)	No. of warm day-times (TX90p)*	1775 - 2018 (year is seen inside the txt files, 2nd column of the data; indexTX90p000027.txt - indexTX90p017289.txt)	aggregated station indices data for all stations within ECA&D.	world	txt (1 txt per station and 1 with stations info)	days		yearly/daily	https://eca.knmi.nl//download/millennium/millennium.php
European Climate Assessment (ECAD)	Maximum of daily minimum temperature (TNx)*	1767 - 2018 (year is seen inside the txt files, 2nd column of the data; indexTNx000017.txt - indexTNx017289.txt)	aggregated station indices data for all stations within ECA&D.	world	txt (1 txt per station and 1 with stations info)	°C		yearly/daily	https://eca.knmi.nl//download/millennium/millennium.php
European Climate Assessment (ECAD)	Mean of daily mean temperature; mean of daily minimum temperature; mean of daily maximum temperature; mean of diurnal temperature range; intra-period extreme temperature	1767 - 2018 (year is seen inside the txt files, 2nd column of the data; indexTNx000017.txt - indexTNx017289.txt)	aggregated station indices data for all stations within ECA&D.	world	txt (1 txt per station and 1 with stations info)	°C			https://eca.knmi.nl//download/millennium/millennium.php

Name	Description	Time interval data	Method	Scale	Type of file	Variable	Descriptor	Database	Web-site
	range; mean absolute day-to-day difference								
E-OBS data access	daily mean temperature (TG), daily minimum temperature (TN), daily maximum temperature (TX), daily precipitation sum (RR)	01/01/1950-31/12/2018 Per 15 year chunks (3rd link) 2019 data per month (4th link)			grid (The ensemble version (indicated with a 'e' after the version number) is available on a 0.1 and 0.25 degree regular grid for the elements; data files are in NetCDF-4 format. The Global 30 Arc-Second Elevation Data Set (GTOPO30), a global raster Digital Elevation Model (DEM) with a horizontal grid spacing of 30 arc seconds (approximately 1 kilometer) developed by USGS is used for the elevation file as well.) gridded data files 2019 per month .nc filetype (4th link); we can see the map and download a png image (when we click download (from the 2nd link), daily				http://c3surf.knmi.nl/dataaccess/access_eobs.php http://c3surf.knmi.nl/maps/eobsdailymaps.php http://c3surf.knmi.nl/dataaccess/access_eobs_chunks.php http://c3surf.knmi.nl/dataaccess/access_eobs_months.php
European Environment Agency (EEA)	Number of extreme heat waves in future climates under two different climate forcing scenarios	2020-2052; 2068-2100	Median of the number of heat waves in a multi-model ensemble of the near future under two scenarios	Europe	.gif, .tif, .png, .xls	days	Number of days in 33 years		https://www.eea.europa.eu/data-and-maps/figures/number-of-extreme-heat-waves-1

Name	Description	Time interval data	Method	Scale	Type of file	Variable	Descriptor	Database	Web-site
European Environment Agency (EEA)	Average temperature anomalies (°C) for Europe between 28 June to 4 July, 2015. Baseline period is 1964–1993.	2015	Average temperature anomalies with respect to the period 1964-1993	Europe	.gif, .tif, .png, .xls	°C	Difference from average temperature in °C		https://www.eea.europa.eu/data-and-maps/figures/extent-of-the-heat-wave
European Environment Agency (EEA)	Spatial distribution of extreme temperature indicators across Europe	1987-2016	number of days	Europe	.gif, .tif, .png, .xls	Days			https://www.eea.europa.eu/data-and-maps/figures/spatial-distribution-of-extreme-temperature
European Environment Agency (EEA)	Observed trends in warm days	1960-2017	Warm days as being above the 90th percentile of the daily maximum temperature	Europe	.gif, .tif, .png, .xls	Days	Days/decade		https://www.eea.europa.eu/data-and-maps/figures/changes-in-duration-of-warm-spells-in-summer-across-europe-in-the-period-1976-2006-in-days-per-decade-10

Table A1.5: Landslide

Name	Description	Method	Scale	Type of file	Descriptor	Database	Web-site
SAFELAND	Identification of landslide hazard and risk "hotspots" in Europe	based on expert judged reclassification and weighting of different factors that are assumed to be important for landslide susceptibility and hazard (International Centre for Geohazards model).	Europe	Geotiff The link downloads a pdf	4 classes	Rainfall-induced	https://www.ngi.no/eng/Projects/SafeLand/#Reports-and-publications
Joint Research Centre Data Catalogue (JRC)	European Landslide Susceptibility Map (ELSUS) Year 2018	heuristic-statistical modelling of main landslide conditioning factors using also landslide location data.	Europe	Geotiff Requieres login (this is processed manually so data can't be obtained immediately) Sent data: 2 folders: 6 datasets (3 dbf, 3 prj, 1 qpj, 2 shp, 2 shx, 1 mshp, 1 asc, 1 clr, 1 cpg, 3 tif) and metadata (6 pdf)	5 classes	Rainfall-induced	https://esdac.jrc.ec.europa.eu/content/european-landslide-susceptibility-map-elsus-v2#tabs-0-description=1
Global Risk Data Platform	Frequency of landslides triggered by earthquakes Year 2018	combination of trigger and susceptibility defined by six parameters: slope factor, lithological (or geological) conditions, soil moisture condition, vegetation cover, precipitation and seismic conditions.	world	Geotiff (2 xml, 1 tfw, 1 tiff)	4 classes	earthquake-induced	https://preview.grid.unep.ch/index.php?preview=data&events=landslides&evcat=1&lang=eng
Global Risk Data Platform	Frequency of landslides triggered by precipitations Year 2018	combination of trigger and susceptibility defined by six parameters: slope factor, lithological (or geological) conditions, soil moisture condition, vegetation cover, precipitation and seismic conditions.	world	Geotiff (2 xml, 1 tfw, 1 tiff)	4 classes	rainfall-induced	https://preview.grid.unep.ch/index.php?preview=data&events=landslides&evcat=2&lang=eng
Global Risk Data Platform	Physical exposition to landslides triggered by earthquakes Year 2018	population grid for the year 2010, provided by LandScanTM Global Population Database (Oak Ridge, TN: Oak Ridge National Laboratory)	world	Geotiff (1 xml, 1 tfw, 1 tiff)		earthquake-induced	https://preview.grid.unep.ch/index.php?preview=data&events=landslides&evcat=3&lang=eng

Name	Description	Method	Scale	Type of file	Descriptor	Database	Web-site
Global Risk Data Platform	Physical exposition to landslides triggered by precipitations Year 2018	population grid for the year 2010, provided by LandScanTM Global Population Database (Oak Ridge, TN: Oak Ridge National Laboratory)	world	Geotiff (1 xml, 1 tfw, 1 tiff)	(people/year)	rainfall-induced	https://preview.grid.unep.ch/index.php?preview=data&events=landslides&evcat=4&lang=eng
Global Risk Data Platform	Economical exposition to landslides triggered by earthquakes Year 2018	A Global Domestic Product grid for the year 2010, provided by the World Bank,	world	Geotiff (1 xml, 1 tfw, 1 tiff)		earthquake-induced	https://preview.grid.unep.ch/index.php?preview=data&events=landslides&evcat=5&lang=eng
Global Risk Data Platform	Economical exposition to landslides triggered by precipitations Year 2018	A Global Domestic Product grid for the year 2010, provided by the World Bank,	world	Geotiff (1 xml, 1 tfw, 1 tiff)	(1000$/year)	rainfall-induced	https://preview.grid.unep.ch/index.php?preview=data&events=landslides&evcat=6&lang=eng
Global Risk Data Platform	risk index for landslide hazard triggered by precipitations Year 2011	designed by UNEP/GRID-Europe for the Global Assessment Report on Risk Reduction (GAR). It was modeled using global data. Credit: UNEP/GRID-Europe.	world	Geotiff (1 xml, 1 tfw, 1 tiff)	from 1 (low) to 5 (extreme)	rainfall-induced	https://preview.grid.unep.ch/index.php?preview=data&events=landslides&evcat=7&lang=eng

Table A1.6: Earthquake

a) Hazard maps

Name	Description	Method	Scale	Type of file	Variable	Descriptor	Database	Web-site
Global Assessment Report on Disaster Risk Reduction 2017	Hazard map	set of parameters that describe the future seismic activity on each of them based on historical records together with relationships to obtain hazard intensities as a function of magnitude and distance	world	Grid file From 'Download section' we can download capraViewer (sw) and files of all the layers of the maps through all the years (Peak Ground & Spectral acceleration (1 grd). Going to 'Download Portal' we get a folder per hazard (Earthquake_hazard_maps). There's a file per year range (several grd files, 1 ame, 2 qml)	peak ground accelerat ion	PGA	250, 475, 975, 1500, & 2475 yrs return period	https://risk.preventionweb.net/capraviewer/download.jsp?tab=9&mapcenter=0,1123252.6982849&mapzoom=2; http://unisdr.envcomp.eu/browse/Hazard/Earthquake_Hazard_maps, https://risk.preventionweb.net/capraviewer/download.jsp?tab=9
Socioeconomic Data and Applications Center (SEDAC)	Global Earthquake Hazard Frequency and Distribution	2.5 minute grid utilizing Advanced National Seismic System (ANSS) Earthquake Catalog data of actual earthquake events exceeding 4.5 on the Richter scale during the time period 1976 through 2002	world	asc (1 asc, 1 prj) requires login	earthqua ke hazard frequenc y	decile		http://sedac.ciesin.columbia.edu/data/set/ndh-earthquake-frequency-distribution
Socioeconomic Data and Applications Center (SEDAC)	Global Earthquake Hazard Distribution Peak Ground Acceleration, v1 (1976–2002)	2.5-minute grid of global earthquake hazards developed using Global Seismic Hazard Program (GSHAP) data that incorporate expert opinion in predicting localities where there exists a 10 percent chance of exceeding a peak ground acceleration (pga) of 2 meters per second per second (approximately one-fifth of surface gravitational acceleration) in a 50 year time span	world	asc (1 asc, 1 prj) requires login	peak ground accelerat ion	4 classes		http://sedac.ciesin.columbia.edu/data/set/ndh-earthquake-distribution-peak-ground-acceleration/data-download

Name	Description	Method	Scale	Type of file	Variable	Descriptor	Database	Web-site
Socioeconomic Data and Applications Center (SEDAC)	Global Earthquake Mortality Risks and Distribution, v1 (2000)	2.5 minute grid of global earthquake mortality risks.		1 asc, 1 dbf, 1 prj requires login				https://sedac.ciesin.columbia.edu/data/set/ndh-earthquake-mortality-risks-distribution/data-download
Socioeconomic Data and Applications Center (SEDAC)	Global Earthquake Proportional Economic Loss Risk Deciles, v1 (2000)	2.5 minute grid of earthquake hazard economic loss as proportions of Gross Domestic Product (GDP) per analytical unit		1 asc, 1 prj requires login				https://sedac.ciesin.columbia.edu/data/set/ndh-earthquake-proportional-economic-loss-risk-deciles/data-download
Socioeconomic Data and Applications Center (SEDAC)	Global Earthquake Total Economic Loss Risk Deciles, v1 (2000)	2.5 minute grid of global earthquake total economic loss risks. A process of spatially allocating Gross Domestic Product (GDP) based upon the Sachs et al. (2003)		1 asc, 1 dbf, 1 prj requires login				https://sedac.ciesin.columbia.edu/data/set/ndh-earthquake-total-economic-loss-risk-deciles/data-download
Global Risk Data Platform	Earthquakes events from ANSS January 1970-June 2015	earthquake events with magnitudes higher than 5.0					01/1970-06/2015	https://preview.grid.unep.ch/index.php?preview=data&events=earthquakes&evcat=1&lang=eng
Global Risk Data Platform	Earthquakes Modified Mercalli Intensity	global estimate of the Modified Mercalli Intensity based on Global Seismic Hazard Assessment Program					1973-2007	https://preview.grid.unep.ch/index.php?preview=data&events=earthquakes&evcat=3&lang=eng
Global Risk Data Platform	Physical exposure to earthquakes 1973-2007	estimate the annual physical exposition to earthquakes of MMI categories higher than a given value (5,7,8,9)					*1973-2007*	https://preview.grid.unep.ch/index.php?preview=data&events=earthquakes&evcat=6&lang=eng

Name	Description	Method	Scale	Type of file	Variable	Descriptor	Database	Web-site
Global Risk Data Platform	Economical exposure to earthquakes 1973-2007	estimate the annual economical exposition to earthquakes of MMI categories higher than a given value (5,7,8,9)					*1973-2007.*	https://preview.grid.unep.ch/index.php?preview=data&events=earthquakes&evcat=7&lang=eng

b) Catalogues

Name	Description	Time interval	Method	Scale	Type of file	Web-site
SHARE	European Earthquake catalogue	1900-2006	Partial excerpt of "The European-Mediterranean Earthquake Catalogue" (EMEC)	Europe	excel file (2 excel files 1000-1899 and 1900-2006) requires registration	https://www.emidius.eu/SHEEC/
International seismological centre	catalogue of earthquakes	1904-2018			csv, kmz requires registration – link received didn't work	http://www.isc.ac.uk/iscgem/download.php
Advanced National Seismic System (ANSS)	catalogue of earthquakes	January 1970 - June 2015	world-wide earthquake catalogue created by merging the master earthquake catalogues from contributing ANSS institutions	World		https://ncedc.org/anss/catalog-search.html

Appendix 2 National hazard maps for Poland

The primary goal of the project is to find solutions that can be applied in a wide range of situations and locations in the context of Europe. As a representative for eastern Europe additional hazard data for Poland are added, since different extreme conditions, from the SAFEWAY Pilots, might occur. This appendix describes the risks associated with these extreme conditions for two case study sites in Poland.

Case study of the expressway S8 and case study of the railway LCS Kutno are located in Łódź Province in central Poland. The climate analysis was done for two main cities – Sieradź (expressway S8) and Kutno (railway section).

Increasing extreme atmospheric phenomena with catastrophic consequences has been recently visible in Poland and in the Łódź Province. There has been an increase of natural disasters related to natural forces, in particular: strong winds, intense precipitation combined with strong discharges, prolonged occurrence of extreme temperatures, floods, etc.

Natural and man-made hazards that occurred or may occur in this area are described briefly in the following chapters.

A2.1 Flood

Along the expressway S8, the flood risk is recognized. Two main rivers: Warta and Grabia present the main flood risk in this area. Since the S8 section was built, there was no flooding. Nevertheless, the probability of flood event is high (10%) in next 10 years. The flood risk areas are highlighted in maps below (Figure A1, Figure A2). Also, it is possible to check flood risk map on the hydrology geoportal – *ISOK Informatyczny System Osłony Kaju* (http://mapy.isok.gov.pl/imap/). The real time monitoring of the water level in rivers can be done through the IMGW-PIB portal:

http://monitor.pogodynka.pl/#map/18.7897,51.5758,13,true,true,12 .

The section of railway Żychlin- Barłogi in the area of Kutno is located in a flood risk terrain because of the Ochnia river. However, if we take into account the aforementioned map on the ISOK website, which determines the probability of flood occurrence in this section, we can see that it is not a threat.

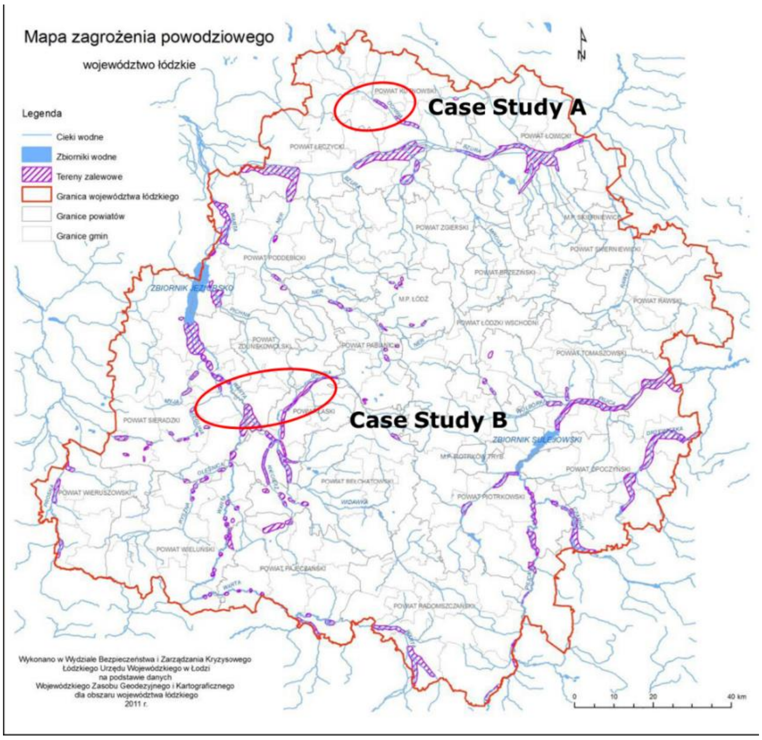

Figure A1: *Flood risk map of the Łódź Province. (Source ISOK; http://mapy.isok.gov.pl/imap/)*

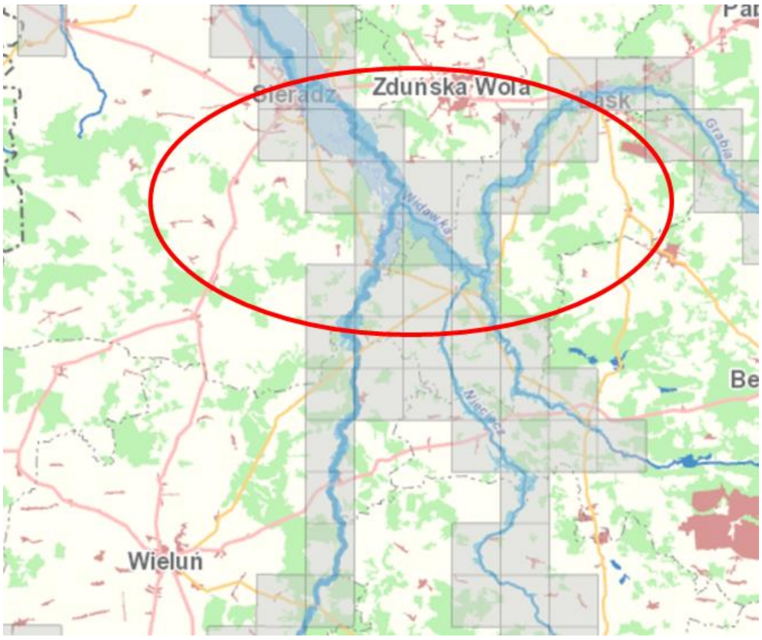

Figure A2: *Flood risk map elaborated by ISOK for the section of the expressway S8. (Source ISOK; http://mapy.isok.gov.pl/imap/)*

A2.2 Wildfire

Potentially, about 83% of the total forest resources in Poland are subjected to wildfire risk[18]. Along the expressway S8 there are many forest areas, which can pose a wildfire hazard. In last years the fire risk was high. Many factors can determine the wildfire risk. One of these factors can be meteorological conditions. Conditions, under which an uncontrolled combustion of the forest material may occur are as follows:

- air relative humidity [%]
- air temperature [$^{\circ}$C]
- moisture of the fuel [%]
- wind velocity [m/s] and direction
- solar irradiance [W/m^2]

Forecasting and monitoring wildfire danger is performed for the whole Poland by the Independent Department of Forest Fire Protection (IDFFP). During the fire season i.e. between March and October inclusive, the IDFFP collects forest fire danger data daily from measurement points of 17 Regional Directorates of State Forests. Forest fire danger is assessed with the IBL method twice a day (at 9:00 a.m. and at 1 p.m.). The actual degree of forest fire danger determines the type of preventive measures which the forestry district or the national park are obliged to undertake. The IBL method is based on three key factors such as: pine litter moisture, relative air humidity, precipitation coefficient. Based on these factors four fire danger degrees are established as shown in Table A1.

Table A1: Description of four fire danger levels provided by the Independent Department of Forest Fire Protection (IDFFP)

Wildfire Risk Level	Relative humidity value [%]			
	9 a.m.		1p.m.	
	Pine litter moisture	Air humidity	Pine litter moisture	Air humidity
0 -No danger	0-60 61-75	96-100 0-100	0-40 41-75	86-100 0-100
1 - Low danger	0-40 41-60	86-95 0-95	0-30 31-40	66-85 0-85
2 - High danger	0-20 21-40	76-85 0-85	0-15 16-30	51-65 0-65
3 - Catastrophic danger	0-20	0-75	0-15	0-50

[18] *http://www.fao.org/docrep/article/wfc/xii/0009-b3.htm*

In Figure A3 and Figure 68, the Fire Weather Index from March to September 2018 is showed on maps generated by Copernicus Emergency Management Service. According to this index, the areas of the interest oscillate mainly between moderate and high danger risk level. The current Fire Weather Index is possible to check on:

http://effis.jrc.ec.europa.eu/static/effis_current_situation/public/index.html

The real-time wildfire risk level can be monitored on:

http://bazapozarow.ibles.pl/zagrozenie/

Wildfire effects on the infrastructure facilities can be disastrous. Nevertheless, it is hard to forecast their malfunctioning. On the expressway S8, viaducts, bridges and overpasses are mainly made of reinforced concrete. In case of wildfire, the malfunction of the structure can be determined after a thorough examination of the entire facility in terms of load capacity because it depends on few important factors:

- element construction, (e.g. fires in solid-wall constructions, especially in box-type cases, fire can be unnoticed while spreading inside), surface type (bituminous materials support combustion), thickness of elements
- type of material and its fire resistance.
- maximum temperature and length of fire.

Concrete bridges are the most resistant to long-term fire, because their spans - due to their large overall dimensions and high thermal inertia of the concrete - are less exposed to the effects of high temperatures. In extreme cases, concrete spalling may occur in the concrete, i.e. the concrete reinforcement casing insulation is detached. Then they are directly exposed to the effects of high temperature, which significantly reduces the strength and bearing capacity of the bridge much faster.

Steel bridges are characterized by the high thermal conductivity causing rapid heating of the structure, also in places far from the source of the fire. The influence of high fire temperatures also leads to changes in the structure of the steel and violation of the static system balance. This creates the risk of deformation of the bridge structure and causing further damage. Steel at elevated temperature loses its mechanical strength properties.

Depending on the design of the bridge/viaduct and the course of the fire, we can encounter extensive damage to the structure, which includes: bending and twisting the entire girders or smaller elements (cross bars, stringers, braces or bridge plates) and minor (local) damage, such as: corrugations, bulges, dents, nicks, cracks, scratches, etc.

The influence of high temperatures on **steel elements** which the railway consists of: loss of mechanical strength properties (e.g. at 600°C, it loses strength after only 7 minutes, at 550°C, the loss of strength is half the initial strength, and at 750°C - about 90% of strength).

When it comes to **concrete elements** and its influence during extremely high temperatures in comparison to steel elements they’re much more fire resistant.

Furthermore, along the section of the Żychlin-Barłogi railway, the fire hazard has a fundamental impact on the strength of track assets, in particular rails and other steel elements like fastenings etc. The main fire risk may be caused by ignition of vegetation along the line, short-circuiting in the traction elements and the fire of the rolling stock.

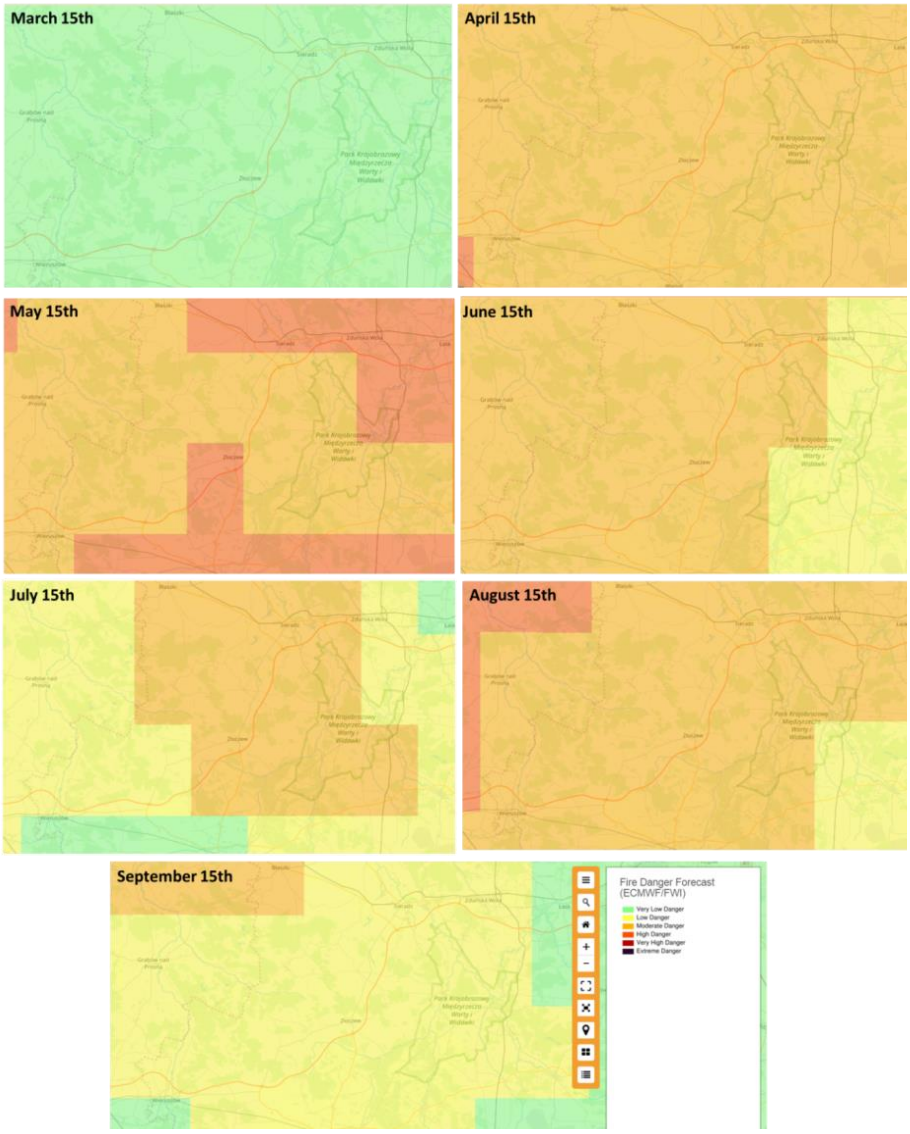

Figure A3: Fire Weather Index from March to September 2018, S8 ROAD. (Source: Copernicus Emergency Management Service)

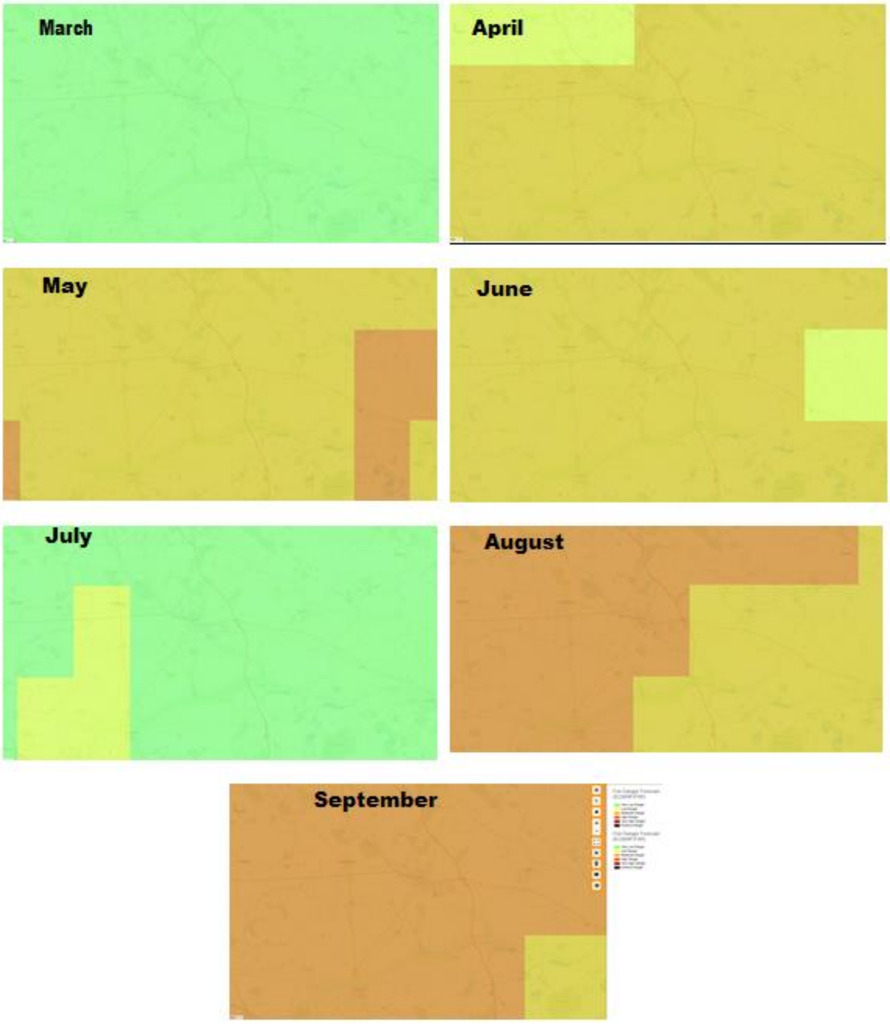

Figure 68: Fire Weather Index from March to September 2018 for railway Żychlin-Barłogi. (Source: Copernicus Emergency Management Service)

A2.3 Heavy rainfall and snowfall

The following weather data show the number of days in the month, when the rain reach a certain value in Sieradz city (Figure A5) and Kutno city (Figure A6), which are the closest city to the analysed case studies: Sieradź (expressway S8) and Kutno (railway section). Weather data are based on hourly weather simulation models from 30 years. These data are elaborated by Meteoblue[19] [20].

---

[19] *https://www.meteoblue.com/pl/pogoda/prognoza/modelclimate/sieradz_polska_3085978*
[20] *https://www.meteoblue.com/pl/pogoda/prognoza/modelclimate/kutno_polska_3094170*

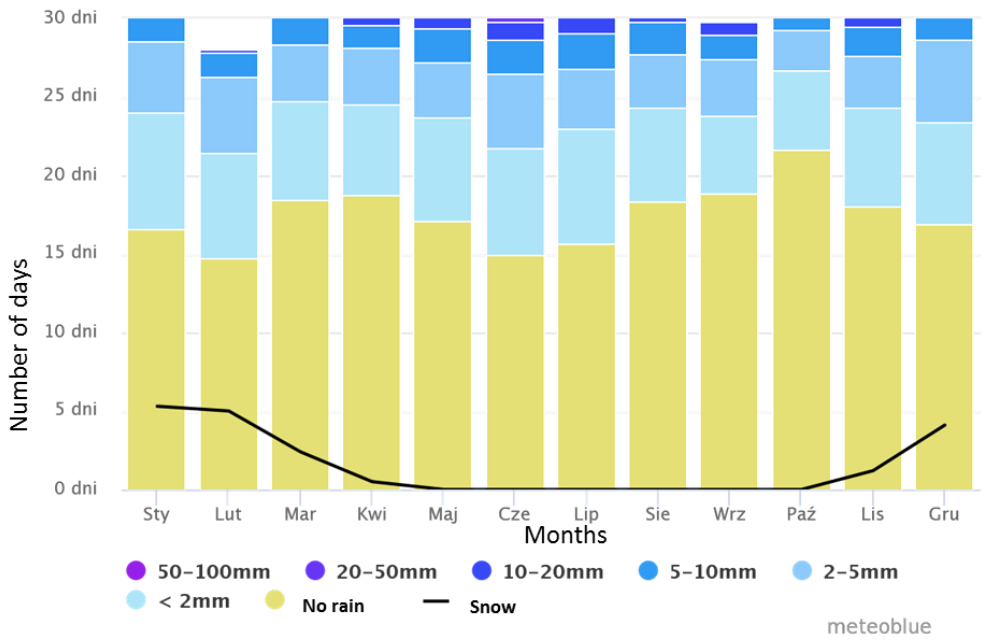

Figure A5: *The amount of precipitation for S8. (Source: Meteoblue; https://www.meteoblue.com)*

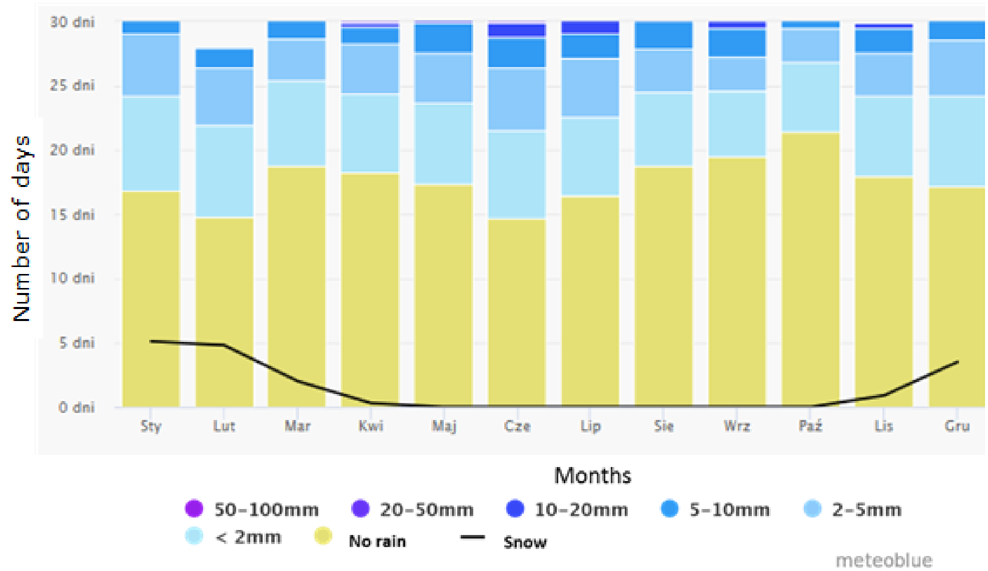

Figure A6: The amount of precipitation for the railway Żychlin- Barłogi. (Source: Meteoblue; https://www.meteoblue.com)

As we can notice the highest probability of rainfall and snowfall occurs from May to August and from November to March, respectively. During this period the malfunctioning of certain infrastructure components (e.g. slope slide) occurs often.

The real-time forecast of precipitation can be checked on ICM Numerical weather forecast service: http://mapy.meteo.pl/

The map below shows the yearly sum of precipitation in Poland (considered period 1971-2000). The average yearly precipitation for the analysed area is between

500-600mm[21]. The red circle shows the area of S8 section and the blue circle is for railway section.

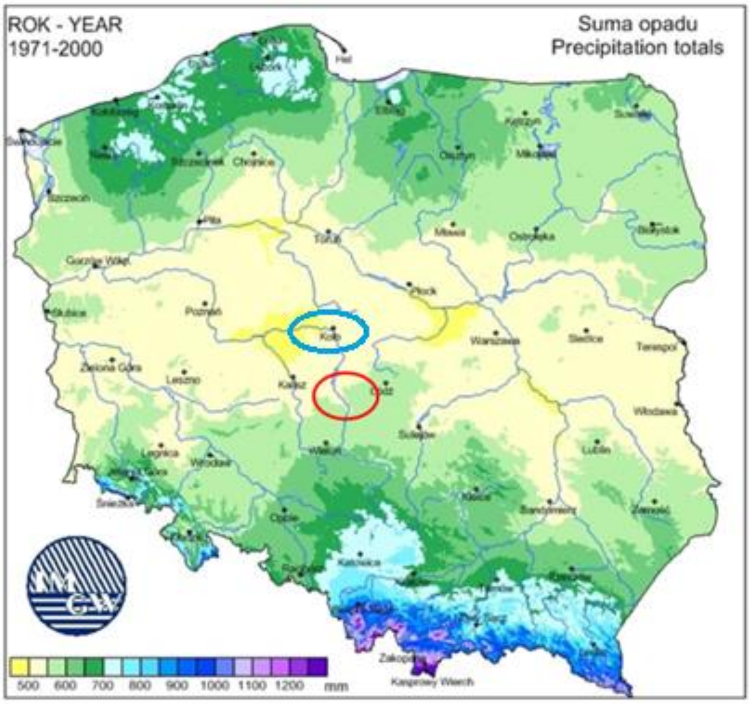

Figure 69: The yearly sum of precipitation in Poland for S8 section and railway section Żychlin-Barłogi. (Source: http://klimat.pogodynka.pl/pl/climate-maps/#Precipitation/Yearly/1971-2000/7/Winter)

A2.4 Strong winds

The following weather data show number of days in the month and classifies them in terms of wind speed in Sieradz city and in Kutno city, which are the closest cities to case studies. Weather data are based on hourly weather simulation models from 30 years. These data are elaborated by Meteoblue. Months with the highest number of days with wind velocity over 50 km/h verifies from October to April (22 days in total).

[21] *http://klimat.pogodynka.pl/pl/climate-maps/#Precipitation/Yearly/1971-2000/7/Winter*

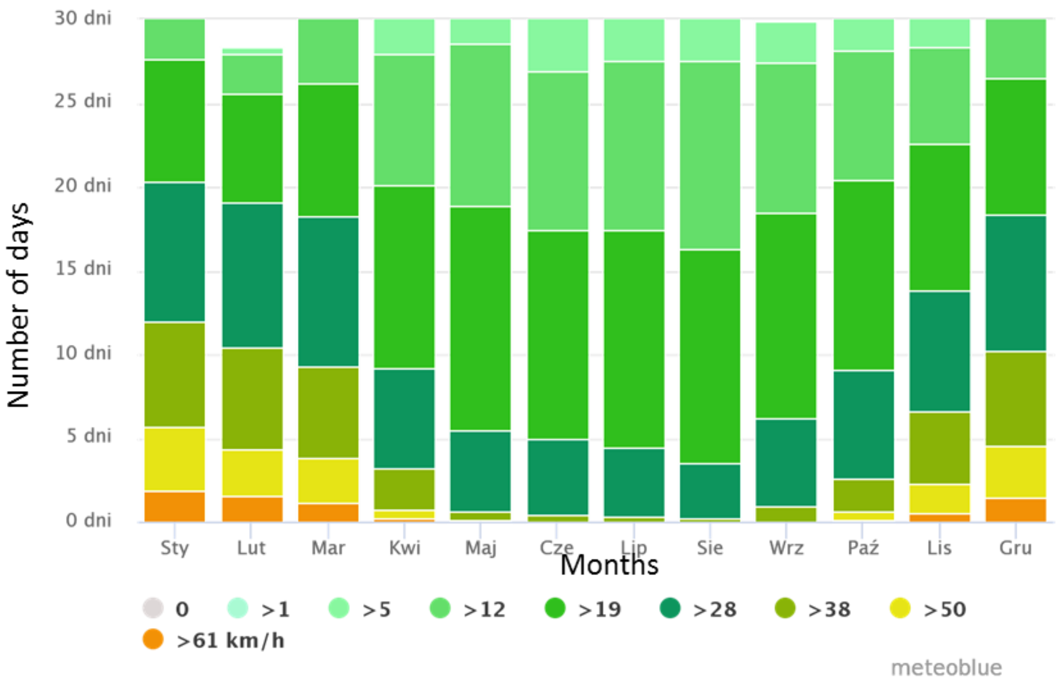

Figure A7:70 The diagram of the number of days in a month when the wind reaches a certain speed for Sieradz city. (Source: Meteoblue; https://www.meteoblue.com)

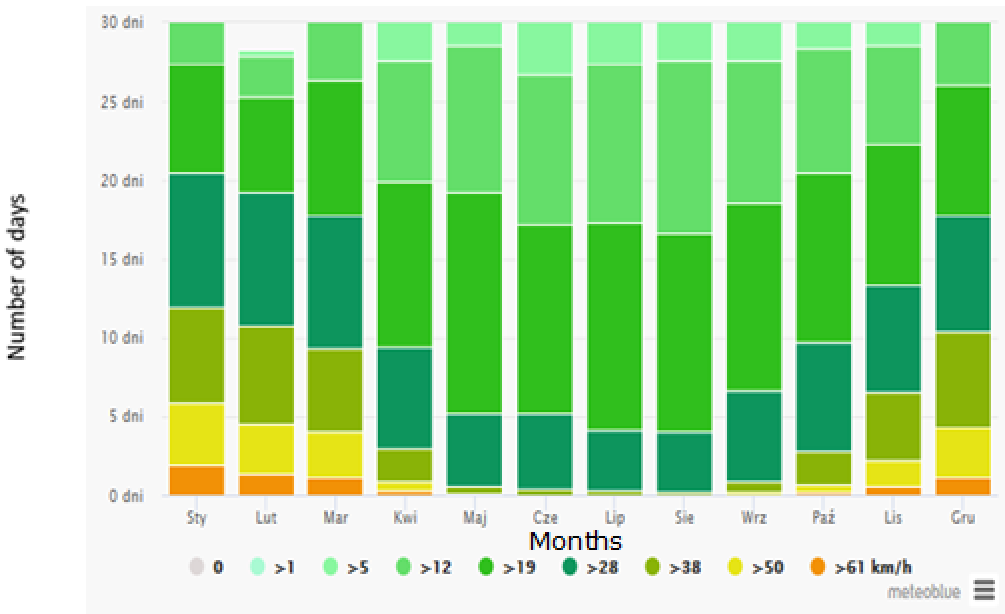

Figure A8: The diagram of the number of days in a month when the wind reaches a certain speed for Kutno city. (Source: Meteoblue; https://www.meteoblue.com)

The real-time forecast of wind velocity and direction can be checked on: https://www.windy.com/51.598/18.739?50.813,18.739,7

A2.5 Extreme temperature, icing and black ice

The following weather data are reported to Sieradz city and Kutno city:

- number of days in the month, when the temperature reaches a certain value
- minimal daily temperature average in each month
- maximal daily temperature average in each month
- average temperature of the hottest day in each month
- average temperature of the coldest night in each month
- sum of precipitation in each month

Weather data are based on hourly weather simulation models from 30 years and are elaborated by Meteoblue.

Months with the highest number of cold days (below 0 °C) verifies from October to March. The coldest temperature is register in January, -11 °C during the night and -3 °C as the lowest daily average temperature. The hottest days, between 30-33 °C, occur from June to August.

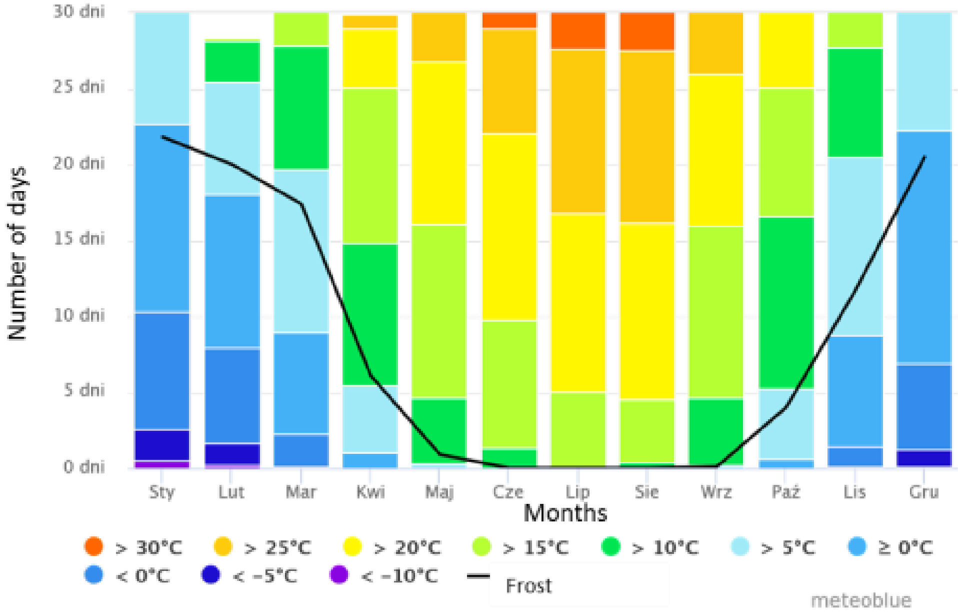

Figure A9: The maximum temperature diagram for Sieradz city. (Source: Meteoblue; https://www.meteoblue.com)

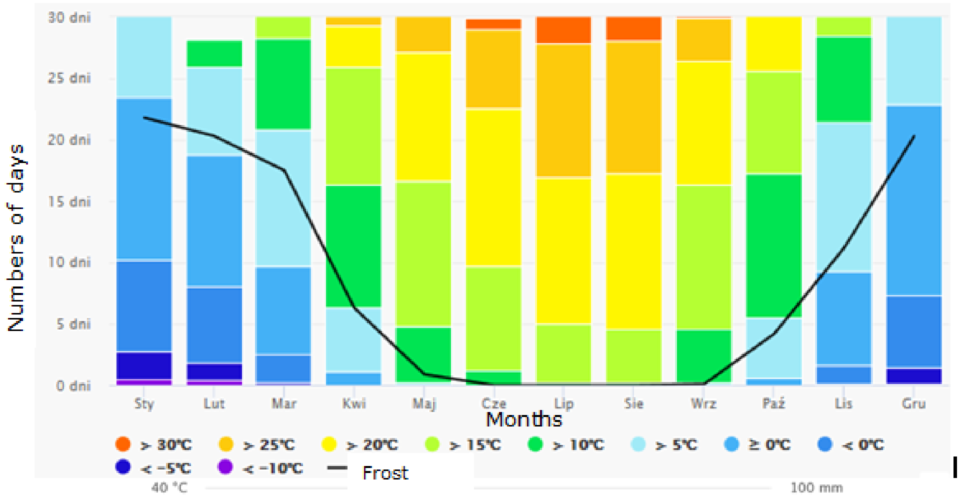

Figure A10: The maximum temperature diagram for Kutno city. (Source: Meteoblue; https://www.meteoblue.com)

On diagrams below there are showed data:

- average maximum daily value (red solid line) shows the maximum temperature of the average day for each month. Similarly,
- average minimum daily value (blue solid line) shows the average minimum temperature.

Hot days and cold nights (red and blue dotted lines) show the average temperature of the hottest days and coldest nights of each month in the last 30 years.

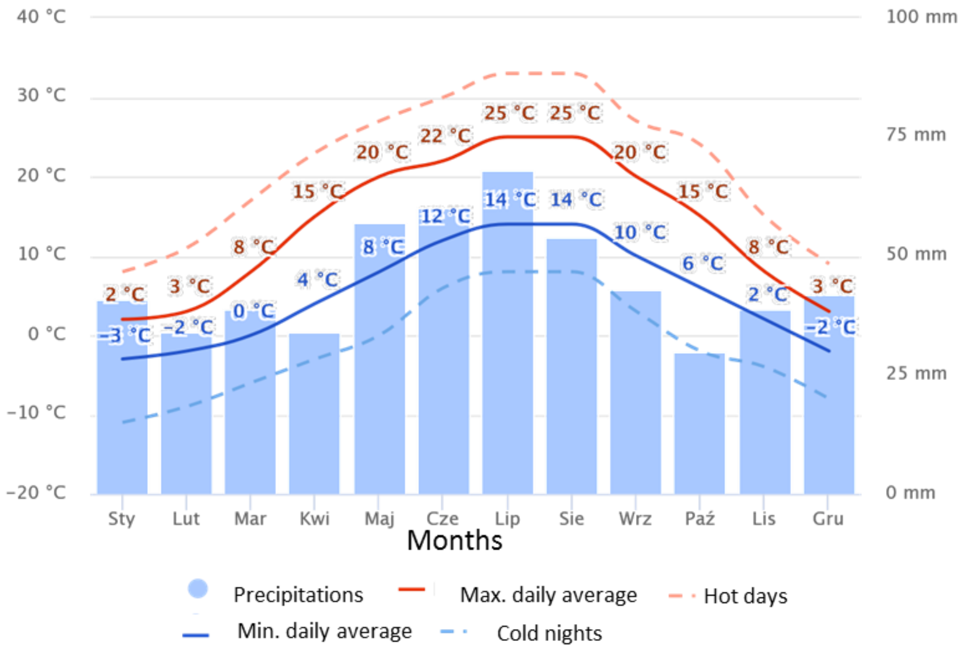

Figure A11: Average temperatures and precipitation diagram for Sieradz city. (Source: Meteoblue; https://www.meteoblue.com)

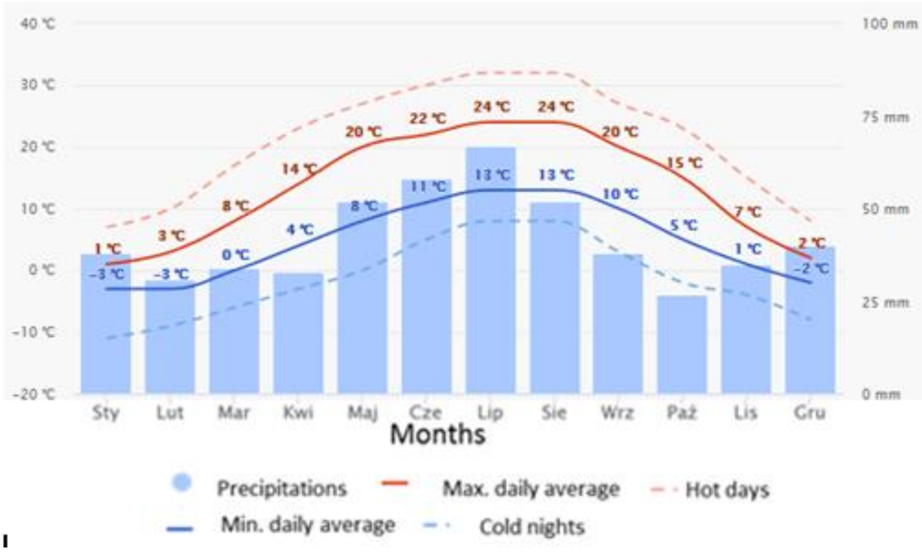

Figure A12: Average temperatures and precipitation diagram for Kutno city. (Source: Meteoblue; https://www.meteoblue.com)

One of the event that may represents a risk for the expressway is the black ice. Black ice is a thin coating of glaze ice on a road surface. It may form when:

- air temperature is below the freezing point (0 °C) and it is raining on the road surface
- air temperature is below the freezing point (0 °C) and moisture in the air condenses and forms dew or fog
- air temperature is below the freezing point (0 °C) and moisture from automobile exhaust condenses on the road surface

To avoid potential consequences of the black ice, it is important to monitor dew point. Dew point is the temperature, to which air must be cooled to become saturated with water vapour.

Black ice can appear on bridges, overpasses and spots on the road shaded by trees or other objects. Bridges and overpasses are prone to black ice because cold air is able to flow underneath the road surface, since it is elevated, therefore lowering the pavement temperature. Shaded spots on the road are prone since they receive less warmth from the sun during the day.

Furthermore, icing represents another risk to the infrastructure. There are three types of icing: clear, rime, and mixed. In most cases, the type of ice is most dependent on the air temperature. Clear ice typically forms when temperatures are around 2 °C to -10 °C and with the presence of large water droplets freezing drizzle, or freezing rain. Mixed ice, a combination of clear ice and rime ice that has the worst characteristics of both, can form rapidly when ice particles become embedded in clear ice and build a very rough accumulation. Mixed ice is most likely to form at temperatures between -10° C to -15° C. Rime ice forms when small droplets freeze immediately on contact with the aircraft surface. It typically occurs with temperatures between -15° C. and -20 ° C.

A2.5 Accidents

A2.5.1 Section of the expressway S8

Poland has made continuous progress, but still reports a higher number of road fatalities than the EU average (75 per million inhabitants compared to the EU average of 49)[22].

The expressway S8 is considered as one of 10 roads with high number of vehicle accidents per 1 km (Figure A13).

Expressway	Number of accidents per 1 km
S86	113
S2	81
S6	40
S79	24
S7	18
S74	15
S1	12
S12	11
S52	11
S8	10

Figure A13: Number of accidents per 1 km (according to Janosik.pl mobile application)

According to data collected by FB Serwis, 252 vehicle collisions occurred in the section of S8 from October 2017 to October 2018. The monthly average cost to eliminate accident damage on the road is between 30-40k PLN (7-9,3k EUR). From 2016 there were 13 fatal accidents and 3 time a helicopter landed to transport injured people. The main reason that may cause collisions are as follows:

- Speeding
- Lane Changes by TIR and other vehicles with a speed limit 90km/h
- Drowsy Driving
- Distraction and use of mobile devices
- Safe distance between vehicles is not respected.

A2.5.2 Section of the railway Żychlin-Barłogi

According to PKP PLK data from 1st January 2004 to 19th November 2018, it is possible to classify several types of accidents on this railway line:

- Accident caused by a passenger or bystander
  In most cases, accidents were caused by unauthorized persons in prohibited areas of railway, jumping out of a moving train, not being cautious when passing through an approaching train.
- duties omission of a linesman (not closed turnpikes),
- due to the fault of the railway employee such as: design errors of engineers, construction errors, driving under the influence of alcohol, arbitrary start of

[22] http://europa.eu/rapid/press-release_MEMO-18-2762_en.htm

work in active tracks without authorisation of a supervisor, bad train maintenance.

- due to natural hazards – like derailment as a result of frost, very strong wind caused the damage of a traction network
- a train defect that could not be detected by an employee for example break of the axle of the wheelset, wheel defects like wheel flat

The number of accidents and number of fatalities, sorted by cause of accident is given in Table A2.

Table A2: Accidents on railway Żychlin-Barłogi, from 1st January 2004 to 19th November 2018

Cause of accident	Number of accidents	Number of deaths
Fault of a passenger or bystander	67	35
Defect that could not be detected by an employee	17	0
Natural hazard	3	1
Fault of the railway employee	27	1